Performance Evaluation of Multicarrier Modulation Techniques Using Discrete Wavelet Transform for 5G Wireless Communication System and Beyond

Gemechu Dinkisa Kumsa

A Thesis Submitted to the Department of Electronics and Communication Engineering

School of Electrical Engineering and Computing

Presented in Partial Fulfillment of the Requirement for the Degree of Master's in Electronics and Communication Engineering (Communication Engineering)

Office of Graduate Studies
Adama Science and Technology University

June,2024
Adama, Ethiopia

Performance Evaluation of Multicarrier Modulation Techniques Using Discrete Wavelet Transform for 5G Wireless Communication System and Beyond

Gemechu Dinkisa Kumsa

Major advisor: Dr. Ram Sewak Singh (PhD)

Co-advisor: Mr. Eshetu Tessema (Msc)

A Thesis Submitted to the Department of Electronics and Communication Engineering

School of Electrical Engineering and Computing

Presented in Partial Fulfillment of the Requirement for the Degree of Master's in Electronics and Communication Engineering (Communication Engineering)

Office of Graduate Studies

Adama Science and Technology University

June,2024

Adama, Ethiopia

DECLARATION

I here by declare that this Master's Thesis entitled "**Performance Evaluation of Multicarrier Modulation Techniques Using Discrete Wavelet Transform for 5G Wireless Communication System and Beyond** " is my Original work and has not been submitted to any University for a similar purpose. That is, it has not been submitted for the award of any academic degree, diploma, or certificate in any other university. The references used in this thesis are duly recognized by proper citations.

Gemechu Dinkisa Kumsa	_____	_____
Name of Student	Signature	Date

RECOMMENDATION OF ADVISORS

We, the advisors of this Thesis, hereby certify that we have read the revised version of the thesis entitled "**Performance Evaluation of Multicarrier Modulation Techniques Using Discrete Wavelet Transform for 5G Wireless Communication System and Beyond**" prepared under our guidance by **Gemechu Dinkisa Kumsa** submitted in partial fulfillment of the requirements for the degree of Master's of Science in Communication Engineering. We recommend that the revised version of the thesis be submitted to the department following the applicable procedures.

Dr. Ram Sewak Singh (PhD)	_____	_____
Major Advisor	Signature	Date
Mr. Eshetu Tessema (Msc)	_____	_____
Co-advisor	Signature	Date

APPROVAL PAGE OF M.SC. THESIS

We, the advisors of this Thesis, entitled "**Performance Evaluation of Multicarrier Modulation Techniques Using Discrete Wavelet Transform for 5G Wireless Communication System and Beyond**" prepared under our guidance by **Gemechu Dinkisa Kumsa** hereby certify that the recommendation and suggestions made by the board of examiners are appropriately incorporated into the final version of the thesis.

Dr. Ram Sewak Singh(PhD)	_____	_____
Major Advisor	Signature	Date
Mr. Eshetu Tessema (Msc)	_____	_____
Co-advisor	Signature	Date

We, the undersigned, members of the Board of Examiners of the thesis by **Gemechu Dinkisa Kumsa** have read and evaluated the thesis entitled "**Performance Evaluation of Multicarrier Modulation Techniques Using Discrete Wavelet Transform for 5G Wireless Communication System and Beyond**" and examined the candidate during open defense. Therefore, to certify that the thesis is accepted for partial fulfillment of the requirement of the degree of Master of Science in Communication Engineering.

_____	_____	_____
Chairperson	Signature	Date
_____	_____	_____
Internal Examiner	Signature	Date
_____	_____	_____
External Examiner	Signature	Date

Final approval and acceptance of the thesis is contingent upon submission of its final copy to the Office of Postgraduate Studies (OPGS) through the Department Graduate Council (DGC) and School Graduate Committee (SGC).

_____	_____	_____
Department Head	Signature	Date
_____	_____	_____
School Dean	Signature	Date
_____	_____	_____
Office of Postgraduate Studies, Dean	Signature	Date

ACKNOWLEDGEMENT

First of all, it is my almighty God who did every good thing in my life and has helped me all over my thesis work. To make this thesis successful, my instructors and my colleagues have contributed a lot. Secondly, I would like to express my deepest gratitude to my main advisor **Dr. Ram Sewak Singh**, and co-advisor **Mr. Eshetu Tessema**, for their guidance, and full support during thesis work. I appreciate their support and patience. I am constantly impressed by their technical intuition, and I have learned a lot from them. They shared with me their academic life experiences. Their experiences motivated me to pass different challenges.

I would like to express my gratitude to my mom, my dad, and all my family members for the comprehensive support they have provided me throughout my life and education.

I would like to thank all my friends, especially Mr. Siressa Etefa, Mr. Galata Germosa, Mr. Galata Tunku, Mr. Roba Dufera, Mr. Daniel Jabessa, and Mr. Galata Yadata who have been helping me with my thesis work by showing me directions, so I have great respect and gratitude for them.

I would like to thank my special family from Gudane Amarti Generation Group, Mr. Kefale Wakjira, Mr. Negasa Diriba, Mr. Gebayo Olana, Mr. Barasa Name, Mr. Bilisuma Beyene and Mr. Hayu Fikadu for their patience in supporting me in every challenge that I faced. I would like to thank Ms.Lomitu Bashu, Ms.Wada Wakjira, and their families for their encouragement, prayers, and positive support. I would like to extend my sincere appreciation to Ms. Buzunesh Wakjira for her invaluable advice and financial support during my endeavors. Additionally, I am grateful to my sister, Ms. Zamiya Adem, and her family for their generous financial assistance and facilitation of essential matters during this time.

I would greatly thank Adama Science and Technology University for sponsoring me to take this master's program opportunity.

TABLE OF CONTENTS

LIST OF TABLES

LIST OF FIGURES

LIST OF ACRONYMS AND ABBREVIATIONS

AMPS	Advanced Mobile Phone System
AWGN	Additive White Gaussian Noise
BER	Bit Error Rate
CDMA	Code Division Multiple Acess
CP	Cyclic Prefix
CP-OFDM	Cyclic Prefix- Orthogonal Frequency Division Multiplexing
DWT	Discrete Wavelet Transform
FBMC-QAM	Filter Bank Multicarrier QuadratureAmplitude Modulation
FBMC-OQAM	Filter Bank Multicarrier Offset QuadratureAmplitude Modulation
FDMA	Frequency Division Multiple Access
FFT	Fast Fourier Transform
FM	Frequency Modulation
F-OFDM	Filtered Orthogonal Frequency Division Multiplexing
IFFT	Inverse Fast Fourier Transform
ISI	Inter Symbol Interference
MCM	Multicarrier Modulation
OFDM	Orthogonal Frequency Division Multiplexing
PAPR	Peak Average Power Ratio
PSD	Power Spectral Density
PSK	Phase Shift Keying
QAM	Quadrature Amplitude Modulation
QPSK	Quadrature Phase Shift Keying
SC-OFDM	Single Carrier- Orthogonal Frequency Division Multiplexing
SMS	Short Messaging Service
SNR	Signal-to-Noise Ratio
UFMC	Universal Filter Multicarrier
WOLA	Weighted Overlap and Added
1G	First Generation
2G	Second Generations

3G	Third Generations
4G	Fourth Generations
5G	Fifth Generations

ABSTRACT

Multicarrier modulation schemes have gained widespread adoption in wireless communication systems when compared to single-carrier modulations. Multicarrier schemes can overcome the challenges posed by multipath fading channels. Various researchers have proposed different multi-carrier modulation techniques to meet customer needs and mitigate the limitations of existing techniques. One widely adopted multi-carrier modulation technique in fourth-generation (4G) technology is Orthogonal Frequency Division Multiplexing (OFDM). However, the current Cyclic Prefix-OFDM (CP-OFDM) falls short of meeting the demands of 5G wireless communication systems because it suffers from significant drawbacks, such as Out-of-Band Emission (OOBE) and dependency on CP. To address the challenges associated with OFDM, different multicarrier modulation techniques such as Filtered-OFDM (F-OFDM) and Filter Bank Multicarrier Modulation (FBMC) have been employed. The growing demand for wireless communication has prompted the need for further advancements in wireless communication systems. In this study, the Discrete Wavelet Transform (DWT) is introduced as an innovative signal analysis approach within multicarrier modulation, offering numerous advantages, including support for high-speed applications, and efficient bandwidth utilization over the existing multi-carrier modulation techniques. The proposed wavelet-based multi-carrier modulation, featuring higher-order Quadrature Amplitude Modulation (QAM), aims to address the limitations of OFDM and other multi-carrier techniques. The performances of each multi-carrier modulation technique with DWT have been analyzed based on performance parameters such as spectral efficiency (SE), Power Spectral Density (PSD), Bit Error Rate (BER), Peak-to-Average Power ratio (PAPR), and Computational Complexity. The performance of wavelet-based multicarrier modulation achieved significantly higher spectral efficiency, lower computational complexity, and reduced BER. Simulation results have shown that the PSD of DWT-F-OFDM achieved a 29.99 dBW/Hz reduction in OOBE compared to the FBMC-QAM techniques. DWT-based multicarrier modulation provides the lowest PAPR compared to the conventional candidate multicarrier modulation techniques. From the result analysis, The PAPR characteristics of haar and bior2.2-based multicarrier schemes reduce the PAPR of OFDM by 3.72,3.66 and 3.36 dB, FBMC-OQAM by 5.18,4.42 and 4.00 dB, and F-OFDM by 2.42, 2.18 and 2.10 dB for higher-order QAM (64-QAM,256-QAM and 1024-QAM)modulation respectively compared to existing candidate multi-carrier modulation techniques. Additionally, the proposed DWT-multicarrier modulation is applied to BER analysis for the Vehicular and Pedestrian channel models. Based on the result analysis, it is observed that the bior2.2,sym4, and haar wavelets multicarrier modulation techniques showed better BER performance for Vehicular A, Vehicular B, and Pedestrian B channel models.

Keywords: *Discrete Wavelet Transform(DWT), Multicarrier Modulation (MCM), Quadrature amplitude modulation (QAM), Wavelet Transform (WT).*

CHAPTER ONE

INTRODUCTION

1.1 Background of the Study

Currently, the field of wireless telecommunication is undergoing substantial expansion. In modern wireless communication, the sending and receiving of signals are based on the principles of electromagnetic wave propagation. Over time, wireless transmission has evolved from radiotelephones to the establishment of cellular networks for mobile communication (Kamal & Din, 2019). Cellular networks must evolve to keep pace with the surging demand for wireless communication. (Abu-dalbouh, 2019). Originally, cellular networks were designed for voice-only applications, utilizing analog transmission channels. However, the evolution of mobile communication stands out as one of the most notable advancements in recent history.

Over time, 5G wireless communication networks have been introduced, with each generation appearing approximately every decade since the 1980s. The journey began with the monopoly of 1G, followed by the impressive popularity of 2G, which gradually incorporated data services. The success continued with the advent of 3G, although its initial attempt to deliver data services was not as successful as anticipated. It was the introduction of 4G that truly revolutionized cellular networks, Empowering applications reliant on data, such as multiplayer services multimedia, and streaming.(Al-jawhar et al., 2021).

To address these challenges and accommodate the exponential growth in wireless network requirements, the development of 5G mobile wireless networks has become imperative. The primary objective behind the introduction of 5G is to significantly improve network capabilities to efficiently handle the constantly growing data traffic and cater to the evolving demands of users in today's data-centric era(Ahmed Solyman & Yahya, 2022).5G is the latest generation of communication networks that follows the previous generations; 1G, 2G, 3G, and 4G. It represents the newest global wireless standard.

Modulation refers to the process of modifying a carrier signal, which is typically a high-frequency waveform, to encode information for transmission over a wireless communication channel(Marian Joseph Jeffery et al., 2020). In analog modulation, modulations are consistently applied following the analog data transmission. Conversely, digital modulation utilizes a discrete signal to modulate an analog carrier signal. This form of modulation could be categorized into single-carrier and multi-carrier modulation systems (Isnawati et al., 2023).

The high-speed data stream is transmitted in parallel across these sub-carriers. Multi-carrier modulation offers a wider symbol interval compared to single-carrier modulation, resulting in improved resilience against inter-symbol interference (Abdel-Atty et al., 2020). Single-carrier modulations offer certain benefits over multi-carrier modulations. In single-carrier modulation systems, the peak-to-average power ratio is very low, which is beneficial for system stability and the use of low-cost equipment in the design of wireless communication systems (Jiang et al., 2016).

To address the challenges posed by multi-path fading, multi-carrier modulations emerged as a favorable alternative. In the case of multi-carrier communications, data is conveyed across multiple frequencies instead of a solitary carrier, effectively partitioning the wide-band frequency selective communication channel into several sub-bands featuring moderately selective fading characteristics (Exam et al., 2019). Currently, Fourth (4G) technology employs CP-OFDM as a multi-carrier modulation technique. Due to the orthogonality property of these sub-carriers, there is no requirement for inserting guard bands between each sub-carrier to prevent inter-carrier interference (Tazeb et al., 2019). However, to mitigate interference between symbols, a cyclic prefix is employed. While the cyclic prefix effectively reduces interference, it also results in a decrease in spectral efficiency. CP-OFDM utilizes rectangular transmit and receive pulses, offering the advantage of reduced computational complexity. However, one drawback of using rectangular pulses is their lack of localization in the frequency domain. Consequently, this can result in significant Out-of-Band Emission (OOBE), where energy is transmitted outside of the intended frequency band (Kishore et al., 2017).

1.2 Motivation of the Study

5G are designed to support IoT devices, smart vehicles, communication between machines, and data rates surpassing 10Gbps and beyond (Patil et al., 2012). To meet the demands of future wireless communication systems, various multi-carrier modulation techniques are being explored such as Filter Bank Multicarrier (FBMC), Weighted Overlap and Added-OFDM (WOLA-OFDM), Filtered-OFDM (F-OFDM), and Universal Filter Multicarrier (UFMC) as a candidate wave-forms. An analysis of multi-carrier modulation techniques is presented in (Kishore et al., 2017; Kundrapu et al., 2019). However, most papers do not consider all performance metrics to draw their conclusion. In this study the detailed analysis of candidate multi-carrier modulation schemes based on DWT for higher-order QAM modulations like 64, 256, and 1024-QAM are discussed.

1.3 Statement of the Problem

The usage of CP which costs on spectral efficiency and poor OOBE parameter of OFDM modulation has limited its potential as a promising approach for wireless communication systems of 5G and beyond. To address the challenges in CP-OFDM, several alternative modulation methods have been proposed for implementation in 5G wireless communication. Therefore, various types of modulation schemes such as FBMC, UFMC, F-OFDM, and WOLA-OFDM have been proposed for 5G wireless communication instead of CP-OFDM. However, an important number of performance parameters should be incorporated and need further improvement for the proposed multicarrier modulation to make it more suitable for 5G and future technologies. To improve the spectral efficiency of multicarrier modulation along with other performance metrics, it becomes necessary to apply other signal processing techniques. Wavelet transform is considered the optimal substitute for signal analysis based on Discrete Fourier Transform (DFT) for multicarrier modulation techniques. This motivates us to research several promising modulation techniques that have been proposed, including OFDM, F-OFDM, and FBMC. In this thesis, the performance of these methods with Discrete Wavelet Transform based on metrics such as Spectral Efficiency, Power Spectral Density (PSD), Peak to Average Power Ratio (PAPR), Bit Error Rate (BER), and Computational Complexity has been analyzed and compared to OFDM, F-OFDM, and FBMC.

1.4 Objectives of Thesis

1.4.1 General Objective

The general objective of this thesis is the performance evaluation of multi-carrier modulation techniques using DWT for 5G and beyond wireless Communication sytems.

1.4.2 Specific Objectives

1. To evaluate the spectral efficiency of candidate multicarrier modulation techniques in the context of 5G wireless communication and beyond.
2. To analyze the bit error rate and peak-to-average power ratio performance of candidates of 5G multi-carrier modulation techniques by applying higher-order QAM.
3. To measure the performance of multicarrier modulation techniques with DWT based on power spectral density and peak-to-average power ratio.
4. To illustrate the bit error rate performance of multicarrier modulation techniques with DWT and compare it to traditional multicarrier modulation schemes.
5. To evaluate the computational complexity of multicarrier modulation techniques with DWT and compare it to conventional techniques.

1.5 Significance of the Study

This research thesis aims to assess the effectiveness of multicarrier modulation techniques used in 5G wireless communication systems, considering the presence of channel uncertainty and fading effects. By studying the behavior of different waveforms under these conditions, this research offers valuable insights into their performance characteristics. Furthermore, this research helps determine whether these modulation schemes meet the requirements of future wireless communication beyond 5G. Discrete Wavelet Transform-based multicarrier modulation is an underexplored area of research, with a limited exploration of crucial performance metrics for evaluating various multicarrier modulation schemes intended for 5G and beyond networks. Thus, this thesis work is helpful to aware and assess the merits and drawbacks of each modulation scheme whether each candidate waveform fulfills the requirement of fifth-generation wireless communication or not, and also to give direction for researchers to do more research.

1.6 Scope of the Study

While OFDM has its own advantages, it also presents certain drawbacks that make it unsuitable as a waveform for future wireless communication systems. To overcome the limitations of OFDM, extensive research has been conducted on various alternative multicarrier modulation schemes. However, a comprehensive and impartial evaluation of these alternative waveforms is lacking, particularly in the context of fading channels and incorporating a wider range of parameters. This thesis aims to address this gap by providing a detailed and objective analysis of the most prominent waveforms considered for the 5G generation. Discrete Wavelet Transform-based multicarrier modulation improves the performance of different schemes under selected channels with important performance metrics. The performance of these schemes can be analyzed across International Telecommunication Union - Radiocommunication Sector (ITU-R) standard channels such as Vehicular and Pedestrian channels.

1.7 Limitation of the Study

This thesis centers solely on simulating the system, utilizing MATLAB as the application software. Simulations are carried out under single-user scenarios, presuming that all accessible resources are assigned to one user.

1.8 Thesis Organization

The structure of this thesis is outlined as follows:

Chapter 1 Introduction: This chapter primarily encompasses the context of the study, problem statement, research objectives, contributions of the study, scope of the study, and limitations of the study.

Chapter 2 Literature Review: This chapter mainly focuses on the Introduction to 5G wireless communication, the use case of 5G technology, requirements of 5G technology, key enabling technology of 5G and beyond, single carrier and multicarrier modulation techniques, and review of related works.

Chapter 3 Design and Methods: This chapter mainly focuses on materials and methodology employed to conduct the research work, multi-carrier modulation techniques, wavelet families, and simulation parameters.

Chapter 4 Results and Discussions: This chapter mainly focuses on simulation parameters, power spectral density comparison, bit error rate comparison, spectral efficiency comparison, Peak-to-average power ratio comparison, and Computational Complexity comparison.

5 Conclusions and Recommendations: This section primarily centers on drawing conclusions and suggesting avenues for future research.

CHAPTER TWO

LITERATURE REVIEW

2.1 Chapter Overview

In this chapter, introduction to 5G wireless communication technologies, Fifth Generation (5G) wireless communication, requirements of 5G wireless communication technologies, key 5G enabling technologies, single carrier and multicarrier modulation techniques, and related literature on candidate waveform of 5G wireless communications that directly related to the objective of this study are reviewed.

2.2 Wireless Communication System

A wireless network of communication involves transmitting information transmitted wirelessly, like radio frequencies, microwaves, or infrared light. This technology serves as the foundation for a range of applications, including cell phones, wireless internet, short-range wireless technology, satellite links, radio broadcasts, TV broadcasting, and various other wireless communication systems (Chataut & Akl, 2020). Typically, such systems comprise a transmitter and a receiver that communicate wirelessly. The transmitter converts data into a signal suitable for transmission over the wireless medium (Tan et al., 2020). The recipient captures the transmission and demodulates and converts it back to the initial data.

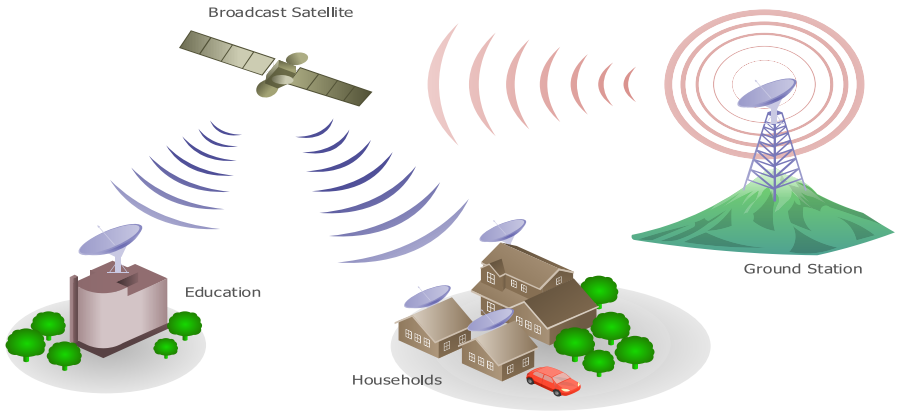

Figure 2.1 Wireless communication medium(Zhang et al., 2016)

One significant benefit of systems is their adaptability and ease. They enable users to communicate nearly any location, freeing them from the limitations of tangible links. This feature makes them especially well-suited for uses like mobile devices and wireless networks, where users require communication while on the move (Tazeb et al., 2019).

2.3 Fifth-Generation Wireless Communication System

The 5th Generation wireless communication technology is a next-generation technology designed to revolutionize wireless networks and meet the evolving demands of modern communication systems. It aims to provide high data rates, low latency, scalability, and seamless connectivity for a wide range of applications and devices (Akyildiz et al., 2016). 5G technology offers several significant advantages, such as excellent data rates, low latency, efficient signal, high spectrum efficiency, improved energy economy, long battery life, and pervasive connectivity (Tazeb et al., 2019).

Key aspects of the 5G Wireless Communication system include:

Diverse Requirements: 5G must support a massive number of low-rate devices, ensure minimal data rate in all circumstances, and enable very low latency data transfer.

Flexibility: The network architecture needs to be flexible to optimize for dynamic scenarios, potentially requiring a hybrid approach for human and machine communications.

Integration of Technologies: 5G integrates wireless and optical access networks to leverage the strengths of both technologies, such as high bandwidth from optical fiber and ubiquitous coverage from wireless networks.

Spectrum Utilization: 5G systems require more spectrum than currently available to achieve data rates on the order of Gbps, leading to considerations of opportunistic spectrum access in various bands.

Candidate Technologies: Technologies like massive MIMO, small cells, waveforms, and optical wireless integration as key components in building and affirming 5G networks.

2.4 The Requirements of 5G Technology

The 5G technology has specific use cases and a vision that requires certain requirements to be met by the future mobile broadband system (ITU-R, 2015) (Alhogbi et al., 2018). Some of the 5G wireless network requirements are as follows.

Peak Data Rate: It denotes the maximum data rate achievable by a mobile station without errors, presuming full utilization of all accessible radio resources for the corresponding connection. The minimum peak data rate is established at 20 Gbps.

Areal Capacity: To cope with the growing demand for wireless data, the 5G RAN needs to have the capacity to enhance its ability to incorporate additional cells within specific regions. This enhancement is anticipated to deliver speeds of up to 10 Mbps per square meter, facilitating the management of the rising mobile data traffic in upcoming times.

Energy Efficiency: To counterbalance the projected 100-fold rise in energy consumption by devices and networks for 5G communication in comparison to 4G, the design of 5G radio access technology needs to prioritize enhanced energy efficiency.

Massive Connectivity: The scope of 5G connectivity extends beyond mobile devices to encompass every device equipped with modem capabilities, facilitating interconnections for purposes such as safety, communication, and enhanced convenience. Projections suggest that 5G will support approximately 10 times more simultaneous Internet of Things (IoT) connections compared to 4G.

Enabling Emerging Technologies: It's anticipated that 5G will play a crucial role in facilitating the rise of technologies such as autonomous vehicles, augmented reality (AR), virtual reality (VR), smart cities, industrial automation, and remote telemedicine. The high speeds, low latency, and massive connectivity of 5G networks support the demands of these advanced applications.

Enhanced Coverage: 5G networks employ various technologies, including small cells, massive MIMO (Multiple Input Multiple Output), and beamforming, to improve coverage and signal strength. This enables reliable connectivity even in crowded areas and remote locations.

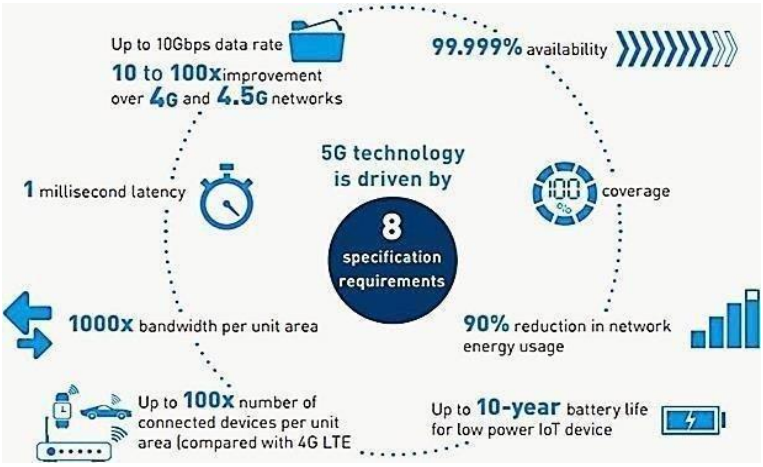

Figure 2.2 Requirements of 5G (Arunachalam et al., 2018)

2.5 The 5G key technologies and techniques

Many new technologies and methods have been developed to align with the implementation of 5G standards. These fresh approaches and technologies will make 5G a highly adaptable and versatile service. The upcoming deployment of 5G wireless communication networks necessitates a significant shift in approach to meet the growing requirements for increased data speeds, reduced network latencies, improved energy efficiency, and consistent

connectivity across various environments (Kamal & Din, 2019). With the imminent introduction of 5G systems, numerous global initiatives and innovative concepts have emerged to address these demands (Akyildiz et al., 2016).

Figure 2.3 The 10 key enabling technologies for 5G (Akyildiz et al., 2016)

Some of the technologies currently being developed for 5G include:

2.5.1Millimeter-Wave communications

Millimeter-wave communication operates at much higher frequencies within the spectrum, allowing for the utilization of a range of new frequency bands and supporting a broad channel bandwidth of up to 2 GHz. However, this presents challenges for handset development, as the typical maximum frequencies and bandwidths are around 2 GHz and 10-20 MHz, respectively. Frequencies above 50 GHz pose complex obstacles for 5G, affecting circuit design, technology, and system utilization due to their limited propagation range, as they are easily absorbed by obstacles. Different countries assign varying frequency spectrums for 5G deployment (Chataut & Akl, 2020).

Millimeter-wave communication is a key technology in 5G networks that enables the delivery of unprecedented data speeds and capacity (Zixuan Wang, 2020). The utilization of Millimeter Wave (mmWave) technology within 5G networks offers a broad spectrum of applications spanning various industries. With its excellent features such as high data speeds, minimal latency, and wide bandwidth, mmWave technology is well-suited for facilitating improved mobile broadband (eMBB) services(Zixuan Wang, 2020).

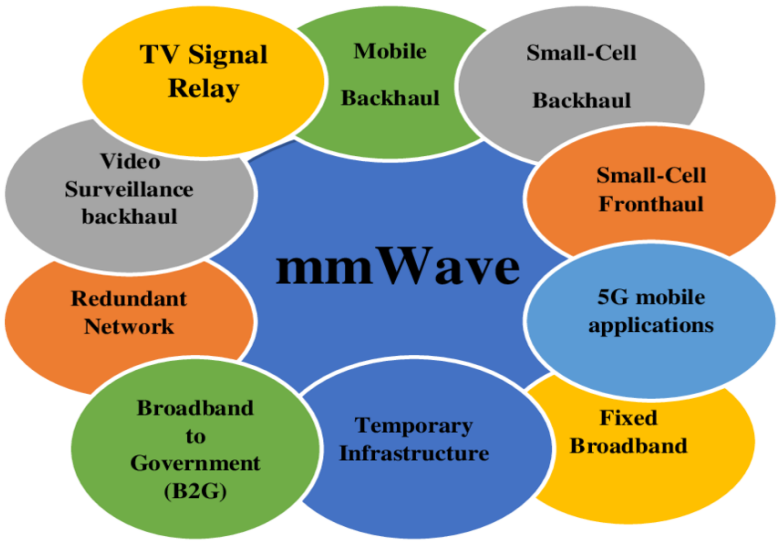

Figure 2.4 MMWave applications and use cases (Saadoon et al., 2022)

2.5.2 Massive Multiple Input and Multiple Output (MIMO)

MIMO systems play a pivotal function in modern wireless networks, being extensively utilized to achieve enhanced efficiency in spectral and energy usage. Before MIMO technology emerged, single-input-single-output systems were prevalent, offering lower throughput and struggling to efficiently support a large user base(Isnawati et al., 2023).

As a result of the increasing demands of users, a variety of innovative MIMO technologies have been developed such as single-user MIMO (SU-MIMO), multi-user MIMO (MU-MIMO), and network MIMO. Consequently, The 5G network is investigating massive MIMO technology as a possible solution to manage the substantial data traffic and growing user base. The advantages of massive MIMO systems have garnered significant attention in various research investigations (Chataut and Akl, 2020).

Massive MIMO is one of the most exciting wireless access technologies for 5G and future networks. It is an evolution of existing MIMO systems in wireless networks. This technology proves adaptable to diverse deployment settings and lays the foundation for forthcoming advancements in wireless communication. Through Massive MIMO, multiple data streams can be transmitted concurrently, boosting system capacity and data transfer speeds. Beamforming directs transmissions to specific users, improving signal strength and expanding coverage.

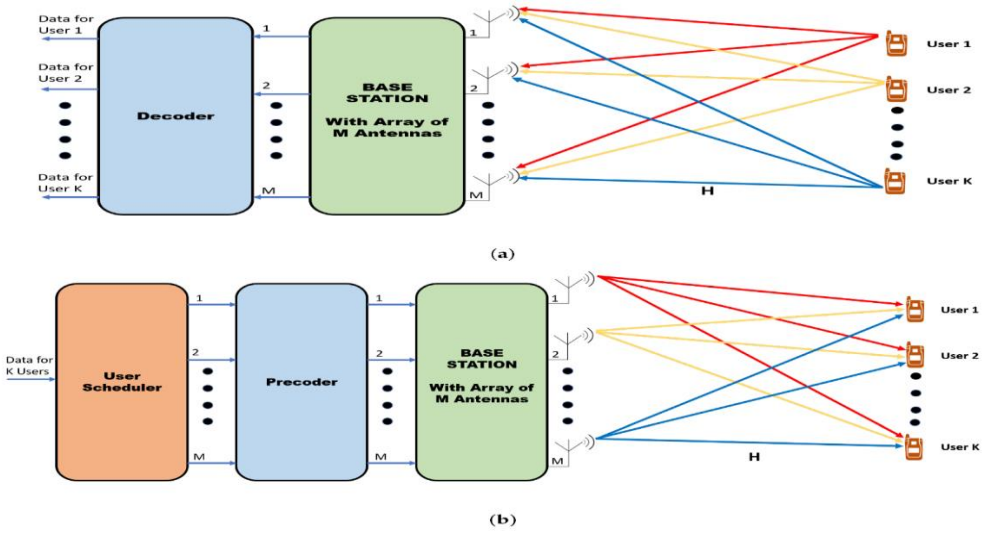

Figure 2.5 Downlink and uplink systems in massive MIMO (Chataut and Akl, 2020)

2.5.3 Network Function Virtualization (NFV)

NFV, which is often used in conjunction with SDN, creates a mutually beneficial relationship. While they are not entirely dependent on one another, using both technologies together offers significant advantages. Network Functions Virtualization (NFV) enables the decoupling of network functions from dedicated hardware devices such as switches and routers, consolidating them on centralized servers (Sharma, 2021). The benefits of NFV include centralized networking, cost savings on hardware, expanded capabilities, reduced power consumption through equipment consolidation, cost efficiency, management of both physical and virtual networks, cloud abstraction, guaranteed network delivery, and more. When NFV is combined with SDN, the resulting network is more versatile, efficient, and cost-effective than traditional hardware-based networks (Sharma, 2021).

2.5.4 Full-Duplex and Green Communication

Full-duplex communication allows for concurrent uplink and downlink transmission within the same frequency band, achieving higher data rates than half-duplex transceivers. Algorithms are employed to mitigate self-interference arising from local antenna transmissions, ensuring acceptable reception quality(Sharma, 2021). Green communication strategies are implemented to reduce energy consumption, especially by base stations that typically consume significant amounts of energy. To enhance energy efficiency, radiofrequency transmit power can be reduced and the transmission of reference signals between base stations and user equipment can be optimized. Service providers can also integrate green energy sources like solar or wind power to reduce the environmental impact of base stations. (Sharma, 2021).

2.6 Modulation in Wireless Communication System

Modulation serves as the process of converting digital data to radio signal waves suitable for transmission over a wireless channel. The process of modulation is a key technique utilized within wireless communication systems for encoding information onto carrier signals for transmission through the airwaves. This technique involves altering specific characteristics of the carrier signal, such as amplitude, frequency, or phase, to signify the data that is being transmitted. Modulation enables efficient and dependable communication by making it possible to transmit data over long distances while simultaneously reducing the impact of noise, interference, and signal degradation (Lu et al., 2014). The focus of this thesis is on 5G enabling technologies, notably modulation techniques for the new air interface. Single-carrier modulations and multi-carrier modulations are the two types of wireless communication systems modulation techniques currently available(Jiang et al., 2016).

2.6.1 Single-carrier Modulations

Single-carrier modulation techniques have a rich historical background and find widespread usage in various wireless communication systems, including traditional 1G, 2G, and 3G systems, as well as the uplink of 4G systems. Single-carrier modulation typically exhibits a lower PAPR than multi-carrier modulation techniques (Jiang et al., 2016). These advantages have led to the continued integration of single-carrier modulation techniques in the 4G standard (Jolania & Sindal, 2023).

However, when compared to multi-carrier modulations, single-carrier modulations exhibit lower effectiveness in handling multipath fading channels, resulting in reduced spectral efficiency. In such scenarios, single-carrier modulation efficiency diminishes as communication system bandwidth expands, leading to shorter symbol intervals and heightened susceptibility to multipath fading. Addressing ISI necessitates the utilization of complex multi-tap equalizers, which in turn escalate system complexity and costs (Jiang et al., 2016).

2.6.2 Multi-carrier Modulations

Multi-carrier modulation splits the total frequency channel into multiple sub-carriers, with the high-speed data stream broken down into multiple lower-speed streams transmitted simultaneously across these sub-carriers. At present, multi-carrier modulation systems are gaining increasing attention for their capability to combat multipath fading. Multi-carrier modulation (MCM) proves to be an effective technique for transmitting data over channels affected by linear distortion. The fundamental concept involves dividing the channel

spectrum into narrowband sub-channels that operate in parallel (Ahmed Solyman & Yahya, 2022). Multi-carrier signaling offers advantages such as simplified equalization, resistance to impulse noise, and flexibility in sub-channel allocation (Hamdar et al., 2023).

Various researchers have explored diverse multi-carrier modulation techniques. In this thesis, we have opted to focus on waveforms that have garnered significant attention from researchers. These waveforms include OFDM, F-OFDM, and FBMC. We analyzed these waveforms using various performance metrics and enhanced the performance of each DWT-based waveform by incorporating the different wavelet families for multi-carrier modulation. The subsequent section presents a review of the relevant literature by different researchers.

2.7 Review of Related Work

Filter Bank Multicarrier Modulation Schemes for Future Mobile Communications is studied by (Nissel et al., 2017). In this study, the authors present a unified framework and discussion for FBMC, evaluate its performance, and compare it with OFDM-based schemes. Parameters like SNR, PSD, Time efficiency, and Throughput are employed as performance metrics to analyze FBMC against OFDM and some of its variants. Performance metrics demonstrate that FBMC facilitates effective coexistence among diverse use cases within the identical frequency band and can be effectively utilized in low-latency transmissions. Even though the results prove that the FBMC is more efficient than OFDM, some performance parameters such as PAPR are not considered. Additionally, the performance of various channel models can also be evaluated.

Wavelet Transform Based MIMO-OFDM application by MATLAB simulation is provided by (Tan et al., 2020). This paper has analyzed the implementation of MIMO-OFDM based on DWT as an alternative to the traditional FFT approach. This implementation involves replacing FFT/IFFT blocks with DWT/IDWT and eliminating the need for Cyclic Prefix (CP) in the transmitter and receiver parts. Comparison of the performance of MIMO-OFDM systems based on FFT and DWT in AWGN and Flat Fading channels. The results of this paper have shown that the DWT-based MIMO-OFDM system is more efficient than the traditional FFT-based system, especially with lower SNR values. However, the study only focused on the lower range of QAM modulation, specifically addressing BER performance. The paper did not consider other crucial metrics essential for demonstrating the performance evaluations of DWT-based OFDM in 5G and beyond communication systems.

The performance of the FBMC system is analyzed by (Wang et al., 2020). In this paper, simulations were conducted to evaluate the Out-of-Band Emission (OOB) and BER

performance of the Filter Bank Multicarrier (FBMC) system, and the results were compared with those of the CP-OFDM system. Various parameters were tested for the FBMC system, including different prototype filters and constellations. The analysis and simulations of the BER performance revealed that both the CP-OFDM and FBMC systems exhibited similar BER performance in an AWGN channel. However, the study didn't consider another channel model with different performance metrics of the system to assess the performance of FBMC over CP-OFDM.

Analysis of PAPR and BER in multicarrier modulation techniques is studied in (Marian Joseph Jeffery et al., 2020). This paper compared three multi-carrier modulation techniques: OFDM, Single Carrier Frequency Division Multiple Access (SC-FDMA), and FBMC. The implementation of FBMC utilizes Poly-Phase Networking (PPN) filter banks, which decompose wideband signals into narrowband signals, thereby reducing the overall system's PAPR. Performance metrics such as SNR, BER, and PAPR have been used to analyze the three modulation techniques across different channel models, including Rayleigh, Rician, and double selective channels. However, the paper does not address how to enhance the weakest aspect of each modulation technique.

Wavelet-based multicarrier modulation technique with PAPR analysis by (Salleh, 2020). The authors analyzed in-depth analysis of the BER and PAPR profiles of multicarrier modulation signals to minimize distortion in high-power amplifiers. Additionally, the studies analyzed using various wavelet families to assess their performance in terms of BER results and evaluate the performance of wavelet-based OFDM systems, such as Wavelet Packet-based OFDM, under different channel conditions and modulation schemes. However, the study didn't consider other metrics, such as PSD with DWT application of OFDM, and the analysis is done within the lower QAM modulation only. The number of performance parameters can be increased, and the channel models might be expanded.

In (Ramakrishnan et al., 2021), the analysis conducted on the FBMC waveform for 5G network-based smart hospitals highlights its suitability as an advanced waveform for such applications. FBMC achieved high spectral performance, making it a strong candidate for the upcoming 5G-centered smart hospitals. Its advantages include a high data rate, absence of spectrum leakage, and reduced sensitivity to frequency errors. This paper presents a comprehensive comparison between OFDM and FBMC modulation techniques.The comparison is conducted based on several performance metrics; BER, Peak Power (PP), PSD, noise-PSD, capacity, and magnitude and phase response. But this paper only considered the two most commonly waveform candidates FBMC and OFDM. Even though the performance

of FBMC has been analyzed for 64-QAM only, the higher order modulation of QAM for more than 64-QAM is not considered.

Analysis of wavelet-based orthogonal frequency division multiplexing (WOFDM) over the LTE 1.25MHz Band is studied by (Sarowa et al., 2020). This paper presented an investigation into the application of wavelet-based OFDM in the context of Long Term Evolution (LTE) systems. The study explores using DWT as an alternative signal analysis technique in high-speed wireless communication, aiming to improve BER performance and system spectral efficiency. The paper also introduced a new way of improving wireless communication systems called wavelet-based OFDM. It shows how using wavelets can make data transmission more efficient and reliable in technologies like LTE. The study included tests with different wavelets to see how they perform regarding error rates. However, the paper didn't consider the effect of wavelet-based OFDM with other performance metrics such as PAPR and PSD with higher order QAM Modulation to better understand its advantages. The impact of the channel model on the wireless communication system within the investigation is also not considered.

The paper (Khan, 2020) examined the performance of three different OFDM-based systems, namely OFDM, W-OFDM, and F-OFDM, using various modulation techniques under Rayleigh fading channel. The study aims to compare these systems in terms of PSD, BER, and SNR. The study has provided some valuable insights into the effects of modulation schemes on SNR and BER. However, it has some limitations such as the lack of context, a limited number of modulation techniques, and the absence of important performance metrics. Furthermore, the conclusion about the superiority of F-OFDM is not credible due to the absence of statistical analysis and inadequate discussion on bandwidth efficiency. The study also lacks the effect of higher-order QAM modulation with other performance metrics.

Performance comparison of multi-carrier communication systems over doubly selective channels is studied (Hasan & Lateef, 2021). This study focused on the comparison of three multi-carrier systems, namely FBMC, F-OFDM, and UFMC, with the widely used OFDM system over a 5G channel. The performance of these systems have been evaluated based on key parameters such as BER, PAPR, and PSD. To ensure a fair comparison, a one-tap frequency domain equalizer have been employed across all multi-carrier systems, and their performance is assessed specifically in the context of 5G channels. The BER performance of the systems was investigated under 5G Vehicular and Pedestrian channel models. Results demonstrate that FBMC exhibits the best BER at high Doppler spreads and the lowest PSD.

However, the performance of the PAPR of FBMC needs some improvement using other signal processing compared to another multi-carrier system. Additionally, the complexity aspect is not addressed.

Filtered-orthogonal wavelet division multiplexing (F-OWDM) technique for 5G and beyond communication systems is provided in (Almutairi & Krishna, 2022). This study introduces a novel modulation technique called F-OWDM replacing fast Fourier transform with wavelet transform as an effective substitute for traditional filtered OFDM for reducing PAPR and BER. The BER and PAPR of the wavelet-F-OFDM system are specifically analyzed when employing wavelets such as Haar, Daubechies, bi-orthogonal, discrete Meyer, and symlet. Additionally, an analysis comparing F-OWDM and conventional filtered OFDM (C-F-OFDM) is presented. However, the authors used lower-order QAM Modulation and the range of comparison can be expanded, incorporating other notable schemes to provide a more comprehensive comparison. Furthermore, An accurate channel model is necessary to precisely assess the performance of the schemes.

The study examines the performance of FBMC-QAM utilizing Hermite filter for 5G Communication and beyond (Dumari et al., 2023). The research presented a comprehensive comparison of different methods of multicarrier modulation, including F-OFDM, WOLA-OFDM, UFMC, and FBMC. This research lies in the evaluation of FBMC employing higher-order QAM with the Hermite filter as a potential solution for wireless communication technology of the 5G systems and provides superior performance of FBMC with Hermite Filter in terms of PSD and BER compared to other modulation techniques, the study highlights the importance of filter design in improving the efficiency and reliability of multicarrier systems. However, the study didn’t consider the effect of the proposed system on the PAPR of the FBMC system.

2.7.1 Research Gap Analysis

The research exhibits a significant gap in addressing crucial performance parameters such as PAPR and Computational Complexity, limiting the comprehensive evaluation of proposed modulation techniques. Moreover, the study's narrow focus solely on lower-range QAM neglects the potential insights higher-order QAM modulation could provide. Essential metrics like PSD and channel models pertinent to real-world scenarios, such as vehicular and pedestrian environments, are overlooked. Neglecting the application of wavelet transform with higher-order QAM modulation further underscores the study's incomplete analysis.

Closing these gaps is essential for advancing the understanding and application of Multicarrier modulation techniques in modern communication systems.

Table 2.1 Contribution and gap of different related works.

Title and Author	Contribution	Gap
FBMC for Future MobileCommunications (Nissel et al., 2017).	Presenting a unified framework and discussion for FBMC, evaluating its performance, and comparing it with OFDM-based schemes.	The study does not consider performance parameters such as PAPR and Computational Complexity.
Wavelet Transform Application Based on MATLAB Simulation (Tan et al., 2020).	The study provides insights into the elimination of the CP and presents a performance comparison between FFT-based and DWT-based MIMO-OFDM systems in AWGN and Flat Fading channels	The study only focused on the lower range of QAM modulation. The paper did not consider other crucial metrics and channel models like vehicular and pedestrian
PAPR and BER Analysis of Multicarrier Modulation Techniques (Marian Joseph Jeffery et al., 2020).	The study implementation of FBMC utilizes Poly-Phase Networking filter banks, which decompose wideband signals into narrowband signals, reducing the overall system's PAPR and BER across Rayleigh, Rician, and Double Selective channels.	The paper does not address how to enhance the weakest aspect of each modulation technique.
Wavelet-Based Multicarrier Modulation Systems with PAPR Analysis (Salleh, 2020).	The studies analyze various wavelet families to assess their performance in terms of BER and PAPR results and evaluate the implementation and performance of wavelet-based OFDM systems, such as Wavelet Packet-based OFDM, under different channel conditions and modulation schemes.	The study didn't consider other metrics, such as PSD with DWT application of OFDM, and the analysis is done within the defined With Lower QAM modulation only.

Analysis of wavelet-based orthogonal frequency division multiplexing (WOFDM) over the LTE 1.25MHz Band is studied by (Sarowa et al., 2020).	The paper also introduces a new way of improving wireless communication systems called wavelet-based OFDM. It shows how using wavelets can make data transmission more efficient and reliable in technologies like LTE.	PAPR and PSD with higher-order QAM Modulation is not considered.
Performance comparison of multi-carrier communication systems over doubly selective channels is studied (Hasan & Lateef, 2021).	This study makes the comparison of three multi-carrier systems, namely FBMC, F-OFDM, and UFMC, and The BER performance of the systems was investigated under 5G Vehicular and Pedestrian channel models.	The performance of the PAPR and PSD of FBMC needs some improvement to make ready for beyond 5G Communication system
Filtered orthogonal wavelet division multiplexing (F OWDM) technique for 5G and beyond communication systems (Almutairi & Krishna, 2022)	This study introduces a novel modulation technique called F-OWDM replacing fast Fourier transform with wavelet transform as an effective substitute for traditional filtered OFDM for reducing the PSD, PAPR, and BER	They didn't consider the effect of wavelet transform with higher-order QAM modulation. An accurate channel model is necessary to precisely assess the performance of the schemes.
Performance of FBMC-QAM utilizing Hermite filter for wireless communication in the 5G Communication and beyond (Dumari et al., 2023).	The study demonstrates the evaluation of FBMC employing higher-order QAM with the Hermite filter as a potential solution for 5G wireless communication systems and provides superior performance of FBMC with Hermite Filter in terms of PSD and BER for Vehicular and Pedestrian Channel.	The study didn't consider the effect of the proposed system on the PAPR which is one of the crucial performance measures to assess the performance of Multicarrier modulation.

CHAPTER THREE

DESIGN AND METHODOLOGY

3.1 Chapter Overview

This chapter primarily focuses on the materials and methods employed in the research, including an overview of multicarrier techniques, system models, multicarrier modulation techniques, the proposed DWT-Multicarrier Modulation, its mathematical models, and the performance metrics used for analyzing the systems.

3.2 Materials

The software tools utilized in this thesis include MATLAB R2022b. MATLAB R2022b is a computational software comprising an Editor for writing code for the entire system.

3.3 Methods

The first step of the research process involves reviewing various literature and identifying any gaps in the existing research. Next, materials that are directly related to the research problem is collected and studied. After analyzing the collected data, a MATLAB code is written on MATLAB R2022b, by understanding the concept. The simulation results are then used to recommend the best solution for the particular and specified case, following the scientific research method.

3.4 Description of the System

Future wireless applications demand higher data rates, but dealing with the fading and uncertain wireless channel becomes challenging at these elevated rates. A potential solution to address the inherent difficulties of the wireless channel and facilitate high-speed communication is the emergence of multi-carrier modulation. At extremely high data rates, single-carrier transmission encounters an issue known as inter-symbol interference (ISI). To overcome this problem, multi-carrier transmission has come to the forefront.

Multi-carrier modulation is a type of FDM, that involves transmitting data throughout numerous restricted bandwidth channels across various frequency ranges. Unlike conventional FDM systems, which segregate sub-carrier signals using guard bands, Multi-carrier modulation segments the entire frequency spectrum into multiple subcarriers. It transmits high-data streams as lower-rate data streams in parallel across these subcarriers. (Tazeb et al., 2019). While each symbol occupies a narrowband frequency range, it is spread over a longer period. As a consequence, this extended symbol duration can lead to the presence of inter-symbol interference (ISI) at the receiver (Dash et al., 2022).

3.5 Wavelet Transform

Wavelet analysis, also known as wavelet transform-based analysis, represents a recent breakthrough in the fields of engineering and communication. It has emerged as a compelling alternative to Fourier analysis due to its distinct capability to examine transient signals characterized by swift alterations. Unlike Fourier analysis, which focuses solely on frequency domain analysis, wavelet analysis allows for simultaneous analysis of signals in both the time and frequency domains. This makes wavelets particularly effective in examining periodic and noisy signals, as they provide insights into their characteristics and behavior at different scales (Almutairi & Krishna, 2022).

Every wavelet family comprises two fundamental functions: the mother wavelet (ψ(t)) and the scaling function (φ(t)), illustrated in equations (3.1) and (3.2), respectively. Consequently, the discrete scaling and translation of ψ(t) can be depicted as shown in Equation (3.3) (Almutairi & Krishna, 2022):

$$\psi(t) = 2^{j/2}\psi(2^j \mathrm{t}) \tag{3.1}$$

$$\phi(t) = 2^{j/2}\ \phi(2^j t) \tag{3.2}$$

$$\psi_{j,k}(t) = \frac{1}{S_O^j}\psi\ \ (\frac{t - kt_0 S_0^j}{S_0^j}) \tag{3.3}$$

Where j and k represent integers denoting the scale and translation indices, respectively, with $S_0 > 1$ serving as a constant dilation step, and τ_0 as the translation factor. The scaling and wavelet functions can be represented as a weighted sum of scaling functions shifted in time, depicted in Equations (3.8) and (3.9)(Almutairi & Krishna, 2022):

$$\phi(t) = \sum_m g(m)\sqrt{2}\ \ \phi(2t - m) \tag{3.4}$$

$$\psi(t) = \sum_m h(m)\sqrt{2}\,\phi(2t - m) \tag{3.5}$$

Where $g(m)$ denotes the coefficients of the scaling filter and $h(m)$ denotes the coefficient of the wavelet. After the translation and scaling of the time variable in (3.4) then it can be represented as in (3.6) (Almutairi & Krishna, 2022).

$$\begin{aligned}\phi(2^j t - k) &= \sum g(m)\sqrt{2}\ \ \phi(2\left(2^j - k\right) - m) \\ &= \ \sum g(m)\sqrt{2}\ \ \phi(2^{j+1}t - 2k - m)\end{aligned} \tag{3.6}$$

Let n = 2k+m and then the equation (3.6) can be represented as in (3.7)

$$\phi\left(2^{j}t-k\right)=\sum_{m} g(n-2k)\sqrt{2}\,\phi\left(2^{j+1}t-n\right) \tag{3.7}$$

Using these functions, a whole part of signals is represented in (3.8) (Almutairi & Krishna, 2022):

$$f(t)=\sum_{k} c_j(k)2^{j/2}\phi\left(2^{j}t-k\right)+\sum_{k} d_j(k)2^{j/2}\psi(2^{j}t-k) \tag{3.8}$$

Within Equation (3.8), the initial sum provides a coarse approximation (approximation coefficient) of the function, while the subsequent sum yields a detailed coefficient:

$$c_j(k)=\langle f(t),\phi_{j,k}(t)\rangle=\int f(t)\phi_{j,k}(t)dt \tag{3.10}$$

From this approximate coefficient is written as:

$$c_j(k)=\int f(t)2^{j/2}\sum_{n} g(n-2k)\sqrt{2}\,\phi\left(2^{j+1}t-m\right)dt \tag{3.11}$$

$$c_j(k)=\sum_{n} g(n-2k)\int g(t)2^{(j+1)/2}\,\phi\left(2^{j+1}t-m\right)dt \tag{3.12}$$

$$=\ \sum_{n} g(n-2k)c_{j+1}(m) \tag{3.13}$$

Similarly for wavelet coefficient:

$$d_j(k)=\sum_{n} h(n-2k)c_{j+1}(n) \tag{3.14}$$

From (3.12) and (3.13), It's evident that DWT values are determined by calculating the weighted sum of DWT coefficients at a larger scale(j+1).

The wavelet analysis process involves two fundamental operations: decomposition, which is performed using the discrete wavelet transform (DWT), and reconstruction, which is achieved through the inverse discrete wavelet transform (IDWT) (Almutairi & Krishna, 2022).

Discrete Wavelet Transform (DWT): The process of decomposing a signal through filtering and downsampling procedures is referred to as the DWT. Given a signal with a length of N, the Discrete wavelet transform comprises Log_2 (N) levels.

At every level, there's a sequence of filtering and sub-sampling steps referred to as decimation. During each step, the signal being input is broken down into a pair of coefficients: the approximate coefficients ($c_j(k)$) and detailed coefficients ($d_j(k)$)(Almutairi & Krishna, 2022). A thorough explanation of the overall representation of decomposition coefficients is given in (3.12) and (3.13)

Inverse Discrete Wavelet Transform (IDWT): The procedure of restoring the initial signal derived from the scaling and wavelet coefficients is widely referred to as the IDWT or the reconstruction process. This reconstruction is accomplished via a sequence of actions, which include upsampling and successive filtering (Almutairi & Krishna, 2022).

$$f(t) = \sum_k c_j(k) 2^{j/2} \left[\sum_m g(m) \sqrt{2}\, \phi\left(2^{j+1} t - 2k - m\right) \right] + \sum_k d_j(k) 2^{j/2} \left[\sum_m h(m) \sqrt{2} \psi\left(2^{j+1} t - 2k - m\right) \right] \quad (3.14)$$

Then, multiplying (3.14) by $\phi\left(2^{j+1} t - 2k\right)$and Performing the integral yields the reconstruction coefficient as in (3.19)(Almutairi & Krishna, 2022):

$$c_{j+1}(k) = \sum_n c_j(n) g(k - 2n) + \sum_n d_j(n) h(k - 2m) \quad (3.15)$$

3.5.1 Wavelet Family

The selection of wavelet functions is determined by the specific application. In this study, five distinct wavelet families were employed for the analysis, and a concise explanation of each family is explained.

1. *Haar wavelet:* The Haar wavelet is a mathematical function used in signal processing and image analysis. It is one of the simplest and most widely used wavelet functions. The *Haar wavelet* is known for its memory efficiency and its ability to preserve the energy of a signal. The mother *haar* wavelet and the *haar* scaling function are presented in;

$$\psi(t) = \begin{cases} 1, & for \;\; 0 \le t < 1/2, \\ -1, & for \frac{1}{2} \le t < 1, \\ 0 & otherwise \end{cases}$$

$$\phi(t) = \begin{cases} 1, & for \;\; 0 \le t < 1 \\ 0, & otherwise \end{cases}$$

It is a type of wavelet that exhibits a distinctive characteristic: it is discontinuous and shares similarities with the step function.

2. Dmey wavelet: The discrete Meyer wavelet, which will be referred to as "dmey" from here on, is an approximation of the Meyer wavelet that is based on a finite impulse response (FIR) filter.

3. Daubechies wavelet: The Daubechies wavelets are wavelets that possess orthogonality and biorthogonality properties. They are commonly denoted as dbN, where N represents the order of the wavelet family.

4. Biorthogonal wavelet: Biorthogonal wavelets are an expanded version of orthogonal wavelet systems that offer increased flexibility and ease of design. They utilize two separate wavelet functions and two scaling functions, with one set dedicated to the decomposition process and the other set specifically used for the reconstruction operation.

5. Symlet wavelets: denoted as symN, are a specific type of wavelet known as least-asymmetric wavelets. They are distinguished by possessing the greatest number of vanishing moments among the Daubechies wavelet family. Daubechies introduced modifications to the original dbN wavelets to achieve symmetry and simplicity in the symlet wavelets.

3.6 Multicarrier Modulation Techniques Model for 5G

Multicarrier modulation (MCM) represents a telecommunications method employed for transmitting data across numerous carrier frequencies. MCM operates by segmenting the spectral range into multiple subcarriers, with each subcarrier responsible for carrying a portion of the overall data. This approach enables more efficient utilization of the available bandwidth, as different subcarriers can be allocated to separate users or data streams (Tazeb et al., 2019).The development of multicarrier modulation methods relies on factors such as spectral containment characteristics, hardware limitations, and the properties of the propagation channel. F-OFDM, UFMC, WOLA-OFDM, FBMC/OQAM, and FBMC/QAM are the expected future-generation modulation techniques.

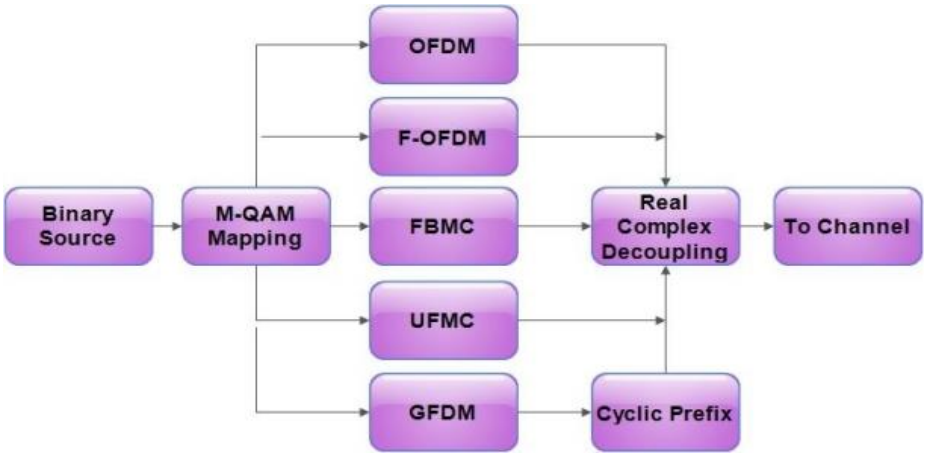

Figure 3.1 Figure of different multicarrier modulation schemes(Shaik & Malik, 2021)

To overcome issues arising from frequency-based disruptions, broadband channels are divided into several subchannels with consistent frequencies and reduced or no interference. This simplifies the equalization process, which relies on single-tap equalizers. The equalization process is crucial for symbol detection through maximum likelihood estimation under Gaussian noise conditions (Shaik & Malik, 2021).

3.6.1 Orthogonal Filter Division Multiplexing (OFDM)

OFDM is a widely utilized multi-carrier modulation technique that plays a prominent role in wireless communication. The OFDM multicarrier modulation is used in current 4G technology. OFDM disperses the available spectrum across numerous subcarriers, where every subcarrier is subjected to modulation by a data signal flow towards maximize bandwidth usage.

Mathematical representation of the OFDM signal, resulting from the modulation of N sub-carriers, can be represented as in (Dumari et al., 2023):

$$s(t) = \sum_{n=0}^{N-1} d_n e^{j2\Pi f_n t} \quad \text{for,} \quad 0 \leq t \leq T_s \tag{3.16}$$

Where d_n represents the intricate data representation, which modulates the N^{th} sub-carrier within the modulation timeframe, and T_s indicates the temporal extent of OFDM symbols.

The subcarrier's orthogonality is guaranteed, in case the separation among neighboring sub-carrier frequencies is identical and sub-carriers are located as in (Tazeb et al., 2019):

$$f_n = \frac{n}{T_s} \quad for = 0,1,2,\ldots,N-1 \tag{3.17}$$

The received signal r(t), derived after radio frequency conversion at the output of the channel, is derived from the convolution of s(t) with the channel impulse response h(t), followed by the addition of a noise signal w(t), as expressed by the equation (3.18) (Tazeb et al., 2019):

$$r(t) = \int_{\infty}^{\infty} s(t-\tau)h(\tau,t)d\tau + \omega(t) \tag{3.18}$$

The discrete-time representation of the received signal with noise is represented as follows (Tazeb et al., 2019):

$$r[n] = h[n] * s[n] + \omega[n]$$
$$= \sum_{u=0}^{T-1} h[\tau]s[n-\tau_u] + \omega[n] \tag{3.19}$$

But the General, the time domain representation OFDM is represented as (Dumari et al., 2023):

$$X_{OFDM} = \frac{1}{\sqrt{N}} \sum_{k=0}^{N-1} x_k \quad x \quad \Pi \quad (t) \quad x \quad e^{-j2\Pi f_k t} \quad \text{for,} \quad \text{n} = 0,1,2,\ldots,\text{N-1,} \tag{3.20}$$

Where x_k denotes the complex symbol derived from a specific constellation, Π (t) symbolizes the filter with a waveform, and N indicates the number of subcarriers. Figure 3.2 shows the Basic block diagram of the OFDM transmitter and receiver part.

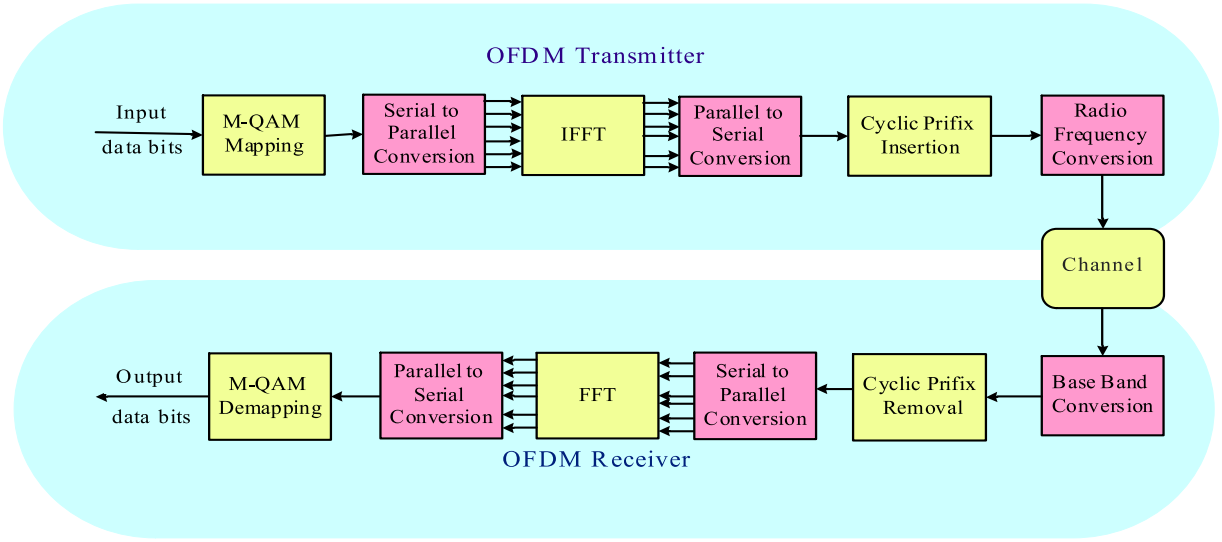

Figure 3.2 Basic block diagram of OFDM system (Dumari et al., 2023)

Figure 3.2 shows the process of mapping digital data to complex symbols utilizing QAM modulation. These entities are then transformed into N streams, each aligned with a subcarrier frequency, via a serial-to-parallel converter. The modulation scheme employs a cyclic prefix to mitigate interference between symbols, but this comes at the cost of reduced spectral efficiency (Dumari et al., 2023). OFDM uses IFFT and FFT blocks in both the Transmitter and Receiver, respectively. CP is added at the transmitter of OFDM and removed at the receiver. It is employed to avoid inter-symbol interference (ISI).

3.6.2 Filtered Orthogonal Frequency Division Multiplexing (F-OFDM)

F-OFDM is a multi-carrier modulation technique that addresses the limitations of OFDM by introducing a filtering operation. In the case of filtered-OFDM modulation, filtering was carried out following the IFFT block at the transmitter to reduce the OOB and thereby minimize the interference among neighboring signals. Filtering plays a crucial role in mitigating side lobe leakage. Filtered OFDM employs multicarrier modulation which incorporates filtering to tackle the drawbacks of OFDM (Ramadhan, 2019). Subsequently, the time-domain signal will be appended with a cyclic prefix of length L*cp*, followed by the application of filter *fi* with a length of L*f*. The basic block diagram of F-OFDM is shown in Figure 3.3

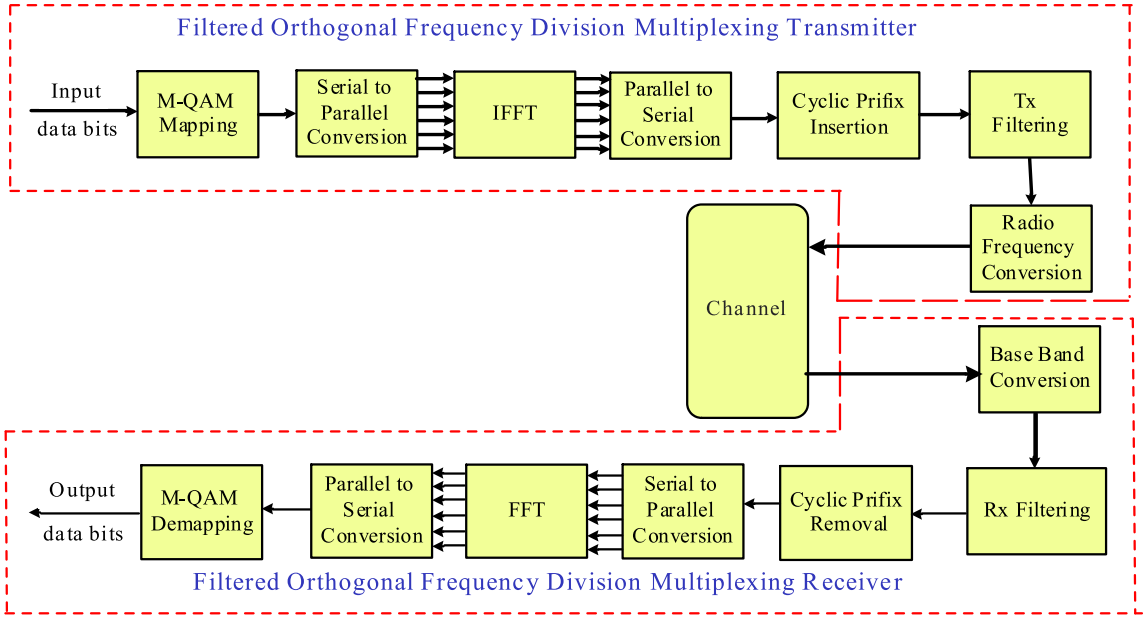

Figure 3.3 Basic block diagram of filtered OFDM system (Dumari et al., 2023)

Figure 3.3 depicts a filter implemented on the signal generated by the CP-OFDM techniques just before transmission. As the signal is in the time domain, the filter is also constructed in the time domain. In the F-OFDM system, a filter is employed across all subcarriers simultaneously. Symbols containing the message are modulated using QAM in the F-OFDM scheme. These encoded symbols from each sub-band are subsequently inputted into N-point IFFT blocks to produce the signal modulated in the time domain, which consists of N samples in length (Dumari et al., 2023). The mathematical representation in the time domain for F-OFDM is presented as (Dumari et al., 2023):

$$X_{F-OFDM} = \frac{1}{\sqrt{N}} \sum_{n=0}^{N-1} x_k \;\; x \;\; f(n) \;\; x \;\; e^{-(j2n\Pi m/N)} \qquad (3.21)$$

Where, *f (n) = P (n). W (n)*, for n = 0,1,2,…, N-1 and x_k represents the complex symbols originating from a specific constellation, f(n) signifies the prototype filter, *P (n)* indicates the ideal bandpass filter, *W (n)* stands for the Hanning Window, and N represents the number of subcarriers. F-OFDM adopts a comparable signal receiver process to a variation of the CP-OFDM modulation scheme, except for an additional step for inverse filtering. (Ahmed et al., 2022).

3.6.3 Filter Bank Multicarrier with offset Quadrature Amplitude Modulation (FBMC/OQAM).

FBMC represents another multi-carrier modulation scheme and stands as a prospective contender for the physical layer of 5G and subsequent generations. To mitigate out-of-band (OOB) spectrum emissions, FBMC applies filtering to each subcarrier. This is achieved by utilizing a filter bank that divides the signal into several sub-bands, each of which is modulated by a separate carrier. FBMC-OQAM, specifically, employs real-valued symbol transmission and reception, involving pre-processing and post-processing stages to convert between complex and real values using OQAM (Abdel-Atty et al., 2020).

The FBMC/OQAM block diagram is illustrated in Figure 3.4.

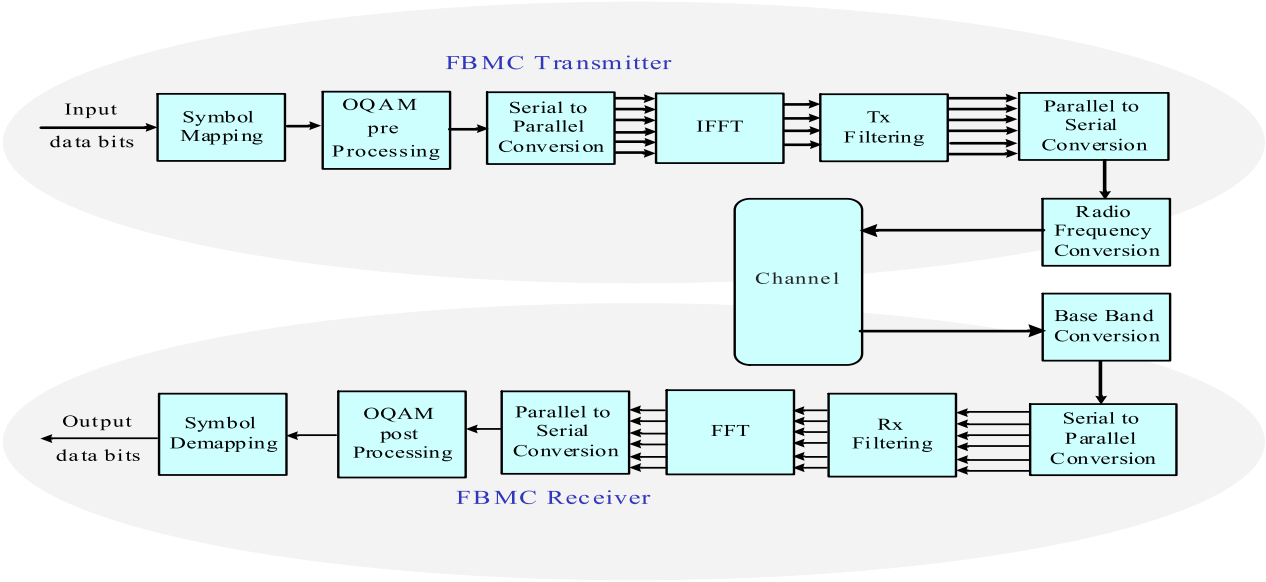

Figure 3.4 Block diagram of FBMC/OQAM system (Jeon et al., 2016)

In FBMC-OQAM, the orthogonality of the subcarriers is preserved through the waveform of the prototype filter and the inherent detection of real values characteristic of OQAM.

Significantly, both the real and imaginary parts of complex data are conveyed through a singular prototype filter, known as PHYDYAS within this context.

The mathematical representation of the signal being transmitted in a discrete-time FBMC-OQAM system is given by (Dumari et al., 2023) as follows:

$$s(n) = \sum_{-\infty}^{\infty} \sum_{m=0}^{M-1} d_{m,k}\theta_{m,k} \;\; f[n - k\tfrac{M}{2}]e^{j2/Mm(n-D)}, \qquad (3.22)$$

Where n denotes the temporal indicator, m denotes the frequency sub-band identifier, k denotes the symbol identifier, $d_{m,k}$ denotes the symbol with real values, M represents the total quantity of subcarriers, and *f(n)* signifies the composite IR. The symbol $d_{m,k}$ is mapped to the space of signals. Additionally, $\theta_{m,k}$ = j^{k+m} introduces an extra phase term. The filter delay, represented by D, is responsible for creating a causal prototype filter f(n) and is determined by D = (L − 1)/2, where L is the length of the filter. (Dumari et al., 2023).

Over multi-path fading channel $h[n]$ and Additive White Gaussian Noise (AWGN) $w[n]$, the received signal is given by as in (Jeon et al., 2016).

$$y[n] = h[n] * s[n] + \omega[n] \quad = \quad \sum_{u=0}^{T-1} h[\tau]s[n - \tau_u] + \omega[n] \qquad (3.23)$$

where τ_u is the multi-path delay and *T* is the number of multi-path delays.

3.6.4 Filter Bank Multicarrier with Quadrature Amplitude Modulation (FBMC/QAM)

FBMC-QAM utilizes two separate prototype filters, known as even and odd filters, which are specifically designated to transmit complex symbols over even-numbered and odd-numbered subcarriers, respectively. The perpendicularity of FBMC-QAM is preserved by the waveform properties of these two standard filters. In terms of the discrete-time baseband model, the modulation signal at the transmitter end can be mathematically represented as. (Jeon et al., 2016).

$$s(n) = \sum_{\infty}^{\infty}(\sum_{p} a_{p,k}g^{e}[n - kM]e^{j\frac{2\pi}{M}m(n-D)} + \sum_{p} a_{p,k}g^{o}[n - kM]e^{j\frac{2\pi}{M}m(n-D)}) \qquad (3.24)$$

Where $g^{e}[n]$ represents an even filter, $g^{o}[n]$ represents an odd filter, and $a_{p,k}$ expresses a complex data symbol using the QAM constellation.

For the ideal channel, the even symbol after demodulation at the receiver *m* sub-carrier at the k_0 time point can be depicted as in (Jeon et al., 2016).

$$a_{p',k'}^{even} = \sum_{n=-\infty}^{\infty} \sum_{k=-\infty}^{\infty} \left(\sum_{p} a_{p,k}\, g_{p,k}^{e} g_{p',k'}^{e*} + \sum_{q} a_{p,k} g_{p,k}^{o} g_{p',k'}^{o*} \right)$$

$$= a_{p',k'} + \sum_{k \neq k'} \left(\sum_{p \neq p'} a_{p,k} g_{p,k}^{e}\, g_{p',k'}^{e*} + \sum_{q} a_{p,k} g_{p,k}^{o} g_{p',k'}^{o*} \right) \quad (3.25)$$

In an optimal channel, the odd symbol after demodulation at the receiver m_0 sub-carrier at k_0 the moment in time can be described as in (Jeon et al., 2016).

$$a_{p',k'}^{odd} = \sum_{n=-\infty}^{\infty} \sum_{k=-\infty}^{\infty} \left(\sum_{p} a_{p,k}\, g_{p,k}^{o} g_{p',k'}^{o*} + \sum_{q} a_{p,k} g_{p,k}^{e} g_{p',k'}^{e*} \right)$$

$$= a_{p',k'} + \sum_{k \neq k'} \left(\sum_{p \neq p'} a_{p,k} g_{p,k}^{o}\, g_{p',k'}^{o*} + \sum_{q} a_{p,k} g_{p,k}^{e} g_{p',k'}^{e*} \right) \quad (3.26)$$

Where, $g_{p,k}^{e}[n] = g^{e}[n - kM] e^{j\frac{2\pi}{M} m(n-D)}$ *and* $g_{p,k}^{e}[n] = g^{o}[n - kM] o^{j\frac{2\pi}{M} m(n-D)}$

The existing system utilizes the PHYDYAS filter as the prototype filter.

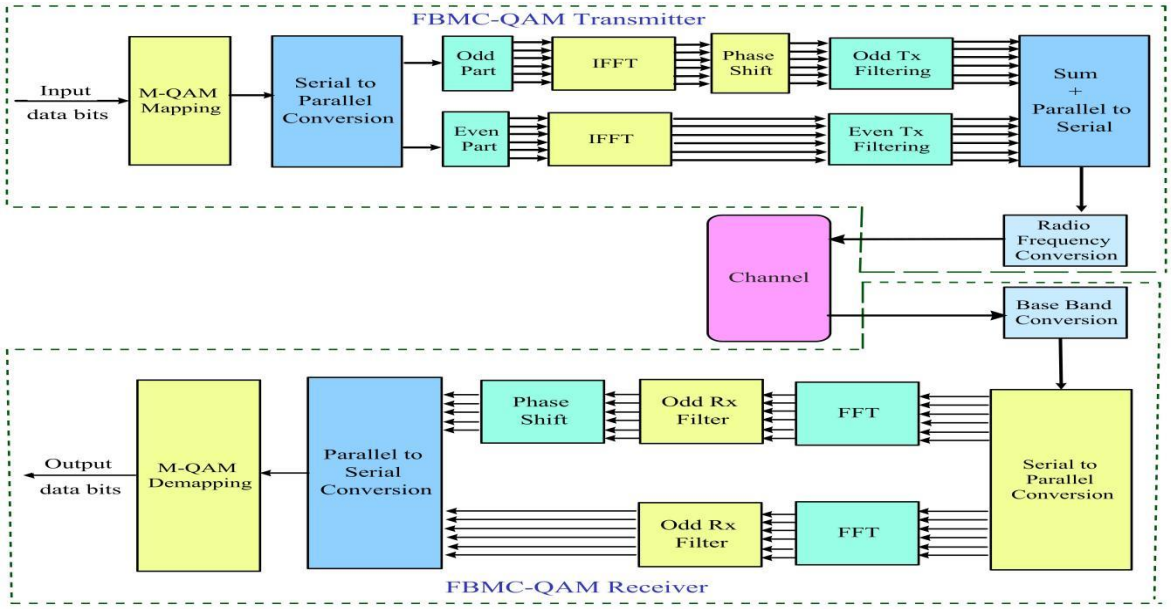

Figure 3.5 Block diagram for FBMC-QAM (Dumari et al., 2023)

3.7 Proposed Discrete Wavelet Transform-Based Multicarrier Modulation Techniques.

The compatibility of DWT-based Multicarrier Modulation technology with future 5G applications has hardly been studied.

Therefore, this study examined the advantages of DWT-based Multicarrier Modulation for 5G and future applications. In a wavelet-based Multicarrier Modulation (MCM) system, each subcarrier exhibits distinct time and frequency resolutions. This system utilizes a filter bank, as opposed to a Fourier transform, for the generation of orthogonal subcarriers.

We made a DWT-based performance analysis for the most important schemes; thus DWT DWT-based OFDM, DWT-based F-OFDM, and DWT-based FBMC-OQAM and DWT-based FBMC-QAM with their performance metrics. we can observe that three commonly used multicarrier schemes will be selected for testing purposes. The selected schemes will involve the use of IDWT in the transmitter and DWT in the receiver.

3.7.1 Discrete Wavelet Transform Based Orthogonal Frequency Division Multiplexing (DWT-OFDM)

In the case of the OFDM transmitter, the IDWT will be applied instead of the IFFT and no cyclic prefix will be required. In the receiver section, the DWT will be applied instead of the FFT block. Since no cyclic prefix is added at the transmitter, no cyclic prefix removal at the receiver part. The proposed block diagram of the DWT-OFDM techniques is shown in Figure 3.6.

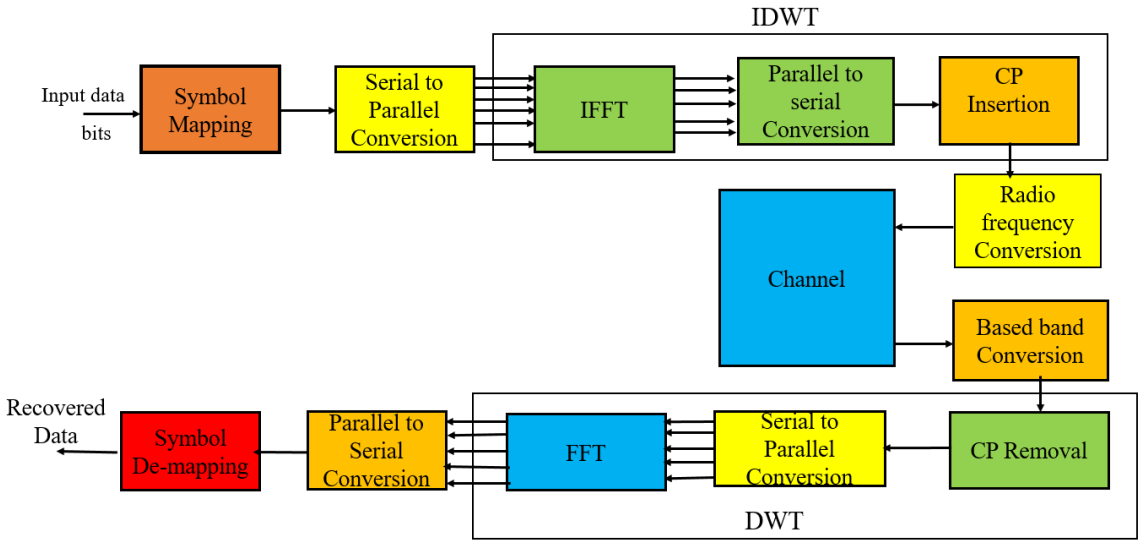

Figure 3.6 Block diagram of the DWT-OFDM system

To derive finite numbers of scales, the scaling function $\phi\,(t)$ is employed. Consequently, the IDWT-OFDM symbol can be interpreted as the weighted sum of Wavelet and scale carriers, as mathematically expressed in the equation (3.27):

$$S(t) = \sum_{j,k} W_{j,k}(t) * \psi_{j,k}(t) + \sum_{k} a_{j,k} * \phi_{j,k}(t) \quad (3.27)$$

Where, $W_{j,k}$ are sequences of wavelets

$a_{j,k}$ are approximation coefficients

The Discrete wavelet Transform based Orthogonal Frequency Division Multiplexing (DWT-OFDM) output is expressed as:

$$X(t) = \left[\left(\sum_{n=0}^{N_s} C_k \, \psi(t - nT_s)\right)\right], \quad (3.28)$$

where *Ck* and *Ts* are complex depictions of the subcarrier symbols and duration of a symbol. Conversely, the inverse process is simulated in the receiver using DWT. The signal undergoes processing before being directed to the demodulator for data recovery. The implementation of OFDM based on DWT is achieved by simply replacing the Fast Fourier Transform (FFT)/Inverse Fast Fourier Transform (IFFT) blocks with DWT/IDWT and eliminating the Cyclic Prefix (CP) insertion and removal in the transmitter and receiver sections, respectively.

3.7.2 Discrete Wavelet Transform-Based Filtered Orthogonal Frequency Division Multiplexing (DWT-F-OFDM)

For F-OFDM, the IDWT will be applied in place of the IFFT, and the use of a cyclic prefix will be omitted. However, transmitter filtering will be employed before signal transmission and Receiver filtering after the signal is recovered from the channel.

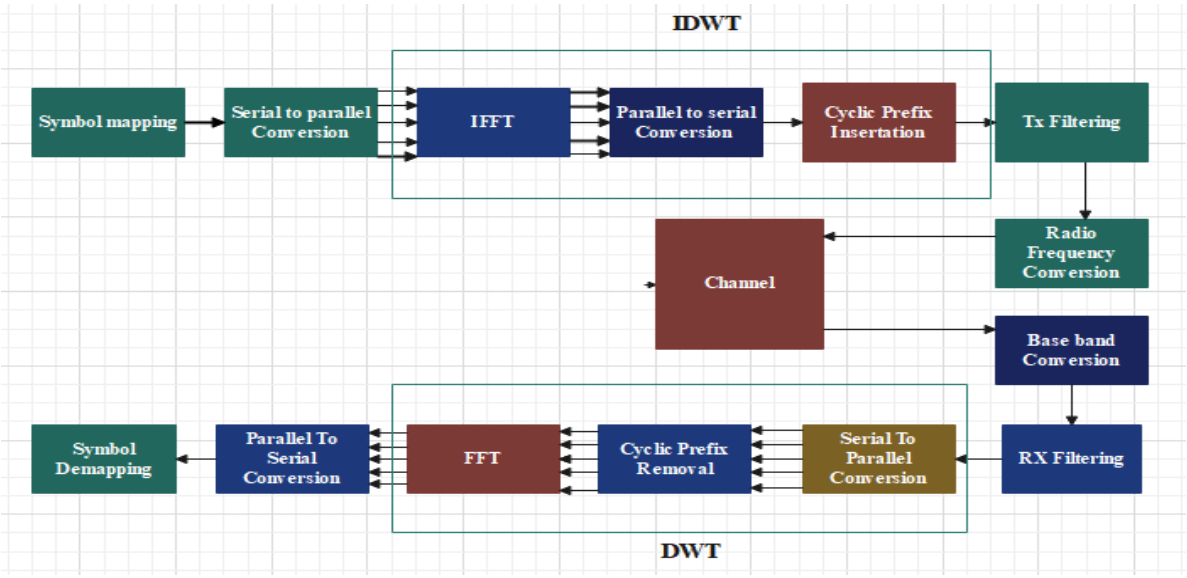

Figure 3.7 Block diagram of the DWT-F-OFDM system

DWT-F-OFDM is a Multicarrier Modulation system based on the wavelet basis, the carriers are expressed and characterized by the wavelet functions.$\psi_{j,k}(t)$, where [j ∈ J0, J – 1], k ∈ [0, 2j-1] and the scaling functions ($\phi_{J0,k}$) (Almutairi & Krishna, 2022).

At the transmitter side, the data can be represented in vector form as $\boldsymbol{b} = [b_1; b_2; \dots; b_B] \in C^{M\times 1}$ where b_k is the signal transmitted in the kth sub-band as represented in (3.25) (Almutairi & Krishna, 2022):

$$b_k = [b_k(1), b_k(2), \dots, b_k\big(M_{B)}\big]^T \in C^{M_B\times 1} \tag{3.29}$$

Within the IDWT block, the QAM modulated signal undergoes up-sampling by a factor of 2 and subsequent convolution with the synthesis Low Pass Filter coefficient, as mathematically expressed in (Almutairi & Krishna, 2022). Subsequently, the results from the HPF and LPF branches are combined and then filtered through a filter f_i with a length of L. The advantage of utilizing Wavelet Transform (WT) lies in the wavelet properties' overlapping nature, which helps maintain the orthogonality of the resulting IDWT signal at the transmitter.

Therefore, in DWT-F-OFDM, there is no need for a Cyclic Prefix (CP) to address the loss of orthogonality caused by time dispersion effects. At the Receiver, the modulation steps are reversed to operate the initial data. Previously, for information retrieval, the received signal undergoes filtering through a matched filter to counteract the channel effects. The processed signal is subsequently fed into DWT operation at the receiver.

3.7.3 Discrete Wavelet Transform-Based Filter Bank Multicarrier with offset Quadrature Amplitude Modulation (FBMC/OQAM).

FBMC/OQAM employs a filter bank to partition the signal into numerous subgroups, each of which is modulated by an individual carrier. To use the IDWT instead of the IFFT in the FBMC-OQAM system, the requirement is to represent the signal using wavelet coefficients instead of Fourier coefficients. To express the signal in terms of wavelet coefficients and then apply the IDWT using the appropriate wavelet functions to reconstruct the transmitted signal in the FBMC-OQAM system. The proposed block diagram of the DWT-FBMC-OQAM techniques is shown in Figure 3.8.

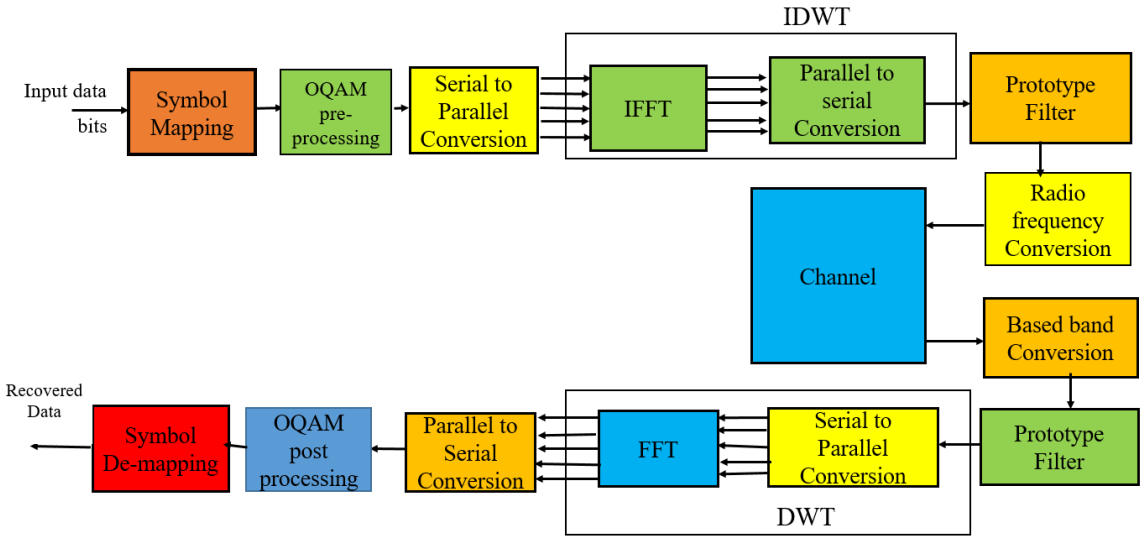

Figure 3.8 Block diagram of the DWT-FBMC-OQAM system

To obtain the wavelet DWT coefficient, we decompose the FBMC-OQAM transmitted signal $s(n)$ into its wavelet coefficients:

$$c(m,k) = \sum_{k}^{M-1} s(n)\,\psi_{m,k}(n) \tag{3.30}$$

Where; s(n) is the model in discrete time, the signal at the transmitting side is represented in equation (3.22), and $\psi_{m,k}(n)$ represents the wavelet function at scale 'm' and translation 'k'.

The IDWT equation for the FBMC-OQAM system transmitted signal can then be written as in (3.16):

$$\hat{s}(n) = \sum_{m=-\infty}^{\infty} \sum_{k=0}^{M-1} c(m,k)\phi_{m,k}\,(n) \tag{3.31}$$

Where; $\hat{s}(n)$ is the IDWT transmitted signal, $c(m,k)$ is the wavelet coefficients, and $\phi_{m,k}(n)$ represents the scale function at scale 'm' and translation 'k'. The wavelet function $\psi_{m,k}(n)$ should be chosen based on the specific wavelet family and properties suitable for the FBMC-OQAM system. In DWT-FBMC/OQAM, it is common to have complex-valued coefficients even if the input signal is real-valued.

3.7.4 Discrete Wavelet Transform-Based Filter Bank Multicarrier with Quadrature Amplitude Modulation (FBMC/QAM).

To utilize the IDWT and DWT instead of the IFFT and FFT in the FBMC-QAM system, we need to express the FBMC-QAM signal in terms of wavelet transforms. The process involves the reconstruction using IDWT at the transmitter and then decomposition using DWT at the receiver. The input data symbols are converted into the FBMC-QAM signal represented temporally, utilizing the Discrete Wavelet Transform (DWT) coefficients. Next, the FBMC-QAM signal is convolved with the even and odd filters *ge*[*n*] and *go*[*n*] respectively, for proper shaping. Lastly, the IDWT is applied to decompose the filtered signal into its respective wavelet coefficients, preparing it for transmission.

To obtain the wavelet DWT coefficient, we decompose the FBMC-QAM transmitted signal *s*(n) into its wavelet coefficients:

$$c(j,k) = \sum_{n=0}^{N-1} s(n).\psi_{j,k(n)} \tag{3.32}$$

Where; s(n) is the discrete-time model, FBMC-QAM signal at the transmitter side which is represented in equation (3.24), and $\psi_{m,k}(n)$ represents the wavelet function at scale 'j' and translation 'k'. To obtain the equation for the IDWT signal ready to be processed with prototype filters, we need to apply the IDWT to the transmitted signal expressed in terms of wavelet coefficients. The IDWT reconstructs the original signal from its wavelet coefficients and is given in (3.29):

$$\hat{s}(n) = \sum_{j}\sum_{k} c(j,k)\phi_{j,k}(n) \tag{3.33}$$

Where; $\hat{s}(n)$ is the IDWT transmitted signal, $c(j,k)$ is the wavelet coefficients, and $\phi_{j,k}(n)$ represents the scale function at scale 'j' and translation 'k'.

To demodulate the even and odd symbols at the receiver using DWT in the FBMC-QAM system, we Convolve the reconstructed FBMC-QAM signal $\hat{s}(n)$ with the even and odd filters *ge*[*n*] and *go*[*n*] respectively to extract the even and odd components:

$$\widehat{s_e}(n) = \hat{s}(n) * g^e[n] \tag{3.34}$$

$$\widehat{s_o}(n) = \hat{s}(n) * g^o[n] \tag{3.35}$$

In this study, we employed a PHYDYAS Filter as a PF in both the transmitter and receiver, serving as even and odd filters, to analyze the bit error performance of FBMC-QAM.

3.8 Performance Metrics

This thesis mainly centers on evaluating the efficiency of multi-carrier modulation methods employing higher-order QAM through diverse performance measures such as Spectral Efficiency, power spectral density (PSD), Peak to peak-to-average power ratio, bit error rate, and Computational Complexity. This section elaborates on the fundamental concept of each performance metric intended for assessment.

3.8.1 Power Spectral Density

Power spectral density (PSD) is a measure of power expressed in dB, normalized to frequency. It serves as a crucial indicator in evaluating the a system's spectral efficiency given waveform technique. PSD is a critical indicator that signifies out of band the level of radiation and the capacity of a waveform to recycle the spectrum and facilitate the coexistence of various services. A lower out-of-band enables users to access the network in an asynchronous mode and to incarnate high mobility.

The PSD of the multicarrier modulation techniques is expressed as:

$$PSD_{MCM}(f) = \frac{1}{T_u}\sum_{k=0}^{N-1}|X_k|^2\delta(f - fk) \tag{3.36}$$

Where T_u is the sysmbol duration, xk is the complex symbol on the k-th subcarrier. δ is the dirac delta function and fk is the frequency of the k -th subcarrier.

3.8.2 Peak to Average Power Ratio

In multicarrier modulation, data is transmitted over multiple subcarriers simultaneously. Each subcarrier is modulated with a lower symbol rate, which helps mitigate the effects of frequency-selective fading channels. The PAPR of Multicarrier Modulation is defined as a measure of the maximum power level relative to the average power level in the transmitted signal.

Mathematically, the PAPR is defined as the ratio of the peak power to the average power of the transmitted signal. It is usually expressed in decibels (dB) and can be calculated as follows (Almutairi & Krishna, 2022):

$$PAPR(dB) = 10\log_{10}({}^{Peak\ \ Power}/_{Average\ \ Power})$$

$$PAPR(dB) = Max\left(\frac{|y(n)|^2}{E[|y(n)|^2]}\right) \tag{3.37}$$

Where $y(n)$ is the transmitted signal in Multicarrier Modulation.

The complementary cumulative distribution function (CCDF) is a widely employed method for assessing the performance of Peak-to-Average Power Ratio (PAPR) reduction techniques. The CCDF represents the likelihood that the PAPR of an OFDM signal surpasses a specified threshold level of $PAPR_0$. A straightforward approximate expression for the CCDF of the PAPR of an OFDM signal with N subcarriers can be formulated as:

$$CCDF = P(PAPR > PAPR_0) = 1 - (1 - e^{-PAPR_0}) \tag{3.38}$$

3.8.3 Bit Error Rate

Bit Error Rate (BER) comparison serves as an additional performance metric for evaluating the efficacy of multi-carrier modulation techniques in communication systems. It measures the number of bit errors that transpire within a designated timeframe, usually articulated as a ratio or percentage to the total number of transmitted bits. Bit Error Rate (BER) measures the frequency of errors that arise during data transmission. The primary causes of BER degradation and transmission channel impairment are noise and multi-path propagation channels, which exhibit random behavior. (Tazeb et al., 2019) .

To find the average BER in a Rayleigh fading channel, we need to average the instantaneous BER over the distribution of γ

$$p(\gamma) = \frac{1}{\gamma}\exp\left(-\frac{\gamma}{-\gamma}\right) \tag{3.39}$$

Where $-\gamma$ is the average SNR

The average BER is obtained by integrating the instantaneous BER over the PDF of γ

$$BER_{QAM} = \int_0^{\infty} BER_{QAM}(\gamma)p(\gamma)d\gamma \tag{3.40}$$

For M-QAM, the average BER in a Rayleigh fading channel is approximated as:

$$BER_{QAM} \approx \frac{4}{k}\left(1-\frac{1}{\sqrt{M}}\right)\frac{1}{-\gamma}\left(1-\frac{1}{\sqrt{\frac{\gamma(M-1)}{3}}}\right)^{2} \quad (3.41)$$

This expression captures the dependence on the modulation order M and the average SNR $-\gamma$ reflecting the performance degradation in fading environments.

For an multicarrier modulation system with N subcarriers, assuming equal power allocation to each subcarrier:

$$SNR_{total} = \frac{P_{total}}{N_0 B} = \frac{N.P_{carrier}}{N_0 B} \quad (3.42)$$

Where P_{total} is the total transmitted power , $P_{carrier}$ is the power per subcarrier , N_0 is noise power and B the bandwidth of each subcarrier.

3.8.4 Spectral Efficiency

Spectrum efficiency, alternatively termed bandwidth efficiency, denotes the volume of data capable of transmission within a given bandwidth in a communication system.

This statistic evaluates how effectively the physical layer protocol and the MAC (media access control) employ a constrained frequency band. Spectral efficiency is crucial for meeting high data rate needs. The literature describes spectral efficiency in several ways. We analyzed spectral efficiency using the definition proposed by (Doré et al., 2017) which is better suited for multi-carrier modulation. The spectrum efficiency is computed by combining time and modulation efficiency (Tazeb et al., 2019):

$$SE_{MC} = TE \times ME \quad (3.43)$$

Where SE_{MC} is Spectrum Efficiency, TE is time Efficiency and ME is Modulation Efficiency of multi-carrier modulation. The concept of time efficiency quantifies the additional time required for transmission, taking into account the time overhead involved (Schaich et al., 2014):

$$TE = \frac{N_{sample\ \ Transmitted}}{N_{Sample\ \ Transmitted}+T_{overhead}} \quad (3.44)$$

where $N_{sample\ Transmitted}$ represents the number of samples in the transmitted signal dedicated to data transmission and $T_{overhead}$ is the overhead sample which will be a cyclic prefix, filter tails, zero padding, etc. For all Multicarrier Modulation; $N_{sample\ Transmitted} = N_M \times N$ where N_M denotes The Number of Symbols Transmitted multicarrier Modulation during in burst time and N is the FFT Number given (Bendimerad et al., 2021).

For the given Multicarrier Modulation schemes, The Overhead time for the sample due to CP , filter tails, and Padding will be given as follows (Bendimerad et al., 2021):

$$\text{For OFDM,} \quad T_{overhead} = N_M Lcp \tag{3.45}$$

Where Lcp is the length of a Cyclic prefix.

$$\text{For FBMC-OQAM,} \quad T_{overhead} = N(K - \tfrac{1}{2}) \tag{3.46}$$

$$\text{For FBMC-QAM,} \quad T_{overhead} = N(K - 1) \tag{3.47}$$

Where N is the Number of FFT given and K is the overlapping factor of the Prototype filter.

$$\text{For F-OFDM,} \quad T_{overhead} = N_M Lcp \tag{3.48}$$

The time Efficiency (TE) of each Multicarrier Modulation is:

$$TE_{OFDM} = \frac{N_M \times N}{N_M \times N + N_M Lcp} = \frac{N}{N + Lcp} \tag{3.49}$$

$$TE_{F-OFDM} = \frac{N_M \times N}{N_M \times N + N_M Lcp} = \frac{N}{N + Lcp} \tag{3.50}$$

$$TE_{FBMC-OQAM} = \frac{N_M \times N}{N_M \times N + N(K - \frac{1}{2})} = \frac{N}{N + N(K - \frac{1}{2})} \tag{3.51}$$

$$TE_{FBMC-QAM} = \frac{N_M \times N}{N_M \times N + N(K-1)} = \frac{N}{N + N(K-1)} \tag{3.52}$$

The SE does not depend on the Number of Symbols Transmitted by multicarrier Modulation during burst time. It depends on the FFT size and Modulation efficiency (ME). The SE of each Multi-carrier Modulation is given as the product of TE and ME. For each multi-carrier Modulation given:

$$SE_{OFDM} = \frac{N_M \times N}{N_M \times N + N_M Lcp} \times ME = \frac{N}{N + Lcp} \times ME \tag{3.53}$$

$$SE_{F-OFDM} = \frac{N_M \times N}{N_M \times N + N_M Lcp} \times ME = \frac{N}{N + Lcp} ME \tag{3.54}$$

$$TE_{FBMC-OQAM} = \frac{N_M \times N}{N_M \times N + N(K-\frac{1}{2})} \times ME = \frac{N}{N + N(K-\frac{1}{2})} \times ME \quad (3.55)$$

$$TE_{FBMC-QAM} = \frac{N_M \times N}{N_M \times N + N(K-1)} \times ME = \frac{N}{N + N(K-1)} \times ME \quad (3.56)$$

Where ME is the Modulation efficiency of Multicarrier Modulation (Doré et al., 2017).

3.8.5 Computational Complexity

Computational complexity, a concept in Computer science, focuses on the computational resources needed for specific tasks. (Tazeb et al., 2019). The complexity of Multicarrier modulation is assessed by taking into account the number of actual multiplications and additions required to carry out the modulation computation.

The computational complexity of a waveform is an important metric for determining how well it can be executed by computers. To understand the formulas for the Multiplication of each Candidate Multicarrier Modulation, we have to know the multiplication complexity formula for *FFT/IFFT and DWT/IDWT*. We assume that there is a total number N of subcarriers accessible, and among them, *No* are utilized with symbols. In the case of FFT, the total number of real multiplications required for an N-point FFT/IFFT using the split radix algorithm is provided by (Tazeb et al., 2019):

$$M_{FFT} = N \log_2 N - 3N + 4, multiplications \quad (3.52)$$

In DWT with a filter of length (L) required LN real multiplications and when a complex constellation is utilized, arithmetic operations need to be computed twice. Therefore, the number of real multiplications is given as $RM = 2LN$. For DWT, the total number of real multiplications required for an N-point DWT/IDWT is given by (Dawood et al., 2015):

$$M_{DWT} = 2LN - 3N + 4, multiplications \quad (3.53)$$

The length of the filter (L) is different for each wavelet family. The wavelet families with lower length of filter have lower Computational Complexity. For wavelet families such as *haar* (L=2), *db6* (L=4), *bior2.2*(L= 6), *sym4* (L=8) and *dmey* (L=24) based on the different Literature.In this study, we used *haar* and *db6* for Computational Complexity Comparison. The number of real multiplications which is used to calculate the complexity for IFFT/FFT and IDWT/DWT is given as follows based on (Tazeb et al., 2019) (Bendimerad,2021).

The complexity is calculated based on the number of real multiplications per multi-carrier symbol. The table presents the number of real-valued multiplications required to transmit one block of OFDM symbols.

Table 3.1 Multiplication of candidate multi-carrier modulation techniques

Candidate Multicarrier Modulation	Number of Complex Multiplication
OFDM (Tazeb et al., 2019)	$2M_{FFT}(N) + 4(N + Lcp) + 4No$
F-OFDM (Bendimerad,2021)	$2(M_{FFT}(N)\log_2 N - 6N + 8 + 2(N + LcpLf) + 2NLf$
FBMC/OQAM (Tazeb et al., 2019)	$4M_{FFT}(N) + 8NK + 4No(1 + Leq)$
FBMC-QAM(Dumari et al., 2023)	$2N\log_2\frac{N}{2} + 2(N)\log_2(N) - 9N + 16 + 8(NK + 1)$
DWT-OFDM	$2M_{DWT}(N) + 4N + 4No$
DWT-F-OFDM	$2(M_{DWT}(N)\log_2 N - 6N + 8 + 2(N + LF) + 2NLF$
DWT-FBMC-OQAM	$4M_{DWT}(N) + 8NK + 4N0(1 + Leq)$
DWT-FBMC-QAM	$2(M_{DWT}(N) + 2M_{DWT}(N) - 9N + 16 + 8(NK + 1)$

Where Lcp represents the length of the cyclic prefix in OFDM and F-OFDM, LF denotes the length of the filter in F-OFDM. No is the number of subcarriers that carry data symbols in FBMC and OFDM. In FBMC systems, it is generally sufficient to employ a 1-tap equalizer, denoted as Leq.

CHAPTER FOUR

RESULT AND DISCUSSION

This chapter illustrates the performance of multi-carrier modulation techniques with Discrete Wavelet Transform in comparison with conventional techniques. Their performance is measured based on key metrics such as PSD, PAPR, BER, SE, and computational complexity. The effectiveness of these multi-carrier modulation schemes in meeting the fundamental requirements of emerging communication networks is evaluated. The simulation parameters adhere to ITU standards.

4.1 Simulation Parameters

Table 4.1 General parameters for simulation

Types	**Parameters**	**Numerical Value**	**Remark**
General Parameters	Sub-carrier Spacing	15KHz	ITU Standard (ITU-R, 2015)
	Sampling frequency	15.36MHz	ITU Standard (ITU-R, 2015)
	Number of Sub-carriers	600/1024	Can Vary
	Modulations Order	64,256,1024	Higher Order QAM
	Number of Symbols	512	(Almutairi & Krishna, 2022)
	Wavelet Families	*Haar,db6,dmey,sym4 ,bior2.2*	(Almutairi & Krishna, 2022)
CP-OFDM	Length of Cyclic prefix	72	As in LTE
F-OFDM	Filter type	Hanning Window	(Almutairi & Krishna, 2022)
	Filter Length	513	
	Number of subbands and subcarriers in each	50/12	(Almutairi & Krishna, 2022)
FBMC-OQAM	Overlapping factor	4	For the best side lobe
	Prototype filter	PHYDYAS filter	(Dumari et al., 2023)
FBMC-QAM	Overlapping factor	4	For the best side lobe
	Prototype Filter	PHYDYAS Filter	(Dumari et al., 2023)

4.3 Spectral Efficiency Comparison

In this study, the Spectrum efficiency of the candidate Modulation is analyzed in two ways;

i) Based on the number of symbols transmitted multicarrier modulation.

This section compares spectrum efficiency expressed in bits/second/hertz, vs the number of transmitted multi-carrier symbols for each multi-carrier modulation in terms of time and modulation efficiency.

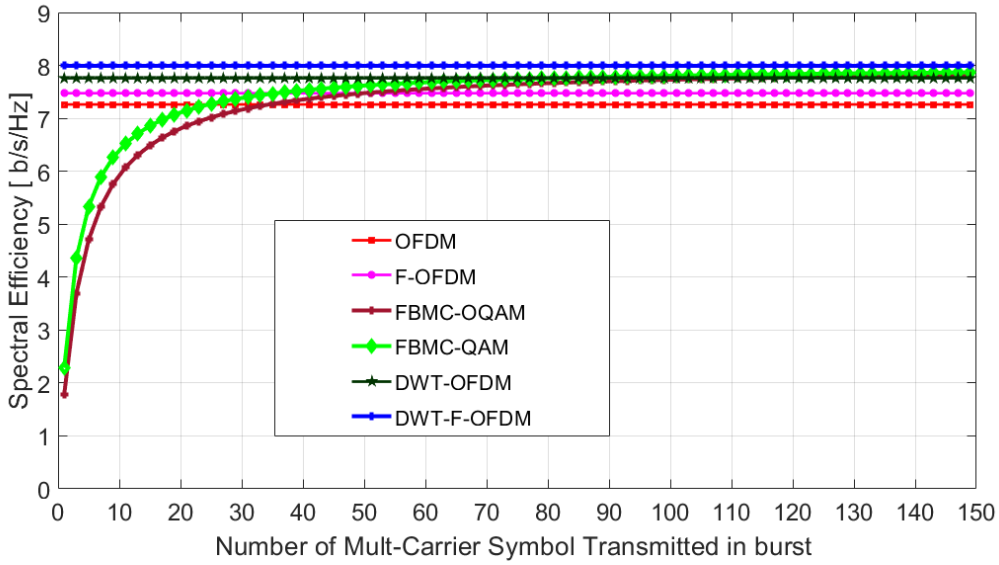

Figure 4.1 Spectral efficiency of DWT-based multicarrier modulation techniques

Figure 4.1 illustrates the spectral efficiency across various DWT-based multi-carrier modulation techniques. From the result, the Spectral efficiency of FBMC depends on the variation of multi-carrier symbols transmitted in time bursts. For a higher number of multicarrier symbols, FBMC-QAM has higher spectral efficiency than other conventional candidate multi-carrier modulation. Although the spectral efficiency of other Multi-carrier modulation schemes remains unaffected by the number of multi-carrier symbols transmitted per symbol, the spectral efficiency of DWT-based multi-carrier modulation surpasses that of conventional techniques.

Based on the results, the Spectral Efficiency (SE) of DWT-OFDM and DWT-F-OFDM exceeds that of the FBMC-QAM system, which in turn demonstrates higher Spectral Efficiency compared to the conventional system. In general, DWT-based multi-carrier modulation techniques exhibit superior spectral efficiency compared to conventional methods. This is due to the efficient utilization of wavelet transforms, which enable DWT-based systems to achieve higher spectral efficiency while maintaining robustness against symbol count variations.

ii) Based on the number of subcarriers.

The spectral efficiency of multicarrier modulation can be evaluated by investigating the relationship between spectral efficiency and the number of subcarriers.

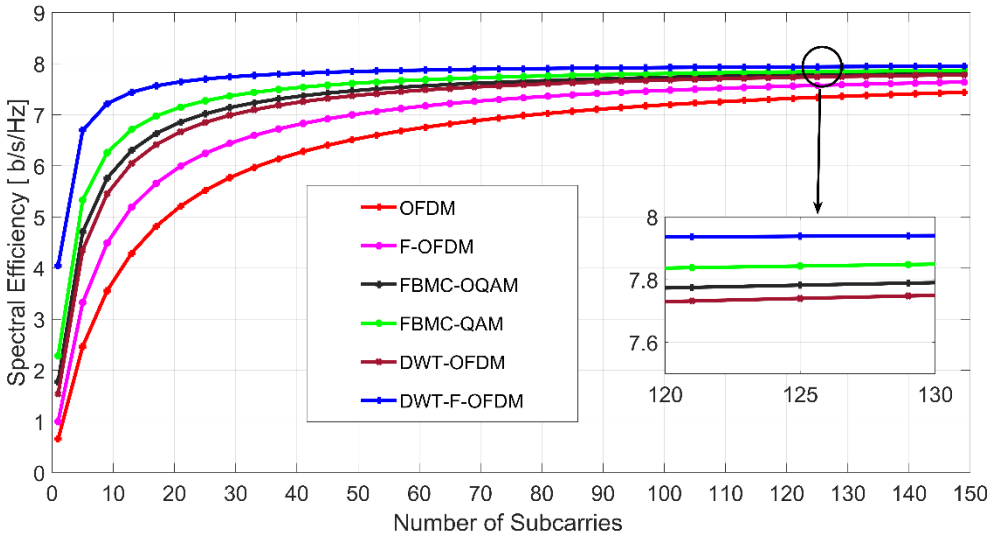

Figure 4.2 Spectral efficiency of DWT- multicarrier modulation schemes for changing the number of subcarriers.

Figure 4.2 shows SE analysis of various multicarrier modulation schemes, including DWT-based and conventional techniques by varying the number of subcarriers. It was observed that FBMC-QAM exhibits higher SE than the candidate conventional multicarrier modulation. However, the DWT-OFDM and DWT-F-OFDM schemes demonstrated higher SE than all the other candidate multicarrier modulation techniques. This implies that the utilization of the DWT in these schemes gives an advantage in terms of spectral efficiency. The DWT-based multicarrier modulation techniques utilize the properties of wavelets to achieve improved frequency localization and sharp variation of the signal representation, resulting in enhanced spectral efficiency.

4.3 Power Spectral Density Comparison

Power spectral density is the power is expressed in dB, and its normalized frequency. The PSD indicates both the bandwidth efficiency of the proposed DWT-based multicarrier modulation techniques and the interference from adjacent channels caused by side-lobe effects.Normalized frequency denotes a value possessing the dimension of frequency, in units of cycles per sample. It is calculated as $fn = f / fs$ where f represents a regular frequency and *fs* represents the sampling rate.

The PSD regulates the extent of out-of-band emissions, which may interfere with neighboring channels or services. Managing the PSD aids in reducing out-of-band emissions and ensuring adherence to regulatory standards.

Figure 4.3 illustrates the comparison of PSD versus normalized frequency analysis across various wavelet families alongside conventional F-OFDM.

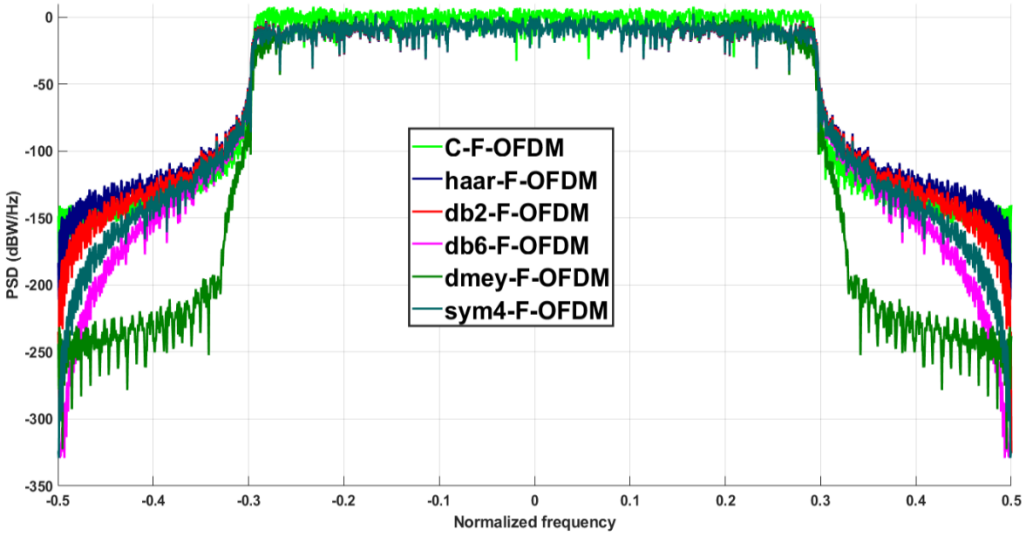

Figure 4.3 Power spectral density analysis of F-OFDM with different wavelets families for sub-carrier spacing 15kHz, number of sub-carriers 600.

Figure 4.3 shows the power spectral density analysis of different wavelet families with Filtered OFDM for the sake of the effect of each wavelet family in DWT with integration of multicarrier Modulation. The Power Spectral Density is estimated using MATLAB through a periodogram approach employing a rectangular window. Each wavelet family can influence the out-of-band emission (OOBE) of the candidate multi-carrier modulation techniques. To optimize multi-carrier modulation techniques of minimal OOBE, wavelet families with minimal side lobes are necessary. Analysis of the power spectral density for various wavelet families with Filtered-OFDM indicates that the *dmey* wavelet family outperforms faster than others as shown in Figure 4.4. By considering these findings, one can effectively choose wavelet families that align with particular communication needs. This approach facilitates the effectiveness of spectral utilization and enhances overall system performance.

Figure 4.4 illustrates the power spectral density analysis of CP-OFDM, C-F-OFDM, FBMC-OQAM with PHYSDAS Filter and FBMC-QAM with PHYSDAS Filter.

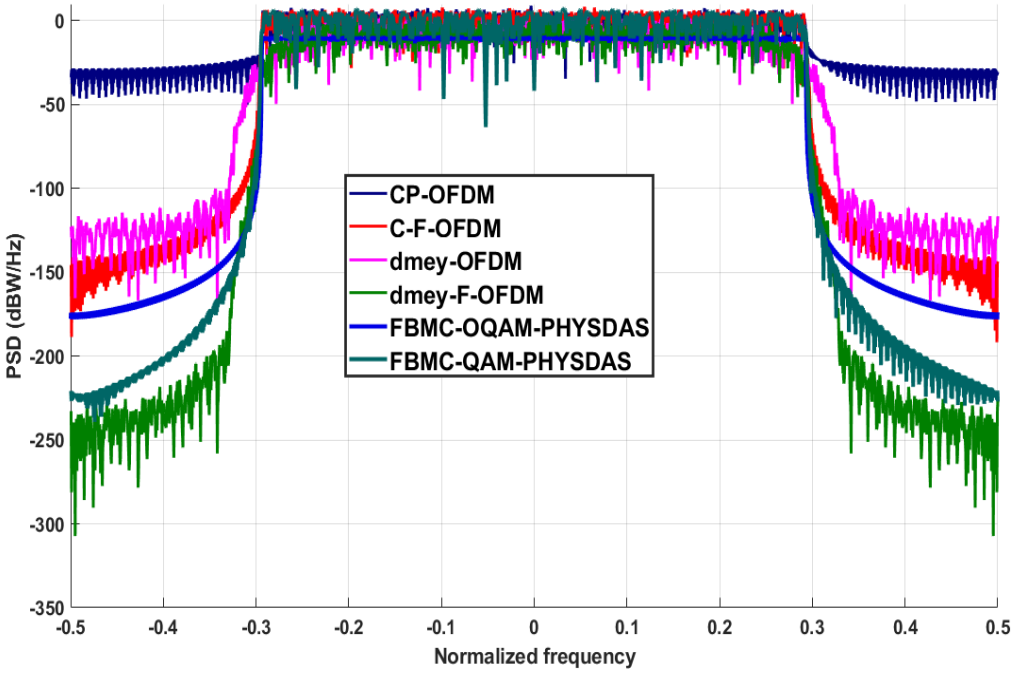

Figure 4.4 The power spectral density analysis DWT-based Multicarrier modulation with different wavelets families for sub-carrier spacing 15kHz, number of sub-carriers 600.

Figure 4.4 shows the simulated result for 600 sub-carriers by taking candidate multicarrier modulation techniques with *dmey wavelet* family from DWT with a single level of decomposition. From The DWT families, *dmey wavelet* family with F-OFDM has attractive PSD characteristics compared to the considered candidate multicarrier modulation techniques for spacing is chosen at 15KHz the same as the LTE.

Let us examine the PSD of multi-carrier modulation techniques with a normalized frequency of -0.5. For CP-OFDM, the PSD is -29.317 dBW/Hz; for F-OFDM, it's -145.65 dBW/Hz; for FBMC-OQAM with PHYDYAS filter, it's -175.78 dBW/Hz; for FBMC-QAM with PHYDYAS, it's -220 dBW/Hz; for OFDM using the *dmey* Wavelet family, it's -129.12 dBW/Hz; and for F-OFDM using the *dmey* Wavelet family, it's -250.7 dBW/Hz. These findings indicate that DWT-F-OFDM employing the *dmey* wavelet family exhibits the lowest out-of-band emission. The side lobe generated by DWT-F-OFDM using the selected *dmey* wavelet family is minimal, facilitating the coexistence of various services. The PSD governs the level of out-of-band emissions, which can cause interference with adjacent channels or services. Controlling the PSD helps in minimizing out-of-band emissions and ensuring compliance with regulatory requirements.

Table 4.2 The PSD of candidate modulation schemes with DWT at normalized frequencies of -0.5 and -0.4.

Candidate Multicarrier Modulation		Normalized Frequency	
		-0.5	-0.4
CP-OFDM	Power Spectral Density(dBW/Hz)	-29.317	-27.575
C-F-OFDM		-145.653	-137.138
FBMC-OQAM with PHYSDAS		-175.78	-166.423
FBMC-QAM with PHYSDAS		-220.715	-200.254
dmey-OFDM		-129.182	-127.778
dmey-F-OFDM		-250.7	-229.56

Because of the adoption of *dmey* wavelet family in *dmey*-F-OFDM with QAM Modulation, a certain amount of PSD improvement was achieved over OFDM and FBMC. When analyzing the PSD of DWT-F-OFDM with the *dmey* wavelet family and FBMC-QAM with the PHYSDAS filter on a dBW/Hz scale for a normalized frequency of -0.5, a significant improvement of 29.99 dBW/Hz was observed.

4.4 Peak to Average Power Ratio Comparison

One major drawback of multicarrier modulation (MCM) techniques is their high PAPR. The PAPRs of multicarrier modulation are defined as a measure of the maximum power level relative to the average power level in the transmitted signal. The relationship between CCDF-PAPR is a critical aspect of the multicarrier modulation schemes. It estimates the probability of PAPR surpassing a specified threshold and assists in determining the ideal range for PAPR variation. The study analyzed the PAPR of the DWT-based multicarrier modulation systems based on parameters like modulation order and compared the PAPR characteristics of DWT-based multicarrier modulation with those of existing techniques.

Figure 4.5 illustrates the comparison of PAPR versus CCDF for various multicarrier modulation schemes employing 64-QAM modulation. The figure illustrates a comparison of the PAPR for various multicarrier modulation schemes, namely CP-OFDM, C-F-OFDM, FBMC-OQAM with PHYDYAS filter, and FBMC-QAM with PHYDYAS filter. The analysis of PAPR performance for these candidate waveforms is conducted to comprehend the influence of DWT on each type of candidate multicarrier modulation techniques.

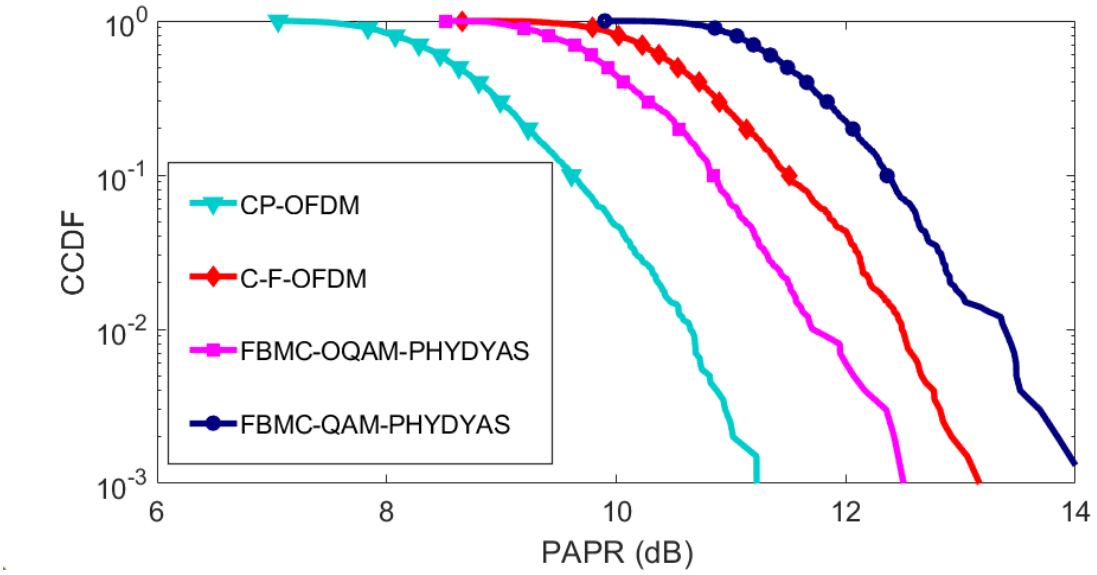

Figure 4.5 Comparison of PAPRs of different existing multi-carrier modulation using 64-QAM modulation.

From Figure 4.5, FBMC-OQAM and OFDM benefit from the orthogonality of their subcarriers, resulting in reduced PAPR. However, the flexibility provided by pulse shaping in FBMC-QAM and F-OFDM comes at the cost of increased side lobes and spectral leakage, leading to higher PAPR. Additionally, FBMC-OQAM and OFDM achieve lower PAPR due to time-frequency localization and the use of highly localized subcarriers, which help in lowering the PAPR. In contrast, FBMC-QAM and F-OFDM exhibit wider subcarriers and broader frequency responses resulting in higher PAPR.

4.4.1 PAPR Analysis of DWT-OFDM and DWT-F-OFDM Multicarrier Modulation Techniques With Higher Order QAM Modulation.

In this section, the study analyzed the effect of each wavelet family on the analysis of PAPR for DWT-OFDM and DWT-F-OFDM using the higher-order QAM Modulation (256-QAM, and 1024-QAM). The analysis was done for different wavelet families selected and contrasted the findings with the traditional CP-OFDM and C-F-OFDM. The investigation explores the impact of various modulation mappings on PAPR within the considered multicarrier modulation techniques.

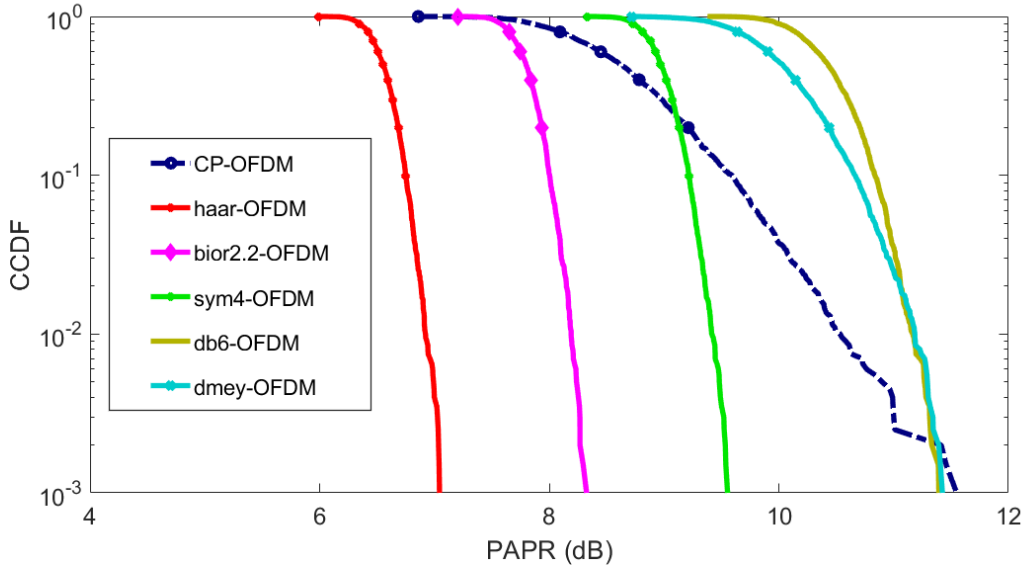

Figure 4.6 Comparison of PAPRs of DWT-OFDM with CP-OFDM for different wavelet families using 256-QAM modulation.

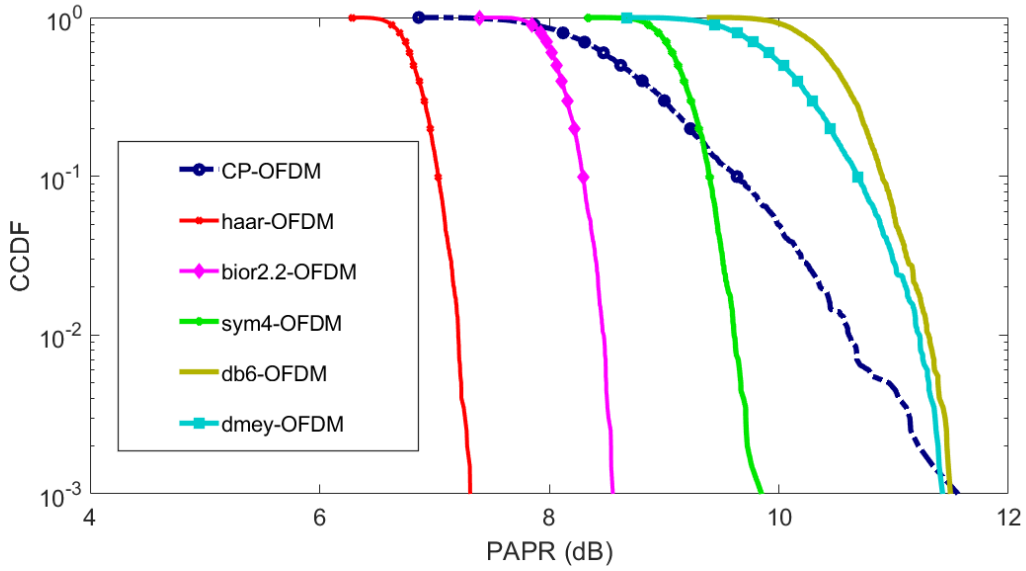

Figure 4.7 Comparison of PAPRs of DWT-OFDM with CP-OFDM for different wavelet families using 1024-QAM modulation.

Figures 4.6, and 4.7 show how higher-order QAM modulation mapping affects the PAPR of the DWT-OFDM approach. The results indicate that the PAPR of the DWT-OFDM system surpasses that of the CP-OFDM approach. Various wavelet families, as listed in Table 4.1, were employed for this analysis. It's evident from the result analysis that the *haar*, *sym4*, and *bior2.2* wavelets offer superior PAPR performance compared to CP-OFDM.

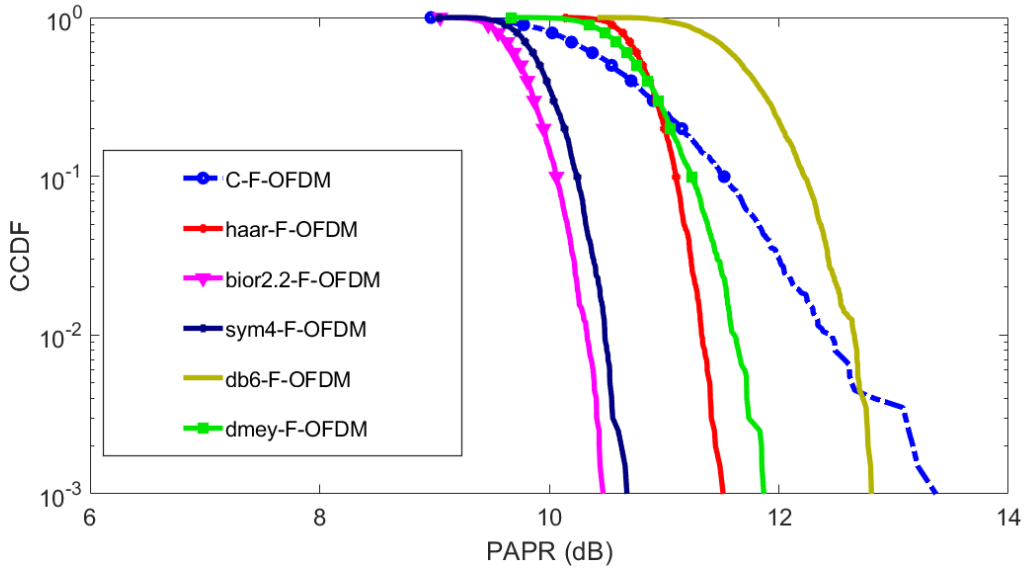

Figure 4.8 Comparison of PAPRs of DWT-F-OFDM with C-F-OFDM for different wavelet families using 256-QAM modulation.

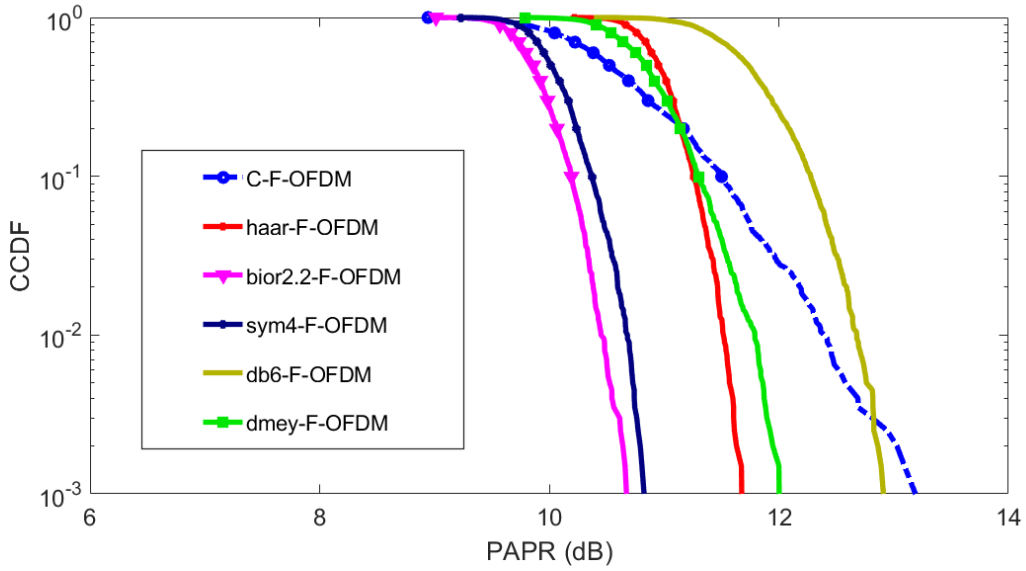

Figure 4.9 Comparison of PAPRs of DWT-F-OFDM with C-F-OFDM for different wavelet families using 1024-QAM modulation.

Figures 4.8, and 4.9 shows how higher-order QAM modulation mapping affects the PAPR of the DWT-F-OFDM system. The results reavels that the PAPR of the DWT-F-OFDM system outperforms that of the C-F-OFDM system. By evaluating the PAPR across different modulation schemes in the DWT-F-OFDM system, it is clear that the *bior2.2*-F-OFDM and s*ym4*-F-OFDM systems demonstrate superior PAPR performance relative to C-F-OFDM.

4.4.2 PAPR Analysis of DWT-FBMC-OQAM Multicarrier Modulation Techniques Using Higher Order QAM Modulation.

In this part, the study analyzed the effect of each wavelet family on the analysis of DWT-FBMC-OQAM using the higher-order QAM Modulation (256, and 1024-QAM).

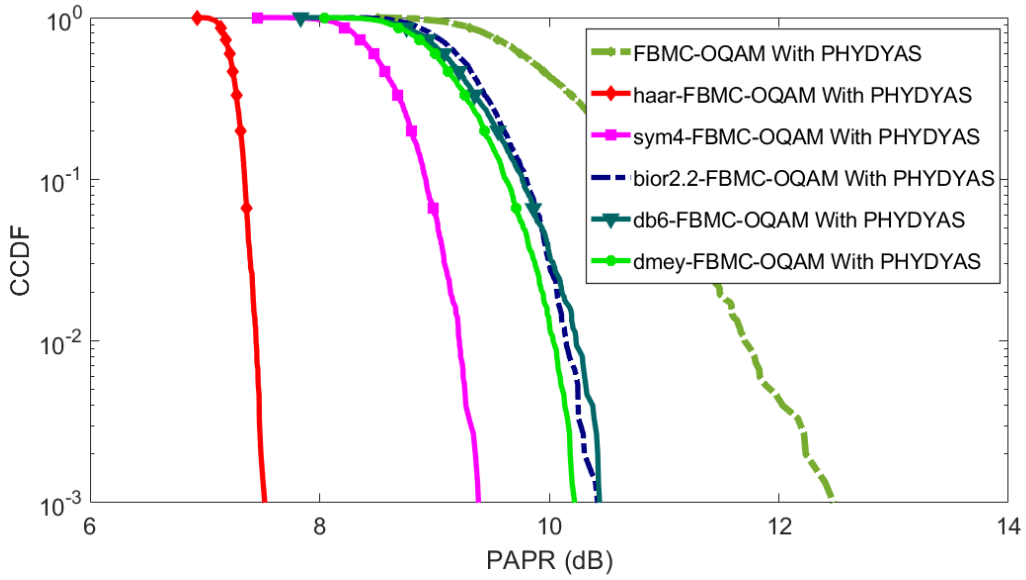

Figure 4.10 Comparison of PAPRs of DWT-FBMC-OQAM with PHYDYAS prototype filter and FBMC-OQAM for different wavelet families using 256-QAM modulation.

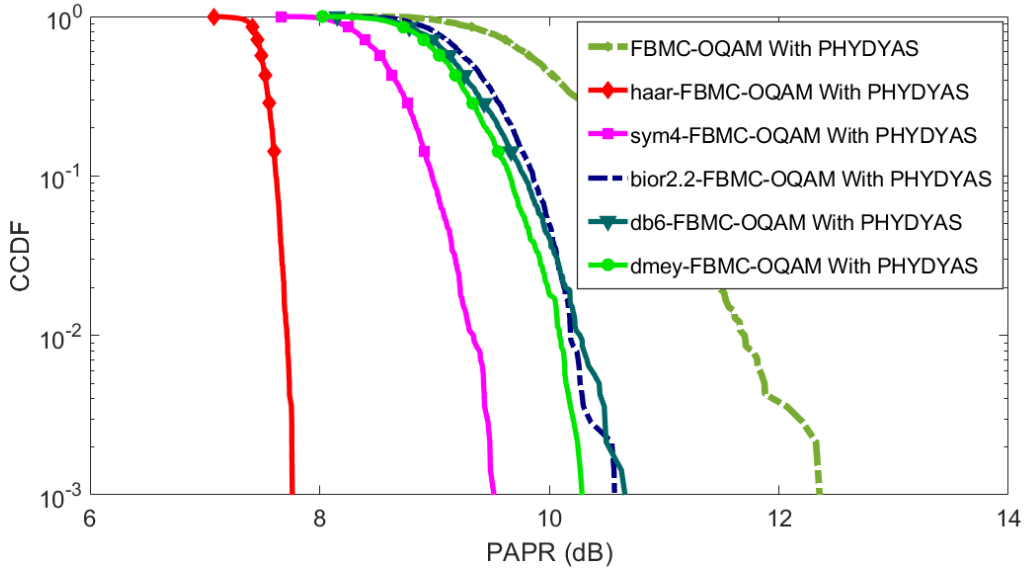

Figure 4.11 Comparison of PAPRs of DWT-FBMC-OQAM with PHYDYAS prototype filter and FBMC-OQAM for different wavelet families using 1024-QAM modulation.

Figure 4.10, and Figure 4.11 show the effect of different higher-order QAM modulations on the PAPR of the DWT-FBMC-OQAM with the PHYDYAS prototype Filter. The PAPR of all wavelet families outperforms those of the FBMC-OQAM systems. Although all wavelet families provide better PAPR than conventional FBMC-OQAM, *haar,* and *sym4* provide better performance than other wavelet families. The Numerical justification of the graph is shown in Table 4.3 for the highest-performance wavelet families from the suggested schemes.

Table 4.3 Comparison of PAPRs of DWT-based multicarrier modulation with existing schemes for different wavelet families using higher-order QAM modulation.

Multicarrier Modulation	QAM order		CCDF values	
			10^{-3}	10^{-2}
CP-OFDM	256		11.22	10.59
	1024		11.25	10.61
C-F-OFDM	256		12.84	12.46
	1024		13.08	12.50
FBMC-OQAM with PHYSDYAS	256		12.55	11.75
	1024		12.65	11.81
haar-OFDM	256		7.04	6.95
	1024		7.35	7.19
bior2.2-OFDM	256		8.39	8.17
	1024		8.52	8.44
bior2.2-F-OFDM	256		10.56	10.33
	1024		10.66	10.43
Sym4-F-OFDM	256		10.67	10.46
	1024		10.78	10.62
haar- FBMC-OQAM with PHYSDYAS	256		7.48	7.43
	1024		7.81	7.73
sym4-FBMC-OQAM with PHYDYAS	256		9.39	8.92
	1024		9.5	9.30

Table 4.3 shows the PAPR values of each DWT-based multicarrier scheme. Most of the wavelet families have better performance than the conventional schemes, However, among all the different wavelets, the *haar, sym4,* and *bior2.2*, they exhibit lower PAPR performance compared to the existing techniques. Based on the simulation results, *haar-OFDM,* and *haar-FBMC-OQAM* achieve the lowest PAPR performance compared to CP-OFDM and conventional FBMC-OQAM, respectively.

From the result analysis of DWT- F-OFDM schemes, *bior2.2-F-OFDM* demonstrates the lowest PAPR relative to C-F-OFDM for the considered higher-order QAM modulations. The analysis suggests that most wavelet families used in candidate multicarrier modulation schemes achieved the desired PAPR performance than conventional techniques. This indicates that the Fourier transform (FT) uses more energy in contrast to the Wavelet Transform (WT).

The study analyzed the PAPR for the selected wavelet family across all available options to understand the improvement within each selected multicarrier modulation scheme. Figure 4.12, figure 4.13, and Figure 4.14 show the effect of *haar* and *bior2.2* on each candidate multicarrier Modulation.

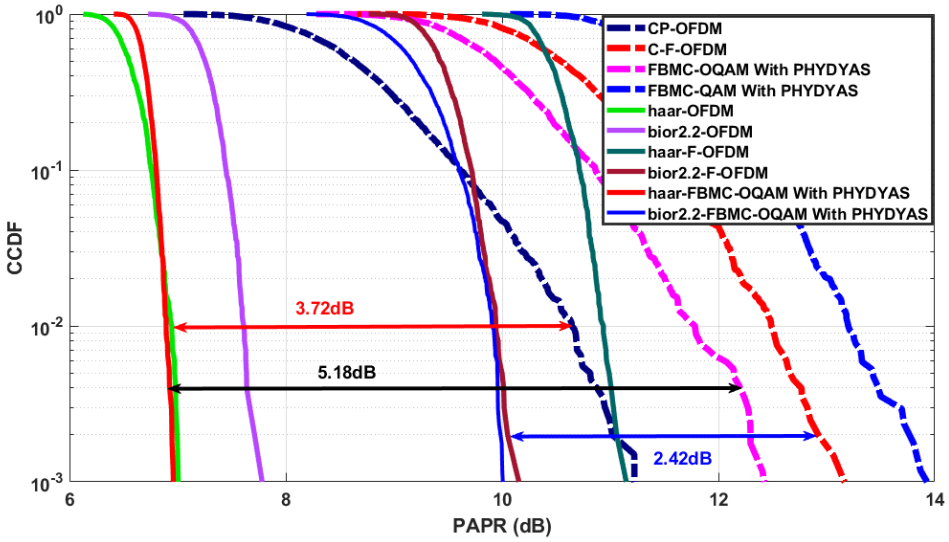

Figure 4.12 Comparison of PAPRs of DWT-based candidate multicarrier modulation using 64-QAM modulation for *haar* and *bior2.2* wavelet families.

From Figure 4.12 It is clear that the *haar*-OFDM provides a PAPR performance improvement of 3.72 dB at 10^{-2} CCDF compared to the CP-OFDM. And, the PAPR of *haar*-FBMC-OQAM with PHYDYAS prototype filter improves to 5.18 dB at $4x10^{-3}$ CCDF and *bior2.2*-F-OFDM improves to 2.42 dB at $2x10^{-3}$ CCDF compared to the Conventional system's using 64-QAM modulation order.

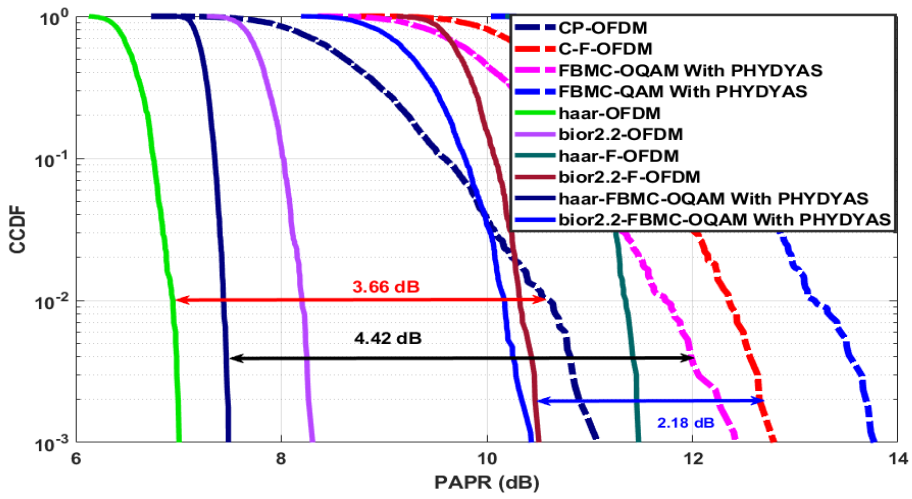

Figure 4.13 Comparison of PAPRs of DWT-based candidate multicarrier modulation using 256-QAM modulation for *haar* and *bior2.2* wavelet families.

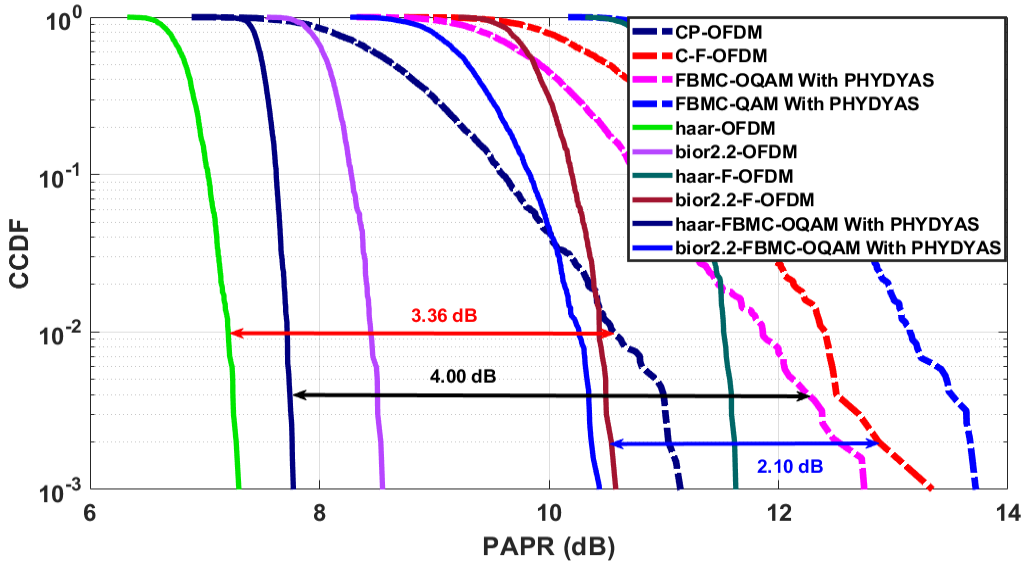

Figure 4.14 Comparison of PAPRs of DWT-based candidate multicarrier modulation using 1024-QAM modulation for *haar* and *bior2.2* wavelet families.

Figure 4.13, and Figure 4.14 show a Comparison of PAPRs of DWT-based Candidate Multicarrier Modulation using 256-QAM, and 1024-QAM modulation respectively for *haar* and *bior2.2* wavelet families. The *haar*-OFDM offers performance in PAPR of 3.66 dB for 256-QAM and 3.36dB for 1024-QAM at 10^{-2} CCDF compared to the CP-OFDM. Additionally, the PAPR of *haar* -FBMC-OQAM with PHYDYAS prototype filter improves to 4.42 dB for 256-QAM and 4.00dB for 1024-QAM at $4x10^{-3}$ CCDF and *bior2.2*-F-OFDM improves to 2.18 dB for 256-QAM and 2.10 dB for 1024-QAM at $2x10^{-3}$ CCDF compared to that of the Conventional techniques.

The PAPR performance of the DWT-based multicarrier modulation schemes outperforms that of the existing techniques because the DWT-based system involves a lower number of signal analyses compared to the existing techniques. In the study,different wavelet families are considered and almost all families achive good PAPR performance compared to traditional techniques. We can also conclude that the PAPR performance of wavelet-based modulation depends on the wavelet family selected and the modulation order.

4.5 Bit Error Rate Comparison

Comparing the bit error rates (BERs) serves as a performance metric for assessing the effectiveness of multi-carrier modulation techniques in communication systems. Figure 4.18 illustrates the comparison between the bit error rate and signal-to-noise ratio for M-QAM (4-QAM, 16-QAM, 64-QAM, 256-QAM, 1024-QAM). The performance analysis of modulation order is used to understand the impact of higher-order modulation on Massive Communication. The thesis simulated the transmission of 1000 OFDM symbols using a Rayleigh fading channel. We can conclude that an increase in the signal-to-noise ratio results in a decrease in the bit error rate. Additionally, an increase in the QAM order leads to an increase in the bit error rate. However, lower QAM orders are unable to support a large signal-to-noise ratio. To enable massive communication, higher QAM orders are necessary.

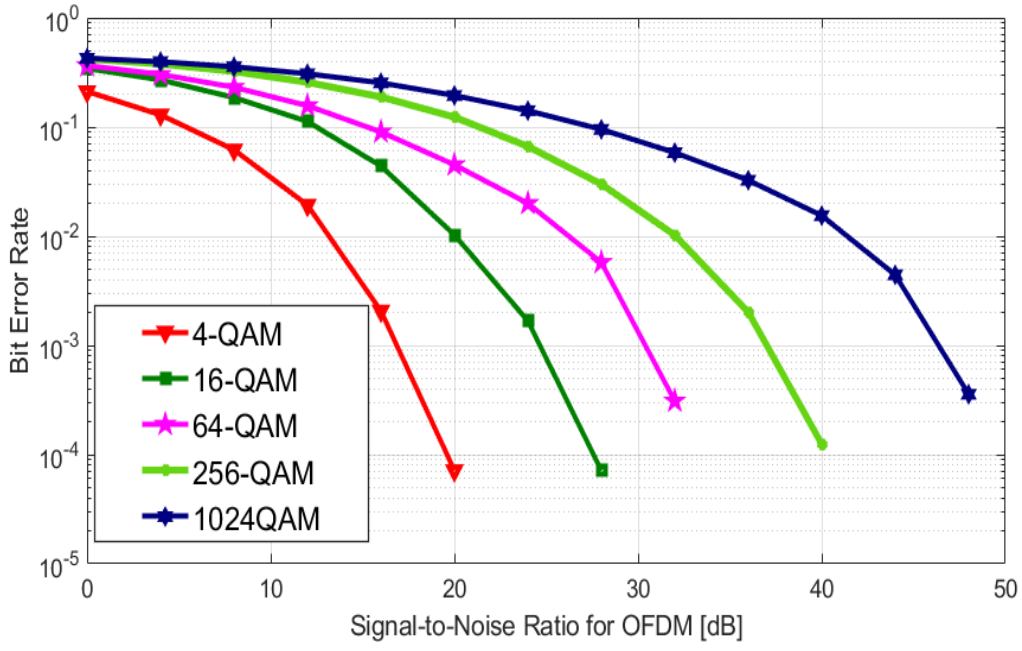

Figure 4.15 Bit error rate performance of OFDM at M-QAM.

The BER performance analysis of M-QAM shows that as the QAM order increases from 4 to 1024, the bit error rate rises significantly, indicating greater susceptibility to noise and errors.

However, higher QAM orders are crucial for supporting the large number of users and achieving higher data rates, necessitating a trade-off between error performance and bandwidth efficiency.

In this study, the BER performance analysis of the DWT-based Multicarrier Modulation was evaluated and compared with existing techniques at higher-order QAM Modulation. The BER performance of the systems utilizing different wavelet families like *haar*, *dmey*, *bior2.2*, *db6*, and *sym4* are analyzed in both vehicular and pedestrian channels.

4.5.1 BER Analysis of DWT-OFDM and DWT-F-OFDM Multicarrier Modulation Techniques for the Vehicular A Channel model.

In this part, BER performance is examined for various higher-order QAM modulations in both the traditional FFT-based OFDM, FFT-F-OFDM system, and the DWT-OFDM, DWT-F-OFDM systems using five different wavelet families. The simulation was done for the evaluation of the proposed system on the candidate multicarrier modulation techniques using the Vehicular A (VehA) channel model. The BER performance is analyzed and compared using the higher order QAM modulations like 256-QAM and 1024-QAM modulation orders.

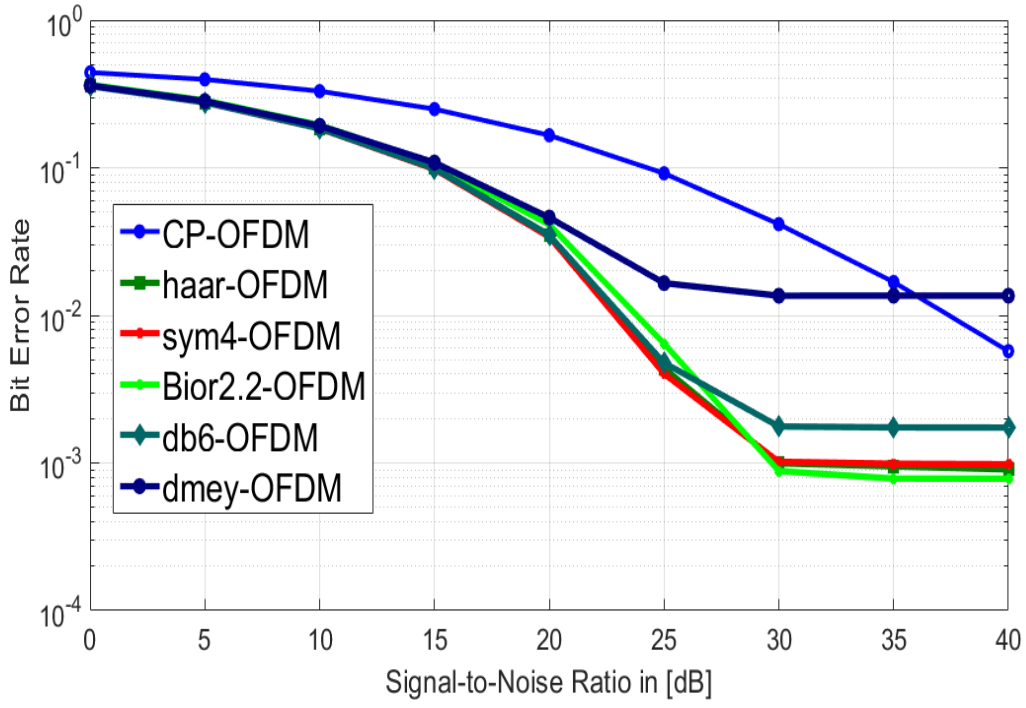

Figure 4.16 BER comparison of DWT-OFDM and CP-OFDM for the VehA channel model using 256-QAM modulation.

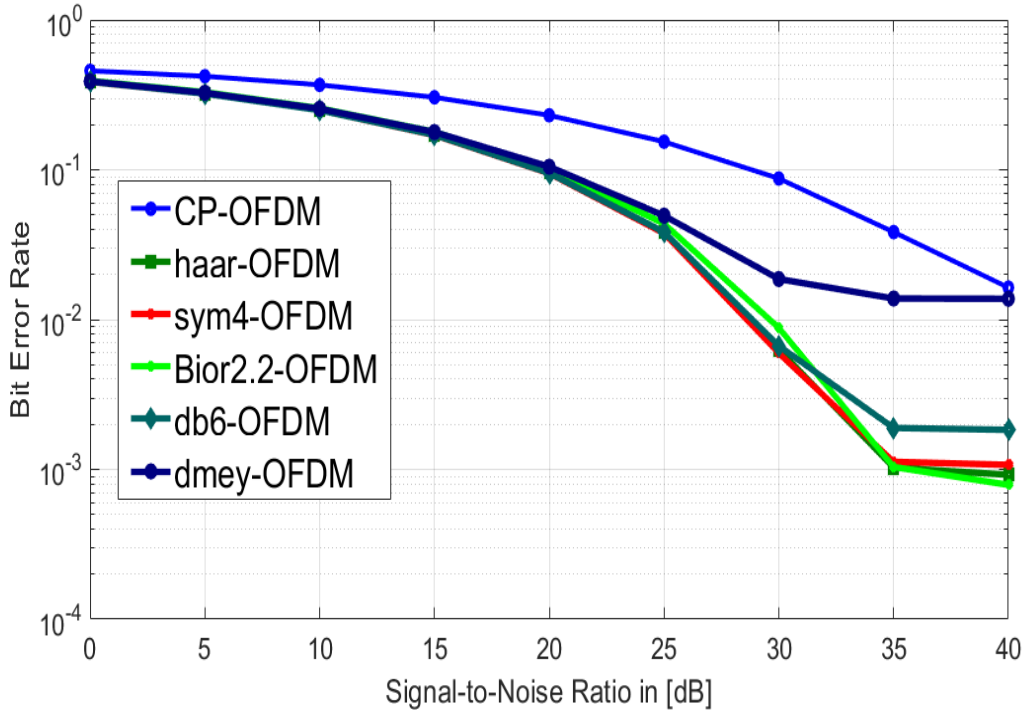

Figure 4.17 BER comparison of DWT-OFDM and CP-OFDM for the VehA channel model using 1024-QAM modulation.

Figures 4.16 and 4.17 illustrate the results of a simulated analysis that compares the performance of DWT-based OFDM systems in terms of the Bit Error Rate (BER) metric. The proposed system uses five different wavelets, and the BER performance of the DWT-OFDM system is compared to that of the existing CP-OFDM techniques for 256-QAM, and 1024-QAM modulation order respectively. The proposed DWT-OFDM system performs better than the CP-OFDM system, and the comparison proved that the Wavelet-based OFDM outperforms the CP-OFDM techniques. Most wavelet families show similar characteristics, except for the *dmey* wavelet. However, the *bior2.2*, *haar* and *sym4* wavelets demonstrate better performance than other wavelets, particularly at a higher SNR for the considered modulation order. This is due to the nature of DWT which is improved orthogonality reduces inter-symbol interference (ISI) power and makes the system less susceptible to Doppler shift effects.

Figure 4.18, and Figure 4.19 show the BER performance of DWT-F-OFDM with C-F-OFDM for the VehA channel model for 256 and 1024-QAM modulation order.

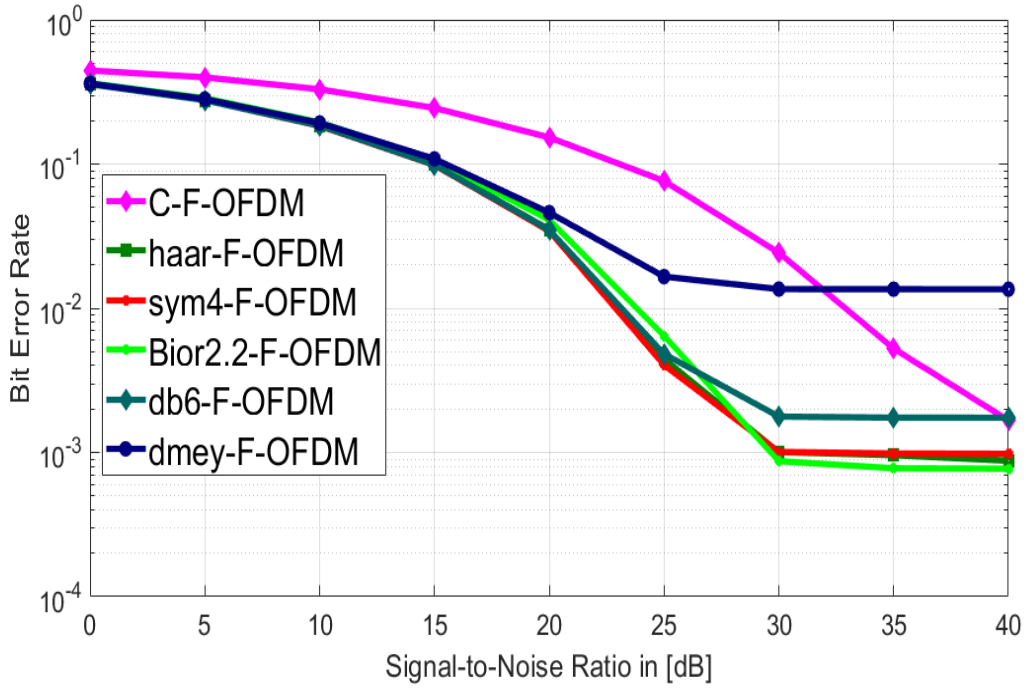

Figure 4.18 BER comparison of DWT-F-OFDM and C-F-OFDM for the VehA channel model using 256-QAM modulation.

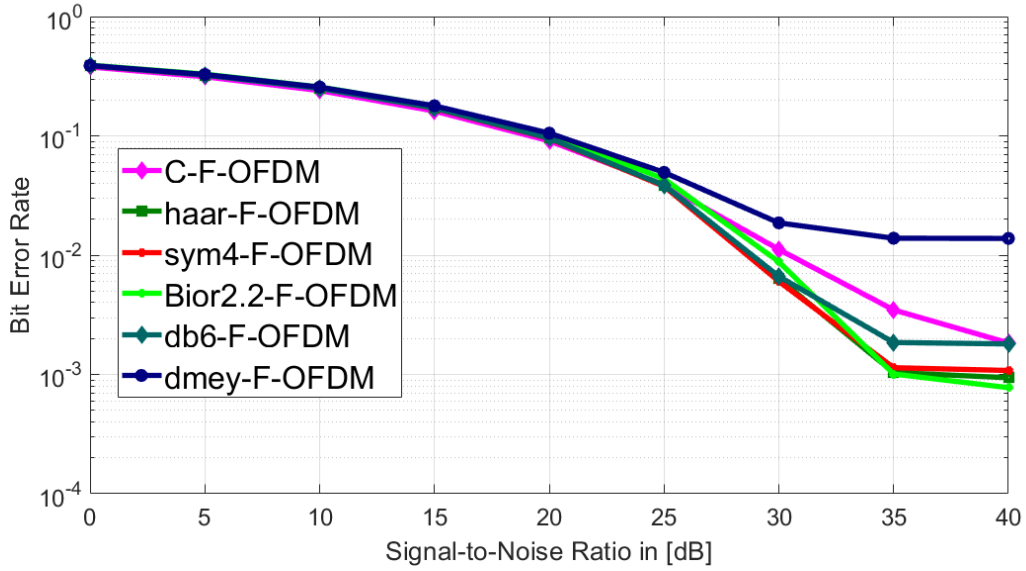

Figure 4.19 BER comparison of DWT-F-OFDM and C-F-OFDM for the VehA channel model using 1024-QAM modulation.

Figures 4.18 and 4.19 illustrate the results of a simulated analysis that compares the bit error rate performance of the DWT-F-OFDM systems to that of the existing C-F-OFDM schemes for 256-QAM, and 1024-QAM modulation order respectively. The proposed DWT-F-OFDM system performs better than the C-F-OFDM system.

However, the *bior2.2*, *haar,* and *sym4* wavelets demonstrate Superior performance than other wavelets, particularly at a higher signal-to-noise ratio for the considered modulation order. Table 4.4 shows the BER values of the most performed selected Wavelet families with the SNR values. From Table 4.4 it can be observed that at SNR 35dB for 256- QAM modulation, the BER of the CP-OFDM is 0.0168, the BER of the *bior2.2*-OFDM is 0.000784 and *haar*-OFDM is 0.000948. Then the difference between BER of OFDM and *bior2.2*-OFDM and *haar*-OFDM is 0.0160 and 0.01585 respectively. This shows the proposed *bior2.2*-OFDM reduces the bit error by 0.0160 of CP-OFDM and *haar*-OFDM reduces the bit error by 0.01585 of CP-OFDM.

At SNR 35dB for 256-QAM modulation, the BER of C-F-OFDM is 0.00525, the BER of *bior2.2*-F-OFDM is 0.000777 and *haar*-F-OFDM is 0.000984. Then the difference between BER of C-FOFDM and *bior2.2*-F-OFDM and *haar*-F-OFDM is 0.004473 and 0.004266 respectively. This shows the proposed *haar*-F-OFDM reduces the bit error by 0.004473 of C-F-OFDM and *haar*-F-OFDM reduces bit error by 0.004266 of C-F-OFDM.

Table 4.4 BER comparison of DWT-OFDM and DWT-F-OFDM with conventional for the VehA channel model using 256, and 1024-QAM modulation.

Multicarrier Modulation	QAM order		SNR values		
			25 dB	30dB	35dB
CP-OFDM	256	BER	9.17×10^{-2}	4.14×10^{-2}	1.68×10^{-2}
	1024		$1{,}54\times10^{-1}$	8.75×10^{-1}	3.84×10^{-2}
C-F-OFDM	256		7.63×10^{-2}	2.42×10^{-2}	5.25×10^{-3}
	1024		3.84×10^{-2}	1.11×10^{-2}	3.47×10^{-3}
bior2.2-OFDM	256		6.44×10^{-3}	8.8×10^{-4}	7.84×10^{-4}
	1024		4.36×10^{-2}	8.8×10^{-3}	1.03×10^{-3}
haar-OFDM	256		4.02×10^{-3}	1.01×10^{-3}	9.48×10^{-4}
	1024		3.84×10^{-2}	6.68×10^{-3}	1.03×10^{-3}
Sym4-OFDM	256		4.02×10^{-3}	1.01×10^{-3}	9.48×10^{-4}
	1024		3.84×10^{-2}	6.68×10^{-3}	1.12×10^{-3}
bior2.2-F-OFDM	256		6.44×10^{-3}	8.7×10^{-4}	7.77×10^{-4}
	1024		3.84×10^{-2}	8.79×10^{-3}	1.00×10^{-3}
haar-F-OFDM	256		4.0×10^{-3}	1.00×10^{-3}	9.84×10^{-4}
	1024		3.84×10^{-2}	6.03×10^{-3}	1.00×10^{-3}
Sym4-F-OFDM	256		4.0×10^{-3}	1.00×10^{-3}	9.84×10^{-4}
	1024		3.84×10^{-2}	6.63×10^{-3}	1.13×10^{-3}

4.5.2 BER Analysis of DWT-FBMC-OQAM and DWT-FBMC-QAM Multicarrier Modulation Techniques for the Vehicular A Channel Model.

Figures 4.20 and 4.21 demonstrate the BER performance comparison of DWT-FBMC-OQAM modulation techniques with the PHYDYAS prototype filter and FBMC-OQAM. The simulation analysis is done for the VehA channel model using 256, and 1024-QAM modulation order.

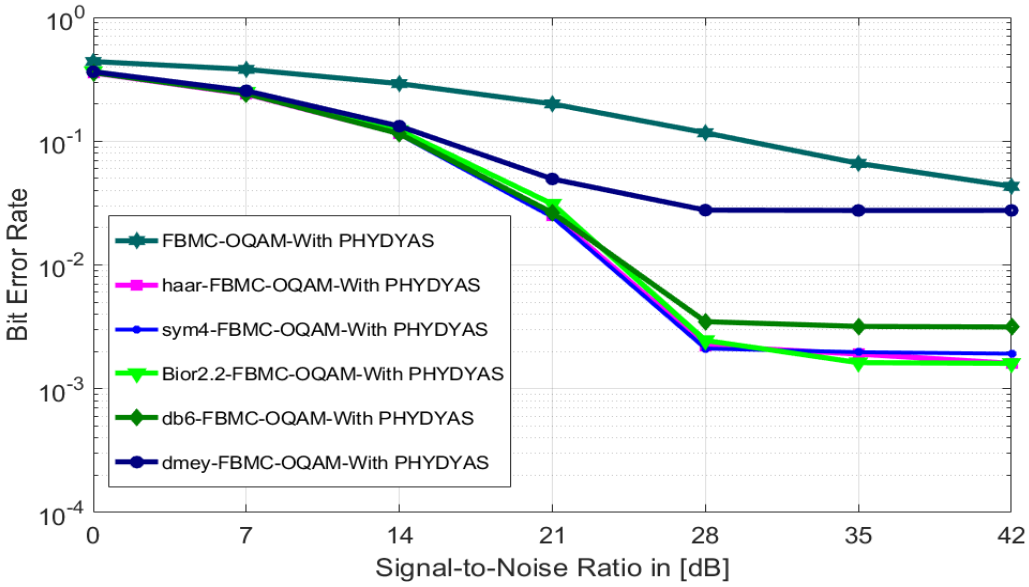

Figure 4.20 BER comparison of DWT-FBMC-OQAM and FBMC-OQAM with PHYDYAS filter for the VehA channel model using 256-QAM modulation**.**

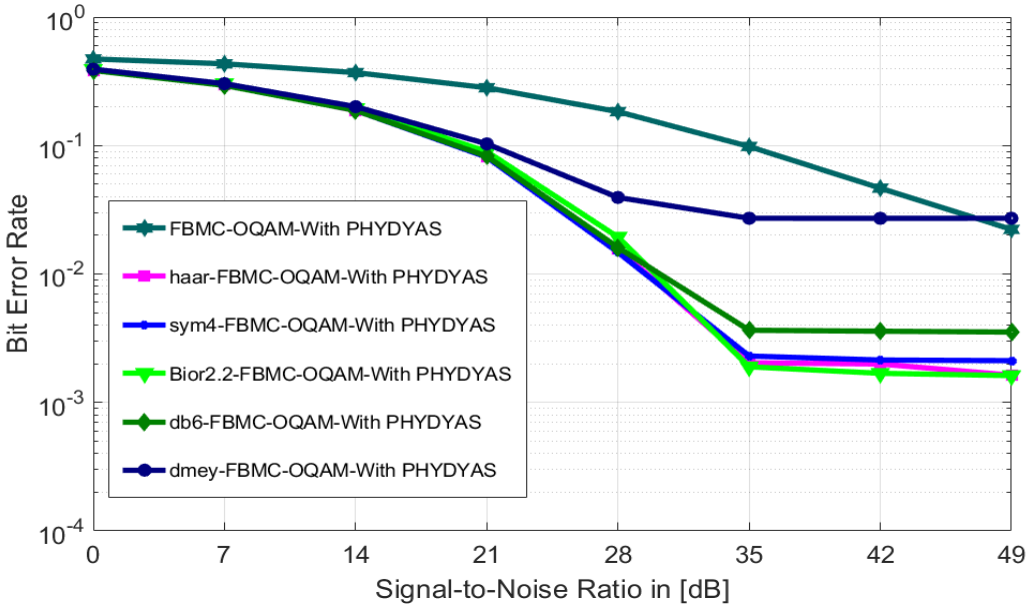

Figure 4.21 BER comparison of DWT-FBMC-OQAM and FBMC-OQAM with PHYDYAS filter for the VehA channel model using 1024-QAM modulation.

Figures 4.20, and 4.21 show the BER performance of the DWT-FBMC-OQAM system with PHYDYAS prototype filter compared to that of the FBMC-OQAM system for 256, and 1024-QAM modulation orders respectively. The proposed DWT-FBMC-OQAM system performs superior the FBMC-OQAM system. However, the *bior2.2*, *sym4,* and *haar,* wavelets demonstrate improved performance than other wavelets.

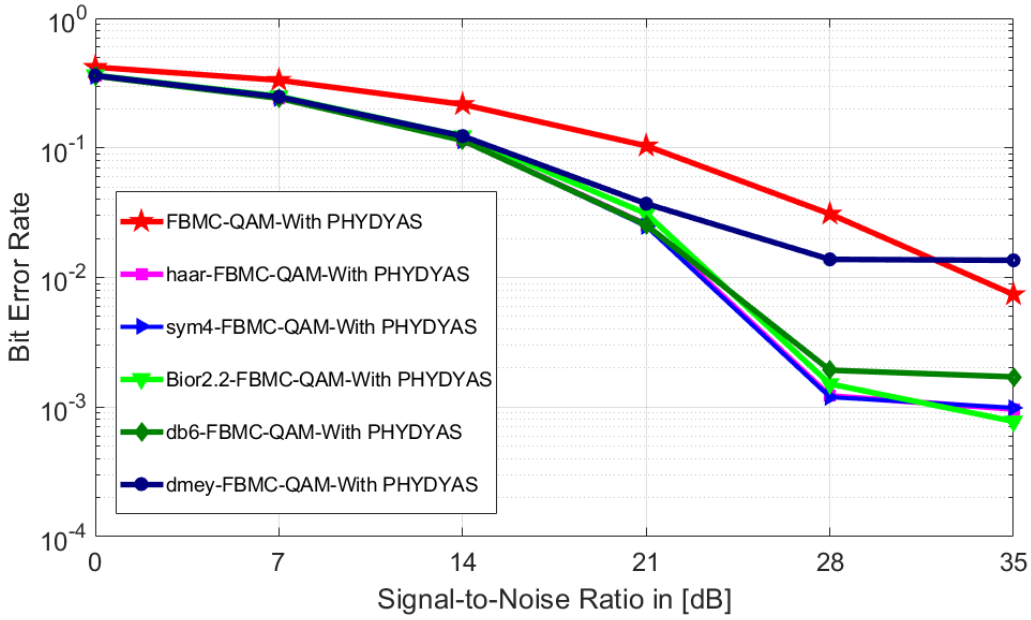

Figure 4.22 BER comparison of DWT-FBMC-QAM and FBMC-QAM with PHYDYAS filter for the VehA channel model using 256-QAM modulation.

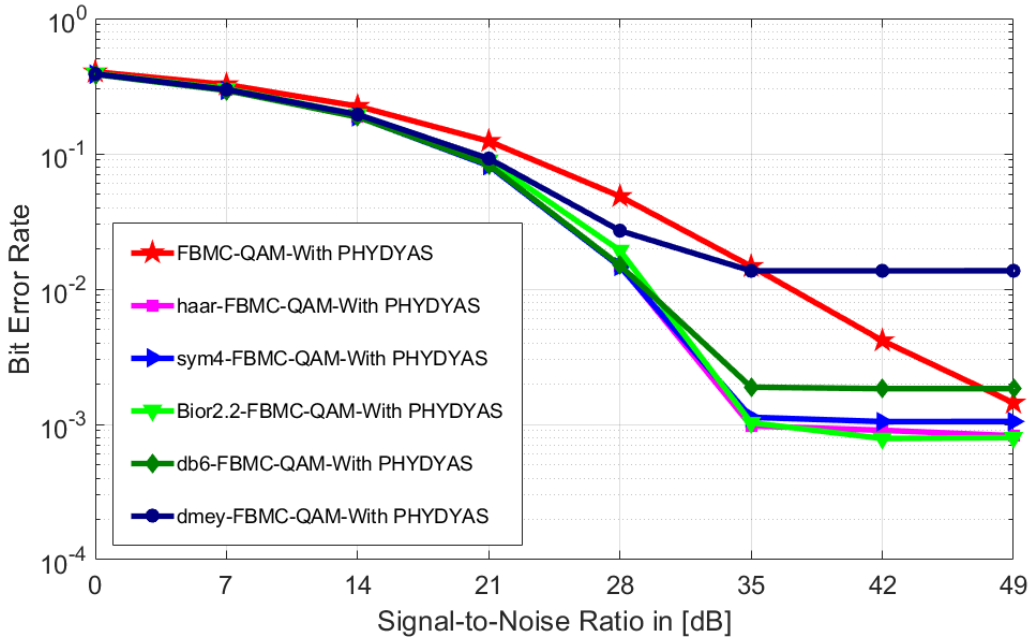

Figure 4.23 BER comparison of DWT-FBMC-QAM and FBMC-QAM with PHYDYAS filter for VehA channel model using 1024-QAM modulation

Figures 4.22 and 4.23 illustrate the BER comparison of the DWT-FBMC-QAM techniques with PHYDYAS prototype filter compared to that of the existing FBMC-QAM system for VehA channel model using 64, 256, and 1024-QAM modulation order respectively. The DWT-FBMC-QAM techniques perform better than the FBMC-OQAM and FBMC-QAM techniques with the PHYDYAS prototype filter. The *bior2.2*, *haar* and *sym4* wavelets show better performance than other wavelets, particularly at a higher SNR for the modulation order. These wavelet families show effects on the improvement of BER and the BER improvement is slightly different as the number of QAM modulations changed. The numerical justification analysis is given in Table 4.5.

Table 4.5 BER Comparison of DWT- FBMC-OQAM and FBMC-QAM With PHYDYAS filter for the VehA channel model using 64, 64, and 1024-QAM modulation.

Multicarrier Modulation	QAM order		SNR values		
			21 dB	28dB	35dB
FBMC/ OQAM PHYDYAS	256	BER	2.00×10^{-2}	1.16×10^{-2}	6.61×10^{-3}
	1024		2.81×10^{-1}	1.83×10^{-1}	9.82×10^{-2}
FBMC/QAM With PHYDYAS	256		9.61×10^{-2}	3.31×10^{-2}	7.79×10^{-3}
	1024		2.16×10^{-1}	1.19×10^{-2}	5.11×10^{-2}
bior2.2-FBMC /OQAM With PHYDYAS	256		3.10×10^{-2}	2.45×10^{-3}	1.62×10^{-3}
	1024		8.97×10^{-2}	1.93×10^{-2}	1.89×10^{-3}
Sym4-FBMC/OQAM With PHYDYAS	256		2.64×10^{-2}	2.11×10^{-3}	1.97×10^{-3}
	1024		8.25×10^{-2}	1.47×10^{-3}	2.29×10^{-3}
haar-FBMC/OQAM With PHYDYAS	256		2.64×10^{-3}	2.45×10^{-3}	1.97×10^{-3}
	1024		8.25×10^{-2}	1.47×10^{-3}	2.03×10^{-3}
bior2.2-FBMC/QAM With PHYDYAS	256		3.10×10^{-2}	1.50×10^{-3}	7.75×10^{-4}
	1024		1.92×10^{-2}	1.1×10^{-3}	7.86×10^{-4}
Sym4-FBMC/QAM With PHYDYAS	256		2.54×10^{-2}	1.19×10^{-3}	9.86×10^{-4}
	1024		1.49×10^{-2}	1.13×10^{-4}	1.0×10^{-3}
haar-FBMC/QAM With PHYDYAS	256		2.54×10^{-2}	1.19×10^{-3}	9.86×10^{-4}
	1024		1.49×10^{-2}	1.0×10^{-3}	9.04×10^{-3}

Table 4.5 shows the effect of BER improvement at specified SNR for DWT-FBMC-OQAM and DWT-FBMC-QAM. At SNR 28dB for 256-QAM modulation, the BER of FBMC-OQAM is 0.016, the BER of *bior2.2*- FBMC-OQAM is 0.00245, and *sym4*- FBMC-OQAM is 0.00211. Then the difference between BER of FBMC-OQAM and *bior2.2*- FBMC-OQAM and *sym4*- FBMC-OQAM is 0.01355 and 0.01389 respectively. This shows the proposed *bior2.2*-FBMC-OQAM improves the bit error by 0.01355 and sym4-FBMC-OQAM improves by 0.01389 of FBMC-OQAM with PHYDYAS Filter.

At SNR 28dB and 256-QAM modulation, the BER of FBMC/QAM is 0.0331, the BER of *bior2.2*- FBMC-QAM is 0.00150, and *sym4*- FBMC-QAM is 0.00119. Then the difference between BER of FBMC-QAM and *bior2.2*- FBMC-QAM and *sym4*- FBMC-QAM is 0.00150 and 0.00119 respectively. This shows the proposed bior2.2-FBMC-QAM improves the bit error by 0.00150 and sym4-FBMC-QAM improves by 0.00119 of FBMC-QAM with PHYDYAS Filter.

4.5.3 BER Analysis of DWT-OFDM and DWT-F-OFDM Multicarrier Modulation Techniques for Vehicular B Channel Model.

In this part, BER performance is examined for various higher-order QAM modulations in both the traditional FFT-based OFDM and F-OFDM schemes compared with the DWT-OFDM and DWT-F-OFDM schemes using five different wavelets. The simulation was done for the VehB channel Model.

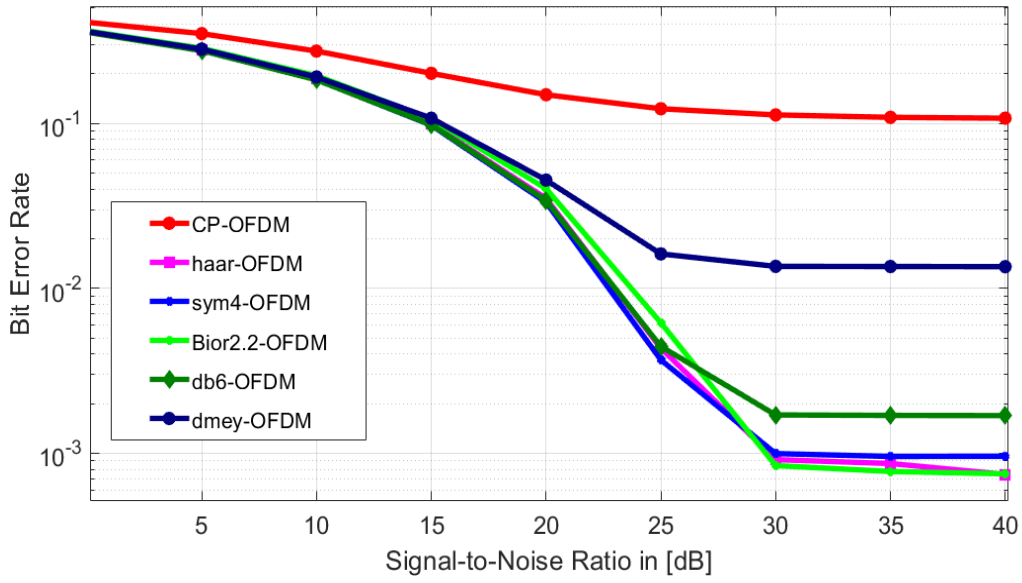

Figure 4.24 BER comparison of DWT-OFDM and CP-OFDM for the VehB channel model using 256-QAM modulation.

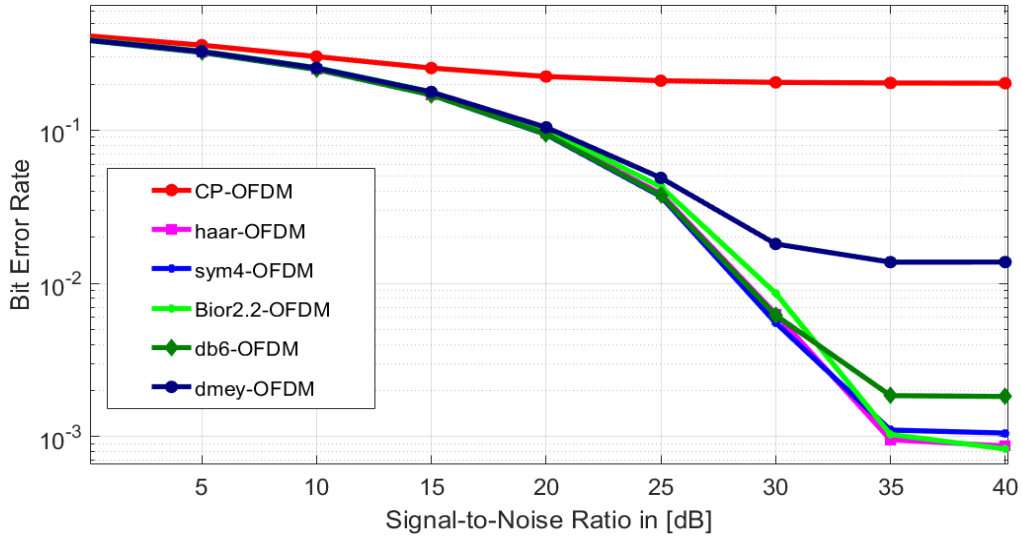

Figure 4.25 BER comparison of DWT-OFDM and CP-OFDM for the VehB channel model using 1024-QAM modulation.

Figure 4.24, and Figure 4.25 show the simulated result of DWT-OFDM for the VehB channel model using 256 and 1024-QAM order of modulation. The result shows the performance comparison of BER with the CP-OFDM for the SNR. The proposed DWT-OFDM schemes more perform than the CP-OFDM schemes. Among the different wavelet families, *sym4*-OFDM and *haar*-OFDM exhibit lower BER values at lower SNR. However, when considering higher SNR scenarios, *bior2.2*-OFDM outperforms all other wavelet families by demonstrating a lower BER.

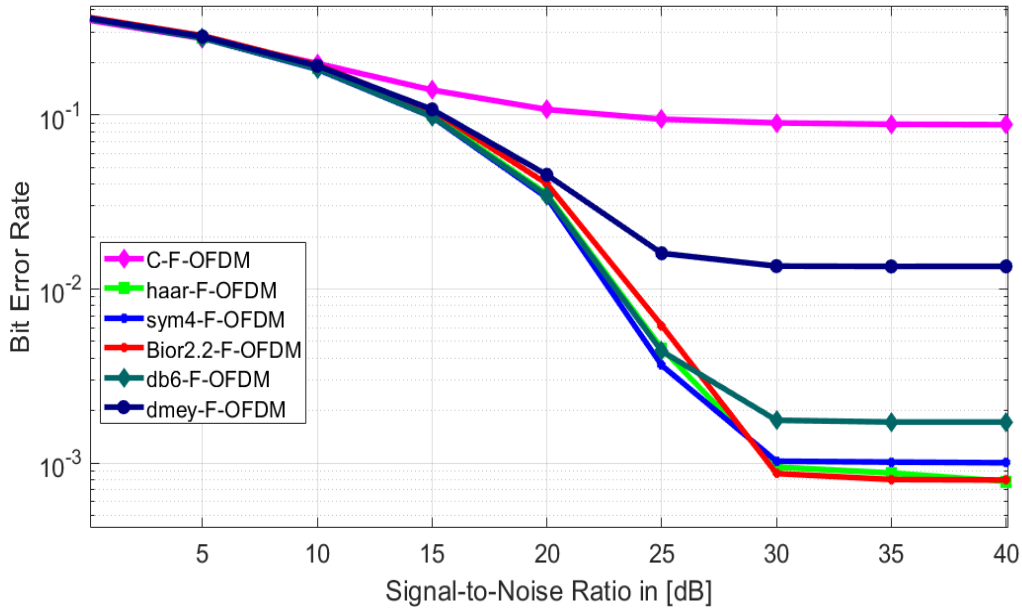

Figure 4.26 BER comparison of DWT-F-OFDM and C-F-OFDM for the VehB channel model using 256-QAM modulation.

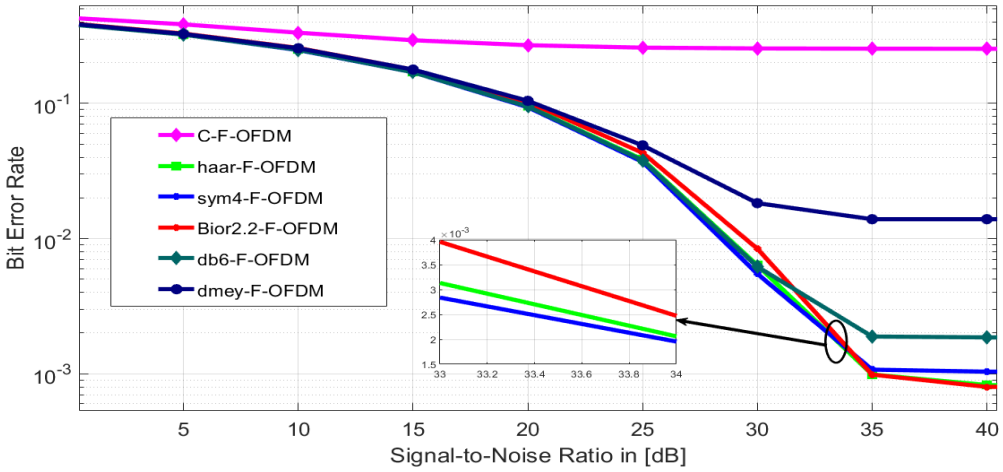

Figure 4.27 BER comparison of DWT-F-OFDM and C-F-OFDM for the VehB channel model using 1024-QAM modulation.

Figure 4.26, and Figure 4.27 show the simulated result of DWT-F-OFDM for the VehB channel model using 256 and 1024-QAM order of modulation. The proposed DWT-F-OFDM system performs superior than the C-F-OFDM system. Among the different wavelet families, *sym4*-F-OFDM and *haar*-F-OFDM exhibit lower BER values at lower SNR. However, when considering higher SNR scenarios, *bior2.2*-F-OFDM outperforms all other wavelet families by demonstrating a lower BER.

Table 4.6 BER comparison of DWT-OFDM and DWT-F-OFDM with conventional for the VehB channel model using 256 and 1024-QAM modulation.

Multicarrier Modulation	QAM order		SNR values		
			25 dB	30dB	35dB
CP-OFDM	256	BER	1.22×10^{-1}	1.12×10^{-1}	1.08×10^{-1}
	1024		2.1×10^{-1}	2.05×10^{-1}	2.03×10^{-1}
C-F-OFDM	256		9.44×10^{-2}	8.99×10^{-2}	8.93×10^{-2}
	1024		2.58×10^{-1}	2.54×10^{-1}	2.53×10^{-1}
bior2.2-OFDM	256		6.17×10^{-3}	8.41×10^{-4}	7.75×10^{-4}
	1024		4.27×10^{-2}	8.62×10^{-3}	1.03×10^{-3}
haar-OFDM	256		4.44×10^{-3}	9.15×10^{-4}	8.66×10^{-4}
	1024		3.75×10^{-2}	5.54×10^{-3}	9.5×10^{-4}
Sym4-OFDM	256		3.68×10^{-3}	9.95×10^{-4}	9.56×10^{-4}
	1024		3.75×10^{-2}	5.54×10^{-3}	1.10×10^{-3}
bior2.2-F-OFDM	256		6.17×10^{-3}	8.69×10^{-4}	8.03×10^{-4}
	1024		4.31×10^{-2}	8.41×10^{-3}	9.85×10^{-4}
haar-F-OFDM	256		4.55×10^{-3}	9.46×10^{-4}	8.76×10^{-4}
	1024		3.79×10^{-2}	6.2×10^{-3}	1.07×10^{-3}
Sym4-F-OFDM	256		3.64×10^{-3}	1.02×10^{-3}	1.01×10^{-3}
	1024		3.78×10^{-2}	5.48×10^{-3}	1.01×10^{-3}

Table 4.6 shows the effect of BER improvement at specified SNR for DWT-OFDM and DWT-F-OFDM for the VehB Channel Model. At SNR 35dB and 256-QAM modulation, the BER of CP-OFDM is 0.108, the BER of C-F-OFDM is 0.0893, the BER of the *bior2.2*-OFDM and *bior2.2*-F-OFDM are 0.000775 and 0.000803. Then the difference between the BER of CP-OFDM and *bior2.2*- OFDM, BER of C-F-OFDM and *bior2.2*- F-OFDM are 0.107225 and 0.088497 respectively. This shows the proposed *bior2.2*-OFDM improves the bit error by 0.107225 of OFDM and *bior2.2*-F-OFDM improves by 0.088497 of C-F-OFDM.

4.5.4 BER Analysis of DWT-FBMC-OQAM and DWT-FBMC-QAM Multicarrier Modulation Techniques for Vehicular B Channel model.

In this part, BER performance is examined for various higher-order QAM modulations in both the traditional FFT-based FBMC schemes compared with the DWT-FBMC schemes using five different wavelets. The simulation was done for the VehB channel Model.

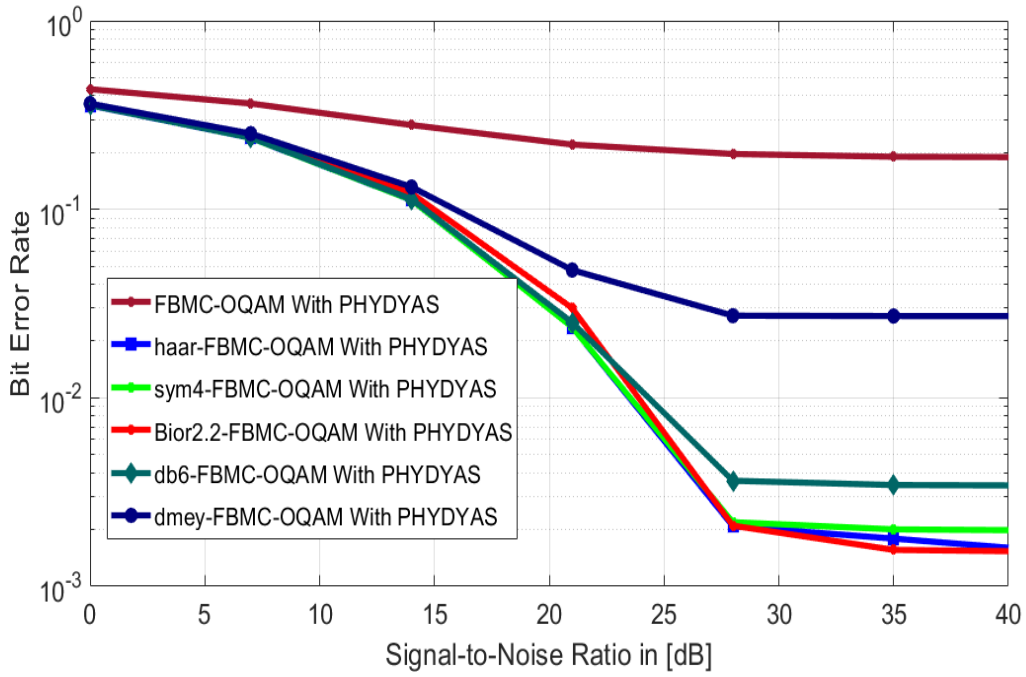

Figure 4.28 BER comparison of DWT-FBMC-OQAM and FBMC-OQAM with PHYDYAS filter for the VehB channel model using 256-QAM modulation.

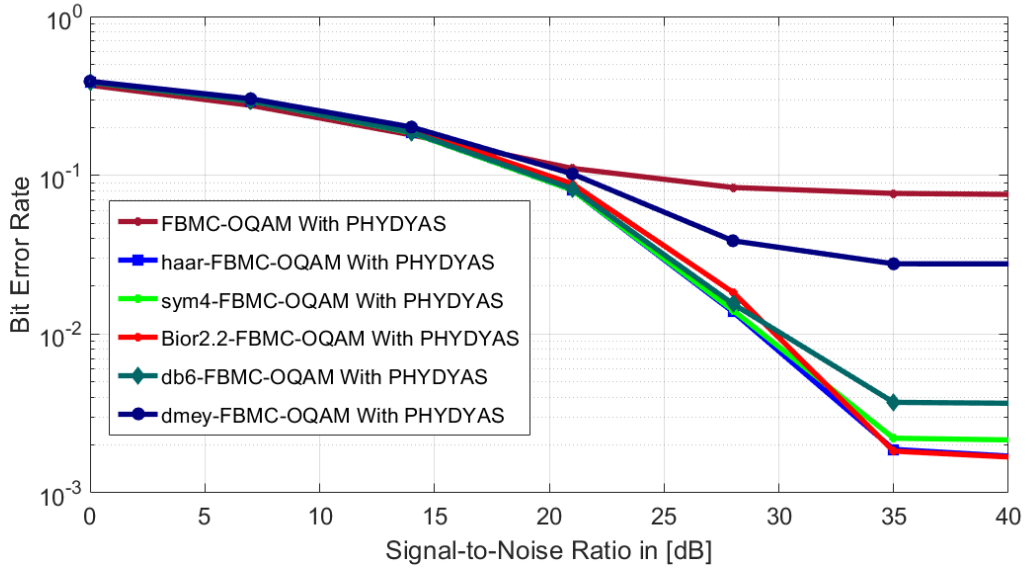

Figure 4.29 BER comparison of DWT-FBMC-OQAM and FBMC-OQAM with PHYDYAS filter for the VehB channel model using 1024-QAM modulation.

Figures 4.28, and 4.29 illustrate BER performance of the DWT-FBMC-OQAM system with PHYDYAS prototype filter is compared to that of the FBMC-OQAM system for 256, and 1024-QAM modulation order respectively for VehB. The proposed DWT-FBMC-OQAM system performs better than the FBMC-OQAM system. However, *bior2.2*, *sym4*, and *haar*, wavelets demonstrate better performance than other wavelets, particularly at a higher Signal-to-noise ratio for the given modulation order.

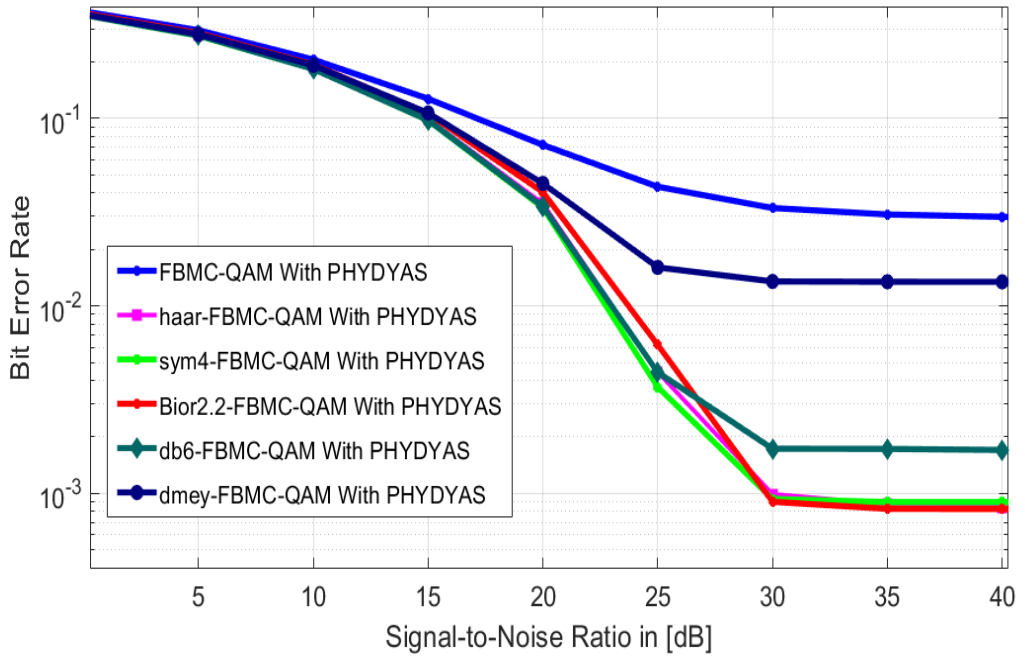

Figure 4.30 BER comparison of DWT-FBMC-QAM and FBMC-QAM with PHYDYAS filter for the VehB channel model using 256-QAM modulation**.**

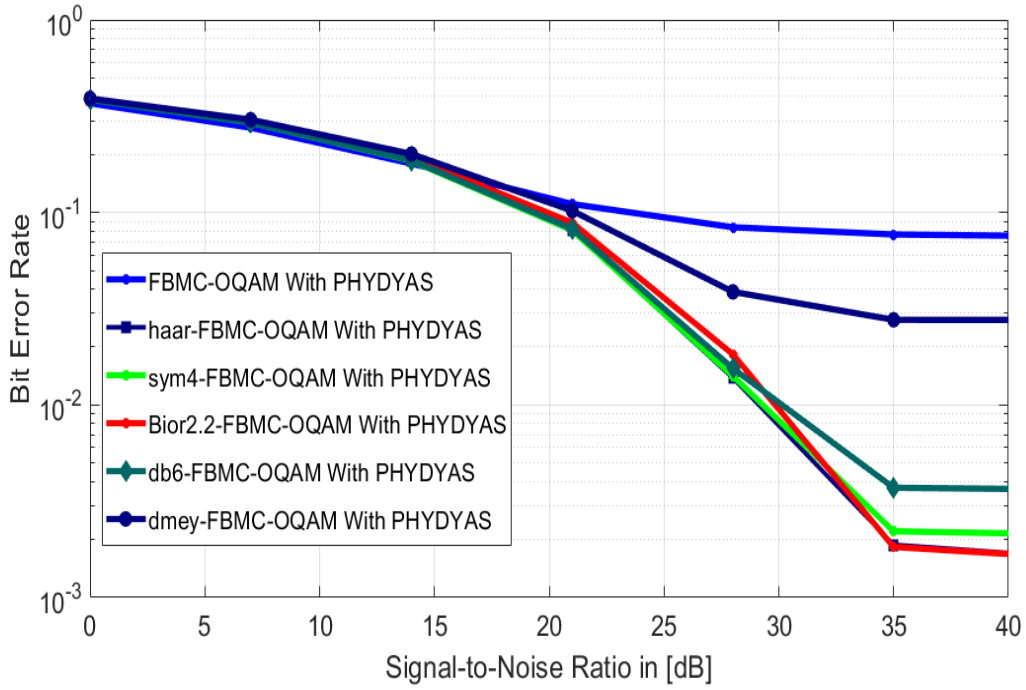

Figure 4.31 BER comparison of DWT-FBMC-QAM and FBMC-QAM with PHYDYAS filter for the VehB channel model using 1024-QAM modulation.

Figures 4.31 and 4.32 illustrate the BER performance of the DWT-FBMC-QAM system with PHYDYAS prototype filter is compared to that of the FBMC-QAM system for 256-QAM, and 1024-QAM modulation order respectively for Vehicular B. The *bior2.2*, *sym4*, and *haar*, wavelets demonstrate better performance than other wavelets, particularly at a higher Signal-to-noise ratio for the given modulation order.

Table 4.7 shows the effect of BER improvement at specified SNR for DWT-FBMC-OQAM and DWT-FBMC-QAM for the Vehicular B Channel Model. At SNR 35dB and 256-QAM modulation, the BER of FBMC-OQAM is 0.190, the BER of FBMC-QAM is 0.0307, the BER of the *bior2.2*- FBMC-OQAM and *bior2.2*- FBMC-QAM are 0.00156 and 0.000826. Then the difference between the BER of FBMC-OQAM and *bior2.2*- FBMC-OQAM, BER of FBMC-QAM and *bior2.2*- FBMC-QAM are 0.18844 and 0.029174 respectively. This shows the proposed *bior2.2*- FBMC-OQAM improves the bit error by 0.18844 of FBMC-OQAM and *bior2.2*- FBMC-QAM improves by 0.029174 of FBMC-QAM.

Table 4.7 BER comparison of DWT- FBMC-OQAM and FBMC-QAM with PHYDYAS filter for the VehB channel model using 64, 256, and 1024-QAM modulation.

Multicarrier Modulation	QAM order		SNR values		
			21 dB	28dB	35dB
FBMC/OQAM With PHYDYAS	256	BER	2.20×10^{-1}	1.96×10^{-1}	1.90×10^{-1}
	1024		1.10×10^{-1}	8.37×10^{-2}	7.68×10^{-2}
FBMC/QAM With PHYDYAS	256		4.32×10^{-2}	3.30×10^{-2}	3.07×10^{-2}
	1024		1.72×10^{-1}	1.58×10^{-1}	1.52×10^{-1}
bior2.2-FBMC/OQAM With PHYDYAS	256		2.99×10^{-2}	2.08×10^{-3}	1.56×10^{-3}
	1024		8.22×10^{-2}	1.83×10^{-2}	1.83×10^{-3}
Sym4-FBMC/OQAM With PHYDYAS	256		2.51×10^{-2}	2.19×10^{-3}	2.00×10^{-3}
	1024		8.22×10^{-2}	1.41×10^{-3}	2.20×10^{-3}
haar-FBMC/OQAM With PHYDYAS	256		2.5×10^{-2}	2.09×10^{-3}	1.79×10^{-3}
	1024		8.22×10^{-2}	1.41×10^{-2}	1.83×10^{-3}
bior2.2-FBMC/QAM With PHYDYAS	256		6.20×10^{-3}	9.02×10^{-4}	8.26×10^{-4}
	1024		4.3×10^{-2}	8.3×10^{-3}	9.69×10^{-4}
Sym4-FBMC/QAM With PHYDYAS	256		3.69×10^{-3}	9.01×10^{-4}	8.98×10^{-4}
	1024		3.77×10^{-2}	5.44×10^{-3}	1.13×10^{-3}
haar-FBMC/QAM With PHYDYAS	256		4.42×10^{-3}	9.89×10^{-4}	8.98×10^{-4}
	1024		3.77×10^{-2}	6.23×10^{-3}	1.03×10^{-3}

In general, when comparing the BER performance of the Vehicular A channel model and VehB channel models, it is true that the BER performance of the Vehicular A model is comparatively better. The BER performance of the VehA channel model is superior to that of the VehB channel model because VehA represents a suburban environment with fewer multipath components, less severe Doppler effects, lower interference, and more consistent statistical variations. In terms of overall analysis of these channel models, the bit error rate decreases as the SNR increases, and it also decreases with higher QAM Modulation. To support higher SNR values, it is recommended to use higher-order QAM as it improves the spectral efficiency of the system. The results from both VehA and VehB channel models indicate that the DWT-based Multicarrier System outperforms all other waveforms.

4.5.5 BER Analysis of DWT-OFDM and DWT-F-OFDM Multicarrier Modulation Techniques for the Pedestrian B Channel Model.

In this part, BER performance is examined for various higher-order QAM modulations in both the traditional FFT-based OFDM and F-OFDM schemes compared with the DWT-OFDM and DWT-F-OFDM schemes using five different wavelets. The simulation was done for the Pedestrian B (PedB) channel Model.

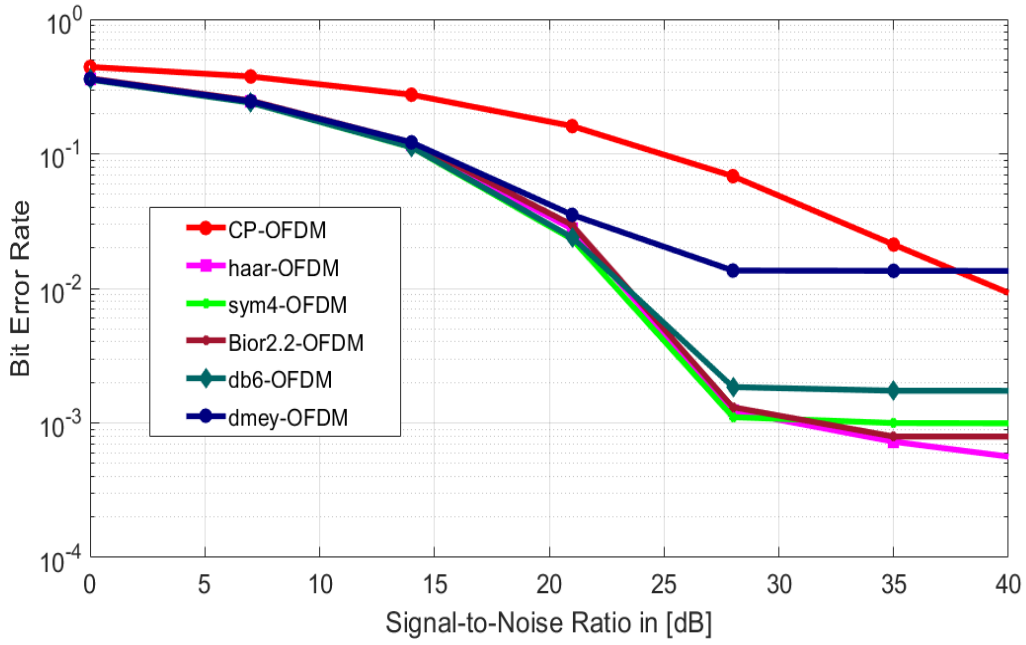

Figure 4.32 BER comparison of DWT-OFDM and CP-OFDM the PedB channel model using 256-QAM modulation.

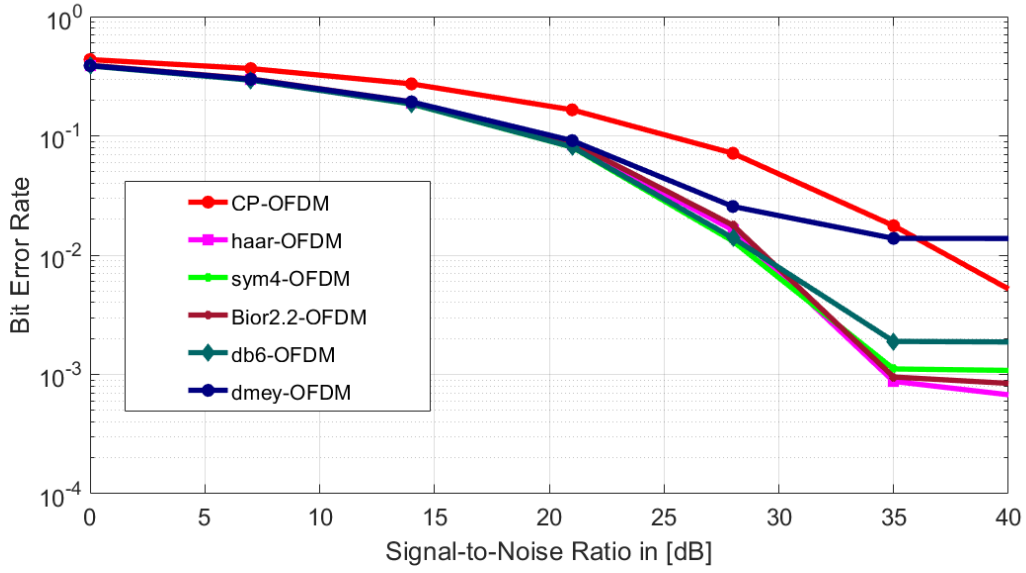

Figure 4.33 BER comparison of DWT-OFDM and CP-OFDM the PedB channel model using 1024-QAM modulation.

Figure 4.33, and Figure 4.34 shows the simulated result of DWT-OFDM for the PedB channel model using 256 and 1024-QAM order of modulation. The proposed DWT-OFDM system performs better than the CP-OFDM system. The *bior2.2*, *sym4*, and *haar*, wavelets demonstrate superior performance than other wavelets, particularly at a higher Signal-to-noise ratio for the given modulation order.

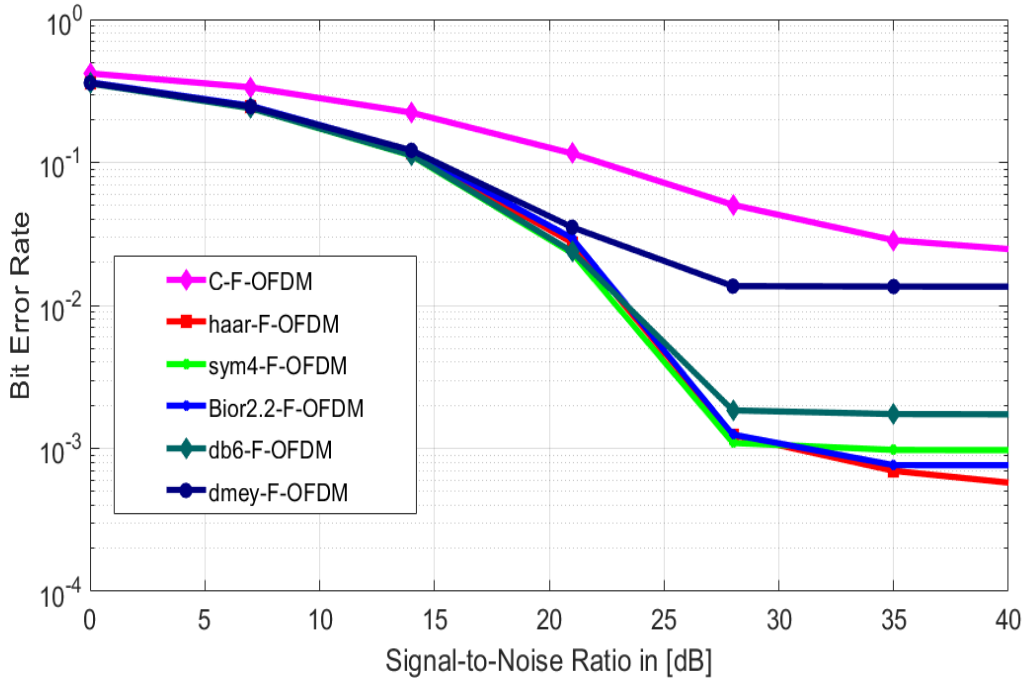

Figure 4.34 BER comparison of DWT-F-OFDM and C-F-OFDM the Pedestrian B channel model at 256-QAM modulation.

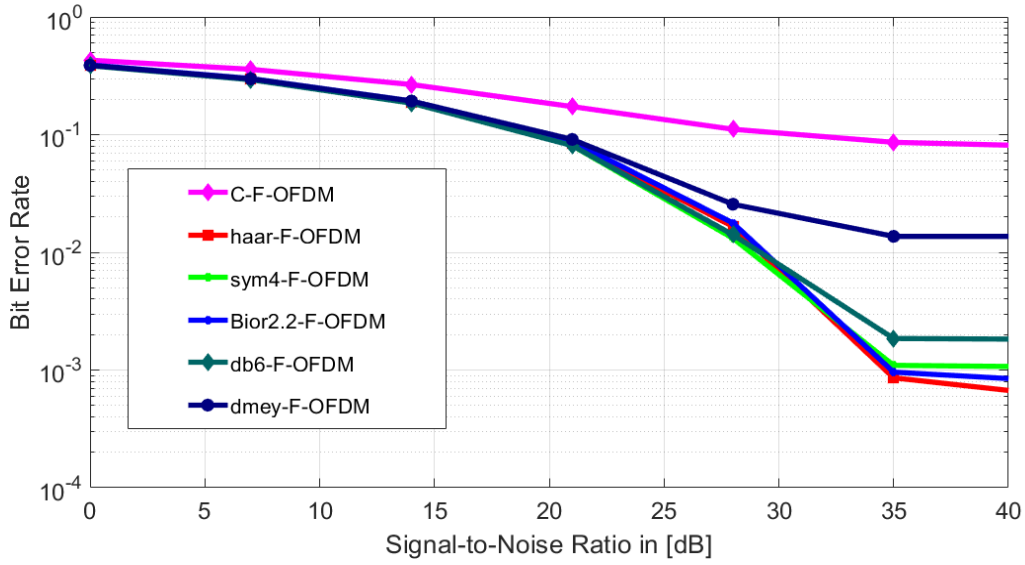

Figure 4.35 BER comparison of DWT-F-OFDM and C-F-OFDM the PedB channel model using 1024-QAM modulation.

Figure 4.47 and Figure 4.48 show the simulated result of DWT-F-OFDM for the PedB channel model using 256 and 1024-QAM order of modulation. The proposed DWT-F-OFDM system performs better than the C-F-OFDM system. The *bior2.2*, *sym4*, and *haar*, wavelets demonstrate desired performance than other wavelets, particularly at a higher Signal-to-noise ratio for the given modulation order.

Table 4.8 BER comparison of DWT-OFDM and DWT-F-OFDM System with for the PedB channel model using 256, and 1024-QAM modulation.

Multicarrier Modulation	QAM order		SNR values		
			25 dB	30dB	35dB
CP-OFDM	256	BER	1.60×10^{-1}	6.81×10^{-2}	2.11×10^{-2}
	1024		1.65×10^{-1}	7.14×10^{-2}	1.76×10^{-2}
C-F-OFDM	256		1.15×10^{-1}	5.05×10^{-2}	2.85×10^{-2}
	1024		1.73×10^{-1}	1.11×10^{-1}	8.60×10^{-2}
bior2.2-OFDM	256		2.96×10^{-2}	1.31×10^{-3}	7.91×10^{-4}
	1024		8.06×10^{-2}	1.78×10^{-2}	9.51×10^{-4}
haar-OFDM	256		2.96×10^{-2}	1.31×10^{-3}	7.2×10^{-4}
	1024		8.06×10^{-2}	1.78×10^{-2}	8.74×10^{-4}
Sym4-OFDM	256		2.96×10^{-2}	1.10×10^{-3}	9.98×10^{-4}
	1024		8.06×10^{-2}	1.30×10^{-2}	8.74×10^{-4}
bior2.2-F-OFDM	256		2.95×10^{-2}	1.24×10^{-3}	7.63×10^{-4}
	1024		8.07×10^{-2}	1.77×10^{-2}	9.58×10^{-4}
haar-F-OFDM	256		2.38×10^{-2}	1.25×10^{-3}	6.96×10^{-4}
	1024		8.07×10^{-2}	1.41×10^{-2}	1.09×10^{-3}
Sym4-F-OFDM	256		3.38×10^{-2}	1.25×10^{-3}	6.96×10^{-4}
	1024		8.07×10^{-2}	1.41×10^{-2}	8.58×10^{-4}

4.5.6 BER Analysis of DWT-FBMC-OQAM and DWT-FBMC-QAM Multicarrier Modulation Techniques for the Pedestrian B Channel model.

In this part, BER performance is examined for various higher-order QAM modulations in both the traditional FFT-based FBMC schemes compared with the DWT-FBMC schemes using five different wavelets. The simulation was done for the PedB channel Model.

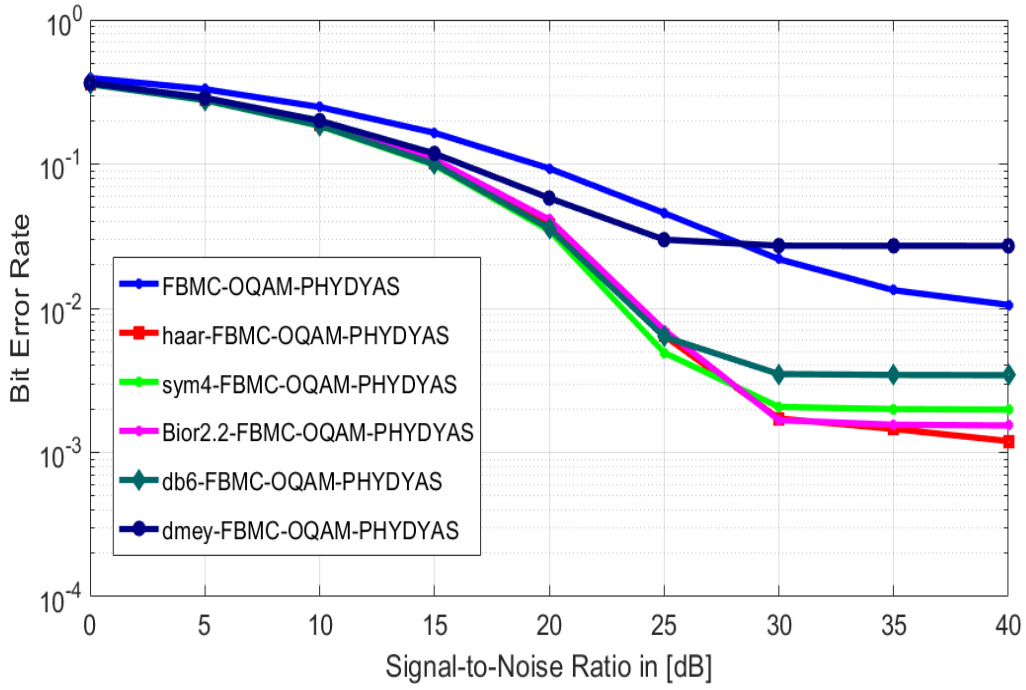

Figure 4.36 BER Comparison of DWT-FBMC-OQAM and FBMC-OQAM with PHYDYAS filter the PedB channel model using 256-QAM modulation.

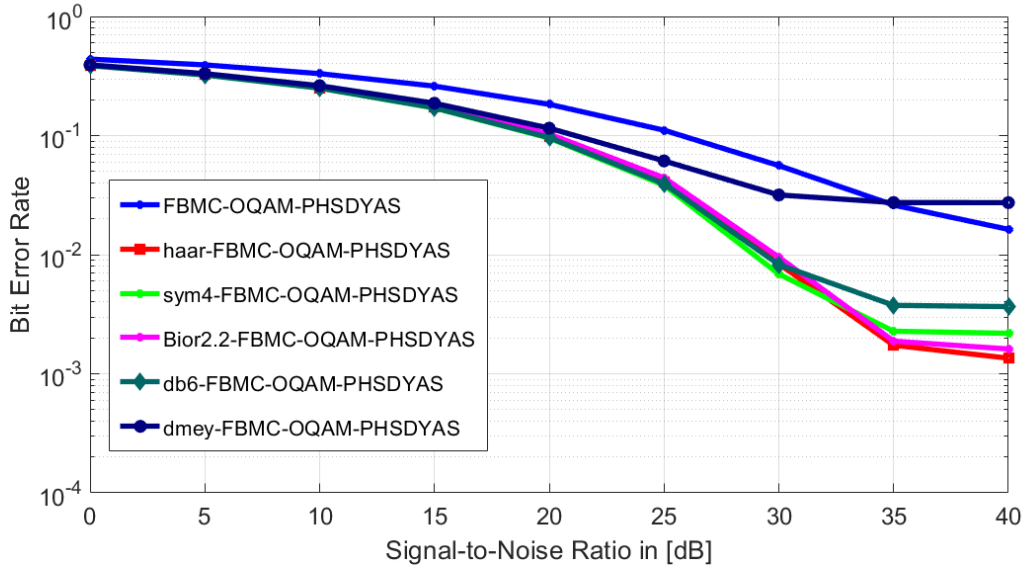

Figure 4.37 BER comparison of DWT-FBMC-OQAM and FBMC-OQAM with PHYDYAS filter the PedB channel model using 1024-QAM modulation.

Figures 4.50 and 4.51 illustrate the BER performance of the DWT-FBMC-OQAM system with PHYDYAS prototype filter is compared to that of the FBMC-OQAM system for 256 and 1024-QAM modulation order respectively for Pedestrian B. The proposed DWT-FBMC-OQAM techniques performs better than the FBMC-OQAM modulation techniques.

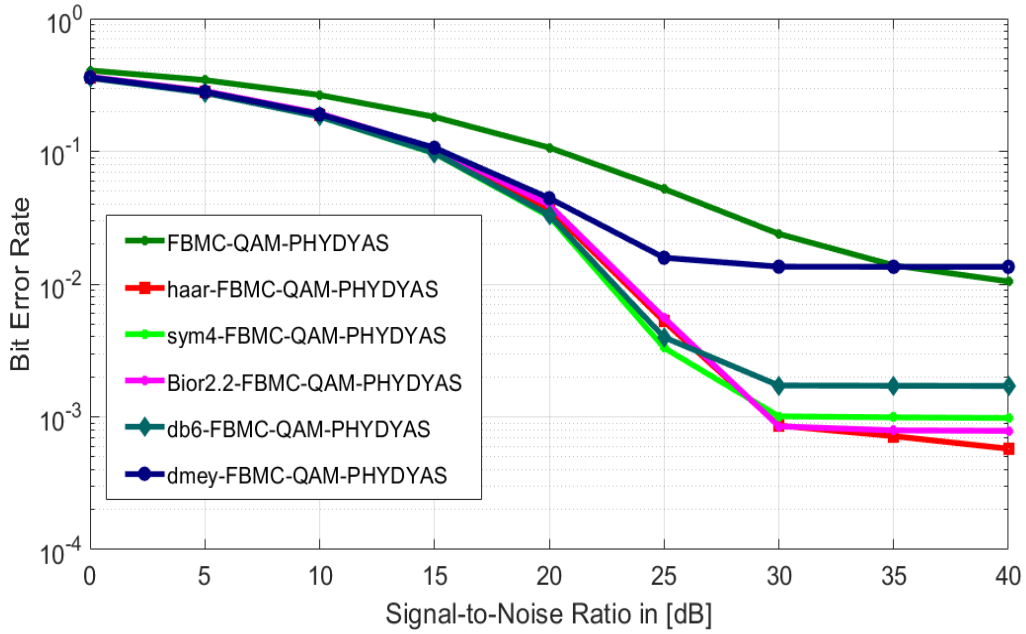

Figure 4.38 BER comparison of DWT-FBMC-QAM and FBMC-QAM with PHYDYAS filter the PedB channel model using 256-QAM modulation.

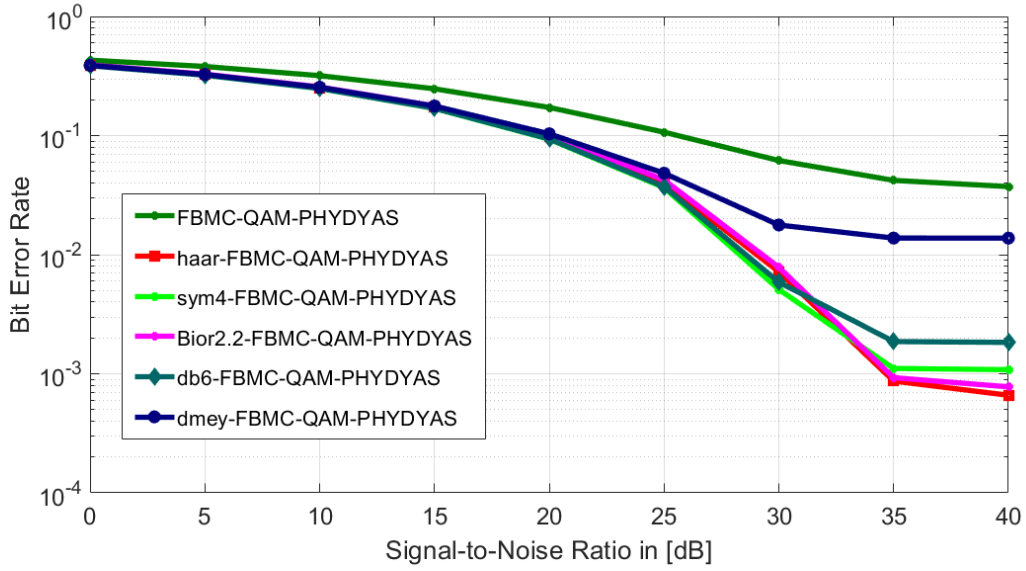

Figure 4.39 BER comparison of DWT-FBMC-QAM and FBMC-QAM with PHYDYAS filter the PedB channel model using 1024-QAM modulation.

Figures 4.39 and 4.40 illustrate BER performance of the DWT-FBMC-QAM system with PHYDYAS prototype filter is compared to that of the FBMC-QAM system using 256, and 1024-QAM modulation order respectively for Pedestrian B. The proposed DWT-FBMC-QAM system performs better than the FBMC-QAM system. Table 4.9 shows the numerical justification of the DWT-based candidate multicarrier modulation techniques.

Table 4.9 BER Comparison of DWT- FBMC-OQAM and FBMC-QAM With PHYDYAS Filter for the PedB channel model using 256, and 1024-QAM Modulation.

Multicarrier Modulation	QAM order		SNR values		
			21 dB	28dB	35dB
FBMC/OQAM With PHYDYAS	256	BER	2.20×10^{-1}	1.96×10^{-1}	1.90×10^{-1}
	1024		1.10×10^{-1}	8.37×10^{-2}	7.68×10^{-2}
FBMC/QAM With PHYDYAS	256		4.32×10^{-2}	3.30×10^{-2}	3.07×10^{-2}
	1024		1.72×10^{-1}	1.58×10^{-1}	1.52×10^{-1}
bior2.2-FBMC/OQAM With PHYDYAS	256		2.99×10^{-2}	2.08×10^{-3}	1.56×10^{-3}
	1024		8.22×10^{-2}	1.83×10^{-2}	1.83×10^{-3}
Sym4-FBMC/OQAM With PHYDYAS	256		2.51×10^{-2}	2.19×10^{-3}	2.00×10^{-3}
	1024		8.22×10^{-2}	1.41×10^{-3}	2.20×10^{-3}
haar-FBMC/OQAM With PHYDYAS	256		2.5×10^{-2}	2.09×10^{-3}	1.79×10^{-3}
	1024		8.22×10^{-2}	1.41×10^{-2}	1.83×10^{-3}
bior2.2-FBMC/QAM With PHYDYAS	256		6.20×10^{-3}	9.02×10^{-4}	8.26×10^{-4}
	1024		4.3×10^{-2}	8.3×10^{-3}	9.69×10^{-4}
Sym4-FBMC/QAM With PHYDYAS	256		3.69×10^{-3}	9.01×10^{-4}	8.98×10^{-4}
	1024		3.77×10^{-2}	5.44×10^{-3}	1.13×10^{-3}
haar-FBMC/QAM With PHYDYAS	256		4.42×10^{-3}	9.89×10^{-4}	8.98×10^{-4}
	1024		3.77×10^{-2}	6.23×10^{-3}	1.03×10^{-3}

In general, when comparing the BER performance of the VehA model, VehB model, and PedB channel models, it is observed that the BER performance of the PedB channel model is better.Because it represents lower mobility scenarios with less severe Doppler effects, multipath propagation, and statistical variations compared to the VehA and VehB channel models. The more stable and less dynamic conditions of the PedB channel result in a more reliable communication link, leading to lower BER.Overall, as the signal-to-noise ratio (SNR) increases, the bit error rate decreases, and this reduction is further improved with higher-order QAM.

To maximize the benefit of a large SNR value, it is recommended to utilize higher-order QAM as it enhances the spectral efficiency of the system. Notably, the findings obtained from the VehA model, VehB model, and PedB channel models indicate that the DWT-based multicarrier modulation techniques outperform all other candidate waveforms.

Discrete Wavelet Transform-based multicarrier modulation exhibits a lower BER compared to conventional methods due to several key advantages. DWT-based systems achieve superior spectral efficiency by efficiently packing data into subcarriers with wavelets, leading to enhanced transmission within the available bandwidth. Additionally, DWT's inherent ability to localize frequency information enables robustness to frequency-selective fading channels, minimizing inter-symbol interference (ISI) and improving BER performance.

Furthermore, the analysis shows that every wavelet-based multicarrier modulation technique outperforms the Conventional schemes in terms of performance over a Vehicular and Pedestrian channel model. The DWT-based multicarrier modulation systems based on *bior2.2*,*sym4,* and *haar* wavelets exhibit superior performance in terms of peak-to-average power ratio and bit error rate characteristics. The spectral analysis indicates that the *dmey* wavelets demonstrate improved power spectral density characteristics when compared to conventional multicarrier techniques.

4.6 Computational Complexity Comparison

Computational complexity analysis of different 5G candidate waveforms with DWT-based are discussed in this section. We have evaluated complexity in terms of the number of real multiplications in each multi-carrier symbol. The primary block contributing to complexity arises from IFFT/IDWT in the transmitter and FFT/DWT in the receiver, respectively. The real number of multiplication calculations for N-Point IFFT and FFT are different from IDWT and DWT. The real number of multiplication for IDWT/DWT multicarrier modulation depends on the choice of the length of filter in each wavelet family.

In this study, the length of *haar* (L=2) and *db6* (L=4) are chosen for computational complexity analysis of DWT-based multicarrier modulation schemes. For simulation, different parameters were considered. Also, the N taken 1024 for all wave-forms, the cyclic prefix is 72 for OFDM and F-OFDM, and The length of the filter for F-OFDM is 513, which is the same as 4G LTE, overlapping factor 4 which has a better side lobe, for FBMC-OQAM, and FBMC-QAM with PHYDYAS prototype Filter.

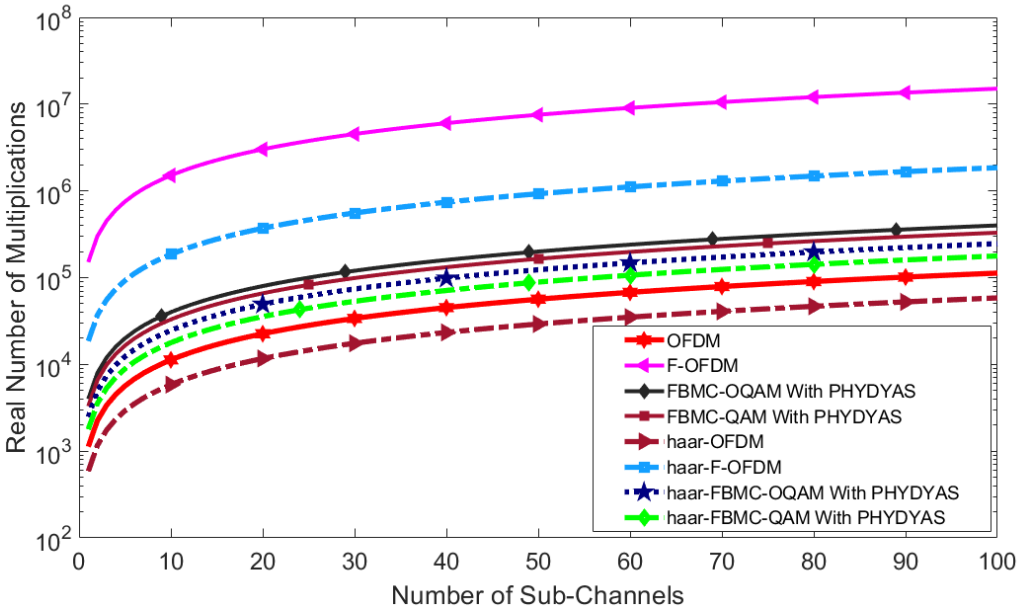

Figure 4.40 Computational complexity of DWT-multicarrier modulation techniques for *haar* (L=2) wavelet family.

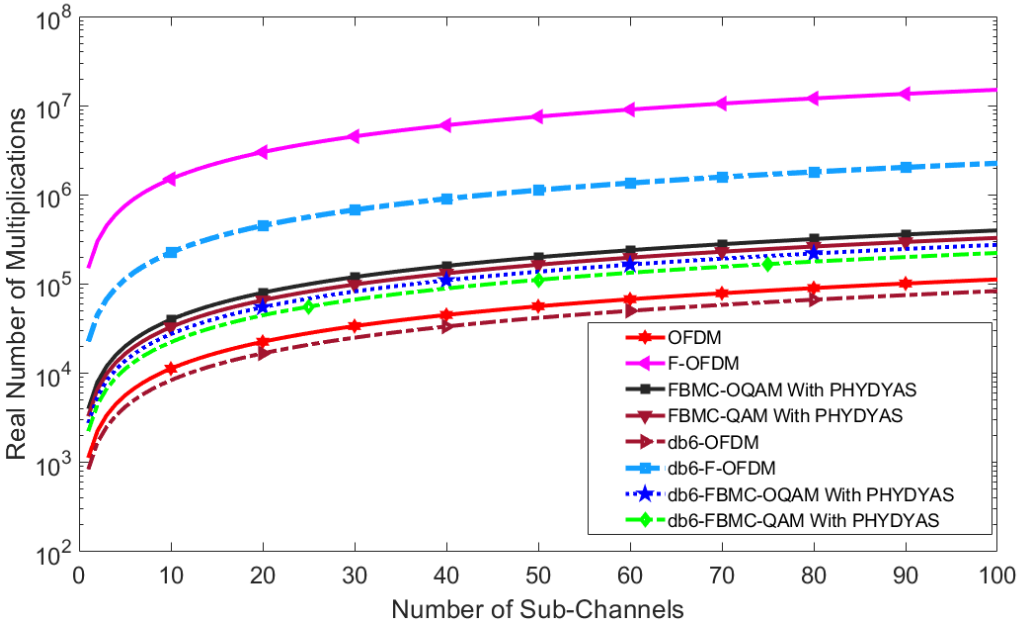

Figure 4.41 Computational complexity of DWT-multicarrier modulation techniques for *db6* (L=4) wavelet family.

Figure 4.55 and Figure 4.56 shows that increasing the number of sub-channels increases the number of real multiplications. The complexity of DWT-multicarrier modulation schemes is small compared to the other conventional multi-carrier modulations. Therefore *haar* and *db6* wavelet families reduce the complexity of each candidate multicarrier modulation.

5. CONCLUSION AND RECOMMENDATIONS

5.1 Conclusion

In this thesis, Discrete Wavelet Transform multi-carrier techniques, such as DWT-OFDM, DWT-F-OFDM, DWT-FBMC/OQAM using the PHYDYAS filter, and DWT-FBMC/ QAM using the PHYDYAS filter have been introduced and compared with existing multi-carrier techniques. The performance of multi-carrier integrated with DWT and conventional multi-carrier techniques was evaluated based on parameters such as SE, PSD, BER, PAPR, and Computational Complexity.

The simulation results demonstrated that the *dmey*-wavelet family exhibited higher PSD compared to other wavelet families. Additionally, the PSD of *dmey*-F-OFDM showed significant improvement over traditional OFDM, FBMC-OQAM, and FBMC-QAM using wavelets. For higher-order QAM modulation, most of the multi-carrier techniques integrated with DWT exhibited lower PAPR performance compared to conventional multi-carrier techniques. However, among the various wavelets, the *bior2.2* and *haar* wavelets demonstrated the lowest PAPR, attributed to the smaller number of signal analyses in the wavelet-based schemes compared to existing techniques. Additionally, it can be deduced that the PAPR performance of wavelet-based multi-carriers depends on factors such as the type of multicarrier technique, the selected wavelet family, and the modulation order. From the simulation results obtained through BER analysis, it was noted that all selected wavelets exhibit comparable BER performance across both Vehicular and Pedestrian channel models. Comparing the BER performance among VehA models, VehB model, and PedB channel models, it is observed that the BER performance of the PedB channel model is better.

Generally, as the SNR increases, the bit error rate decreases, and this reduction is further improved with higher-order QAM. The results obtained from VehA, VehB, and Pedestrian B channel models indicated that the DWT-based multicarrier modulation technique outperformed all other waveforms. The DWT-based multicarrier method based on *bior2.2*,*sym4*, and *haar* wavelets exhibited better performance in terms of BER parameters. The *bior2.2* wavelet offers superior PAPR characteristics and maintains nearly identical spectrum properties to traditional MCM. Additionally, the BER characteristics of *bior2.2* based candidate multicarrier modulation techniques show significant improvement compared to the existing system in considered channels. Therefore, the *bior2.2* wavelet-based modulation is recommended as the optimal model for the proposed DWT-based multicarrier techniques because of its unique bi-orthogonal characteristics for PAPR and BER analysis.

The complexity of DWT-based multicarrier modulation is affected by the length of the filter for the wavelet family. The complexity analysis from the simulation results revealed that *Haar* and *db6* wavelet families exhibit less complexity with the considered candidate multicarrier method. Generally, the analysis suggests that DWT-based multicarrier modulation techniques are the most suitable for 5G wireless communication and beyond, outperforming all other existing waveforms.

5.2 Recommendations

In this thesis, the performance evaluation of multi-carrier modulation techniques using Discrete Wavelet Transform for 5G wireless communication and beyond was carried out based on considered performance metrics. The multi-carrier modulation techniques that have been chosen for comparison are DWT-OFDM, DWT-F-OFDM, DWT-FBMC with OQAM using PHYDYAS filter, and DWT-FBMC with QAM using PHYDYAS filter.

Some points that are recommended for future work are:

1. The analysis in this thesis is carried out using a single transmitting and receiving antenna. In the future, it is recommended to analyze the system's massive MIMO antenna because it enhances spectral efficiency.
2. The PSD evaluation of DWT-based Multicarrier Modulation in the thesis is limited to the integration of DWT with OFDM and F-OFDM only. It is recommended to integrate the DWT with FBMC for PSD analysis

6.REFERENCES

Abdel-Atty, H. M., Raslan, W. A., & Khalil, A. T. (2020). Evaluation and analysis of FBMC/OQAM systems based on pulse shaping filters. *IEEE Access*, *8*, 55750–55772. https://doi.org/10.1109/ACCESS.2020.2981744

Abu-dalbouh, H. M. (2019). *Developing Mobile Tracking Applications for Patient Treatment*. *12*(1), 12–22. https://doi.org/10.5539/cis.

Ahmed, A. S., Al-Amaireh, H., & Kollár, Z. (2022). Multicarrier Modulation Schemes for 5G Wireless Access. *ECTI Transactions on Computer and Information Technology*, *16*(4), 378–392. https://doi.org/10.37936/ecti-cit.2022164.248710

Ahmed Solyman, A. A., & Yahya, K. (2022). Evolution of wireless communication networks: from 1G to 6G and future perspective. *International Journal of Electrical and Computer Engineering*, *12*(4), 3943–3950 . https://doi.org/10.11591/ijece.v12i4.pp3943-3950

Akyildiz, I. F., Nie, S., Lin, S., & Chandrasekaran, M. (2016). *5G roadmap : 10 key enabling technologies*. *106*, 17–48. https://doi.org/10.1016/j.comnet.2016.06.010

Al-jawhar, Y. A., Ramli, K. N., Abas, M., Shahida, N., Salama, M. S., Bashar, A. M., & Khalaf, A. (2021). *Improving PAPR performance of filtered OFDM for 5G communications using PTS*. *43*(February 2020), 209–220 . https://doi.org/10.4218/etrij.2019-0358

Almutairi, A. F., & Krishna, A. (2022). Filtered-orthogonal wavelet division multiplexing (F-OWDM) technique for 5G and beyond communication systems. *Scientific Reports*, *12*(1), 1–15. https://doi.org/10.1038/s41598-022-08248-3

Arunachalam, S., Kumar, S., Kshatriya, H., & Mahendrapatil, P. (2018). *Analyzing 5G : Prospects of Future Technological Advancements in Mobile Analyzing 5G : Prospects of Future Technological Advancements in Mobile*. *May*, 5–11.

Bendimerad, M. Y., Senhadji, S., & Bendimerad, F. T. (2021). *Prototype Filters and Filtered Waveforms for Radio Air-Interfaces: A Review*. *April* . http://arxiv.org/abs/2104.01373

Chataut, and A. (2020). *Massive MIMO Systems for 5G and beyond Networks—Overview, Recent Trends, Challenges, and Future Research Direction*. 1–35 . https://doi.org/10.3390/s20102753

Dash, L., Jayanthi, M., Rohit, M., Patil, R. S., Rupendran, A. M., & Ravi, N. (2022). Feasibility Analysis of Multicarrier Techniques for 5G Communication. *2022 International Conference on Advances in Computing, Communication and Applied*

Informatics (ACCAI), 1–6. https://doi.org/10.1109/ACCAI53970.2022.9752557

Dawood, S. A., Malek, F., Anuar, M. S., & Hadi, S. Q. (2015). *Discrete Multiwavelet Critical-Sampling Transform-Based OFDM System over Rayleigh Fading Channels*. *2015*.

Doré, J. B., Gerzaguet, R., Cassiau, N., & Ktenas, D. (2017). Waveform contenders for 5G: Description, analysis and comparison. *Physical Communication*, *24*, 46–61. https://doi.org/10.1016/j.phycom.2017.05.004

Dumari, H. T., Gelmecha, D. J., Shakya, R. K., & Singh, R. S. (2023). BER and PSD Improvement of FBMC with Higher Order QAM Using Hermite Filter for 5G Wireless Communication and beyond. *Journal of Electrical and Computer Engineering*, *2023*. https://doi.org/10.1155/2023/7232488

Exam, F., Reinforced, A., & Design, C. (2019). *Jimma Institute of Technology*. *October*, 4–6.

Hamdar, F., Maria, C., Gussen, G., Nadal, J., Nour, C. A., & Baghdadi, A. (2023). FBMC / OQAM Transceiver for Future Wireless Communication Systems : Inherent Potentials, Recent Advances, Research Challenges. *IEEE Open Journal of Vehicular Technology*, *4*(September), 652–666. https://doi.org/10.1109/OJVT.2023.3303034

Hasan, F. S., & Lateef, N. Q. (2021). Performance Comparison of Multicarrier Communication Systems Over Doubly-selective Channels. *Periodicals of Engineering and Natural Sciences*, *9*(3), 12–21. https://doi.org/10.21533/pen.v9i3.2075

Isnawati, A. F., Dhia Fikri Zam Zami, & M. Lukman Leksono. (2023). Performance Comparison of FBMC-OQAM and CP-OFDM Using AWGN Channel. *Jurnal Nasional Teknik Elektro*, *1*. https://doi.org/10.25077/jnte.v12n1.1034.2023

ITU-R. (2015). IMT Vision – Framework and overall objectives of the future development of IMT for 2020 and beyond. *Mobile, Radiotetermination, Amateur and Related Satellite Services*, *0*, 1–21. https://www.itu.int/dms_pubrec/itu-r/rec/m/R-REC-M.2083-0-201509-I!!PDF-E.pdf

Jeon, D., Kim, S., Kwon, B., Lee, H., & Lee, S. (2016). Prototype filter design for QAM-based filter bank multicarrier system. *Digital Signal Processing: A Review Journal*, *57*, 66–78. https://doi.org/10.1016/j.dsp.2016.05.002

Jiang, C., Member, S., Zhang, H., & Han, Z. (2016). *Information Sharing Outage-Probability Analysis of Vehicular Networks*. *9545*(c), 1–13 . https://doi.org/10.1109/TVT.2016.2614369

Jolania, S., & Sindal, R. (2023). *Design aspects and Performance analysis of Multicarrier Waveform contenders of 5G and beyond Wireless Networks*.

Kamal, Q., & Din, U. (2019). Proceedings of 2019 16th International Bhurban Conference on Applied Sciences and Technology, IBCAST 2019. *Proceedings of 2019 16th International Bhurban Conference on Applied Sciences and Technology, IBCAST 2019*, 989–993.

Khan, M. H. M. M. H. A. (2020). Performance Analysis of OFDM, W-OFDM, and F- OFDM Under Rayleigh Fading Channel for 5G Wireless Communication. *Proceedings of the Third International Conference on Intelligent Sustainable Systems [ICISS 2020]*, 1172–1177.

Kishore, K. K., Umar, P. R., & Naveen, V. J. (2017). Comprehensive Analysis of UFMC with OFDM and FBMC. *Indian Journal of Science and Technology*, *10*(17), 1–7. https://doi.org/10.17485/ijst/2017/v10i17/114337

Kundrapu, S., Dutt, S. I., Koilada, N. K., & Raavi, A. C. (2019). Characteristic Analysis of OFDM, FBMC and UFMC Modulation Schemes for Next Generation Wireless Communication Network Systems. *Proceedings of the 3rd International Conference on Electronics and Communication and Aerospace Technology, ICECA 2019*, 715–721. https://doi.org/10.1109/ICECA.2019.8821991

Lu, L., Member, S., Li, G. Y., & Swindlehurst, A. L. (2014). *An Overview of Massive MIMO : Bene fi ts and Challenges*. *8*(5), 742–758.

Marian Joseph Jeffery, J., Masapalli, L., Nookala, V. M., Dasari, S. P., & Kirthiga, S. (2020). Peak to Average Power Ratio and Bit Error Rate Analysis of MultiCarrier Modulation Techniques. *Proceedings of the 2020 IEEE International Conference on Communication and Signal Processing, ICCSP 2020*, 1443–1446 . https://doi.org/10.1109/ICCSP48568.2020.9182172

Nissel, R., Schwarz, S., & Rupp, M. (2017). Filter Bank Multicarrier Modulation Schemes for Future Mobile Communications. *IEEE Journal on Selected Areas in Communications*, *35*(8), 1768–1782. https://doi.org/10.1109/JSAC.2017.2710022

Patil, C. S., Karhe, R. R., & Aher, M. A. (2012). *Review on Generations in Mobile Cellular Technology*. *2*(10), 614–619.

Ramadhan, A. J. (2019). *Implementation of a 5G Filtered-OFDM Waveform Candidate*. *May*.

RRamakrishnan, B., Kumar, A., Chakravarty, S., Masud, M., & Baz, M. (2021). Analysis of FBMC waveform for 5g network-based smart hospitals. *Applied Sciences (Switzerland)*, *11*(19). https://doi.org/10.3390/app11198895

Saadoon, H. J., Jamel, T. M., & Khazal, H. F. (2022). The Effects of Different Weather Conditions on 5G Millimeter Waves Propagations at 38 GHz and 73 GHz for Kut-City inIraq.*Wasit Journal of Engineering Sciences* . https://doi.org/10.31185/ejuow.Vol10.Iss2.274

Salleh, J. Z. and M. F. M. (2020). *We are IntechOpen, the world's leading publisher of Open Access books Built by scientists, for scientists TOP 1 %*.

Sarowa, S., Kumar, N., & Singh, R. S. (2020). Analysis of WOFDM over LTE 1.25MHz band. *Wireless Communications and Mobile Computing*, *2020* . https://doi.org/10.1155/2020/8835879

Schaich, F., Wild, T., & Chen, Y. (2014). Waveform contenders for 5G - Suitability for short packet and low latency transmissions. *IEEE Vehicular Technology Conference*, *2015-Janua*(January). https://doi.org/10.1109/VTCSpring.2014.7023145

Shaik, N., & Malik, P. K. (2021). *5G Multi-Carrier Modulation Techniques : Prototype Filters , Power Spectral Density , and Bit Error Rate Performance*.

Sharma, S. (2021). Key Enabling Technologies of 5G Wireless Mobile Communication Key Enabling Technologies of 5G Wireless Mobile Communication. *Journal of Physics: Conference Series*. https://doi.org/10.1088/1742-6596/1817/1/012003

Tan, N. M., Chen, H., Giap, B. D., Le, H., & Nhat, Q. (2020). *Wavelet Transform Application Based on Matlab Simulation Wavelet Transform Application Based on Matlab Simulation*. *March*. https://doi.org/10.25073/2588-1124/vnumap.4459

Tazeb, F., Dereje, A., Co-Advisor, H., Kassaw, A., & Ababa, A. (2019). *Comparative Performance Analysis of Modulation Formats for 5G Wireless System*.

Wang, Y., Song, R., Wang, S., & Wu, W. (2020). Study of the prototype filter and bit error rate for the filter bank multi-carrier system. *2020 5th International Conference on Computer and Communication Systems, ICCCS 2020*, 816–820 . https://doi.org/10.1109/ICCCS49078.2020.9118476

Zhang, X., Chen, L., Qiu, J., & Abdoli, J. (2016). *On the Waveform for 5G*. *November*, 74–80.

Zixuan Wang. (2020). Massive MIMO Detection Algorithms Based on Massive MIMO Detection Algorithms Based on MMSE-SIC , ZF-MIC , Neumann Series Expansion , Gauss-Seidel , and Jacobi Method. *Journal of Physics: Conference Series*. https://doi.org/10.1088/1742-6596/1438/1/012006